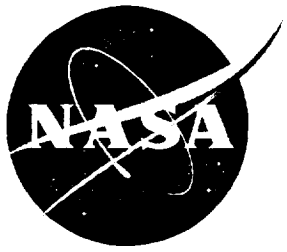

NASA Contractor Report 4668

Computer Program BL2D for Solving Two-Dimensional and Axisymmetric Boundary Layers

Venkit Iyer

Contract NAS1-19672
Prepared for Langley Research Center

May 1995

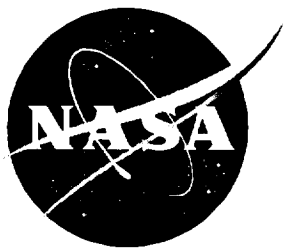

NASA Contractor Report 4668

Computer Program BL2D for Solving Two-Dimensional and Axisymmetric Boundary Layers

Venkit Iyer
ViGYAN, Inc. • Hampton, Virginia

National Aeronautics and Space Administration
Langley Research Center • Hampton, Virginia 23681-0001

Prepared for Langley Research Center
under Contract NAS1-19672

May 1995

Printed copies available from the following:

NASA Center for AeroSpace Information
800 Elkridge Landing Road
Linthicum Heights, MD 21090-2934
(301) 621-0390

National Technical Information Service (NTIS)
5285 Port Royal Road
Springfield, VA 22161-2171
(703) 487-4650

SUMMARY

This report presents the formulation, validation, and user's manual for the computer program BL2D. The program is a fourth-order-accurate solution scheme for solving two-dimensional or axisymmetric boundary layers in speed regimes that range from low subsonic to hypersonic Mach numbers. A basic implementation of the transition zone and turbulence modeling is also included. The code is a result of many improvements made to the program VGBLP, which is described in NASA TM-83207 (February 1982), and can effectively supersede it. The code BL2D is designed to be modular, user-friendly, and portable to any machine with a standard `fortran77` compiler.

The report contains the new formulation adopted and the details of its implementation. Five validation cases are presented. A detailed user's manual with the input format description and instructions for running the code is included. Adequate information is presented in the report to enable the user to modify or customize the code for specific applications.

Keywords

Boundary layer
Computer program
Two-dimensional
Axisymmetric
Compressible flow
Laminar flow control
Transition prediction
Turbulence modeling

TABLE OF CONTENTS

Nomenclature

$a_1,\ a_2,\ a_3$	coefficients in the ξ-direction differencing formula (eq. (18))
$a_{i,j}$	coefficients of the block-tridiagonal system given by eq. (49)
$a^k_{l,m}$	diagonal elements of the linear system given by eq. (22)
$b_{i,j}$	coefficients of the block-tridiagonal system given by eq. (49)
$b^k_{l,m}$	superdiagonal elements of the linear system given by eq. (22)
c_1, c_2	coefficients used in power law for viscosity (eq. (61))
$C_{f,e}$	skin-friction coefficient based on edge conditions, $\tau_w/\left(\frac{1}{2}\rho_e u_e^2\right)$
c_{1k}	$\Delta\zeta_k/2$ (eqs. (24) and (28))
c_{2k}	$\Delta\zeta_k^2/12$ (eqs. (24) and (28))
c_p	specific heat at constant pressure
$e_{i,j}$	coefficients used in the block-tridiagonal system (eqs. (35), (41) and (47))
F	$u\ /\ u_e$
f	an arbitrary function
H	$T\ /\ T_e$
h	heat transfer coefficient, $\dot{q}^*_w/(T_w - T_{aw})$
I	H_ζ
i	index in the streamwise (ξ) direction
j	flag; = 0 indicates two-dimensional flow; = 1 indicates axisymmetric flow
k	index in the boundary-layer normal (ζ) direction
ki	value of index k at the edge of the inner part of the normal grid distribution
ke	index k that corresponds to the boundary-layer edge
k_s	factor for stretching the grid in the ζ direction (eq. (62))
L	F_ζ
l	$(\rho\mu/\rho_e\mu_e)$
l_1	$t^{2j}l\bar{\epsilon}$ (eq. (1))
l_2	$t^{2j}l\tilde{\epsilon}$ (eq. (2))
M	Mach number
M_θ	$M_\infty^2 \sin^2\theta_s$
N_{Pr}	Prandtl number, laminar value
$N_{Pr,t}$	Prandtl number, turbulent value
$N_{St,e}$	Stanton number based on edge conditions, $h/(c_p\rho^*_e u^*_e)$
P	pressure, dimensional
p	pressure, nondimensional (eq. (53))
p_{10}	total pressure at boundary-layer edge (eq. (56)), nondimensional
Q	vector (eq. (14))
$\dot{q}^*_w$	wall heat flux, dimensional
R	gas constant, dimensional
Re	Reynolds number
r	body radius
r^k_l	residual, right-hand side of eq. (22)
S	solution vector
s^*	streamwise length along body surface, dimensional
T	temperature, dimensional

t	transverse curvature term (used in eq. (1) and (2) only)
t	temperature, nondimensional (eq. (55))
t^*	boundary-layer thickness, dimensional
U_∞	free-stream velocity, dimensional
u	velocity in streamwise direction, nondimensional
w	transformed normal velocity
x	Cartesian coordinate in the body axis direction
z	coordinate in the body-normal direction
α	$(\gamma - 1)M_e^2$
β	$\frac{2\xi}{u_e}(u_e)_\xi$
Γ	streamwise intermittency distribution
γ	ratio of specific heats
$\Delta\zeta$	step size in ζ (eq. (15))
δ	displacement thickness
ζ	transformed normal coordinate
θ_s	shock-wave angle
μ	absolute viscosity
ξ	transformed boundary-layer surface coordinate
ρ	density

Subscripts:

aw	adiabatic wall
e	boundary-layer edge
$k = 1$	at the wall
$k = ke$	at boundary-layer edge
ref	reference value
w	wall quantity
0	stagnation condition
ξ, ζ	partial derivatives in ξ or ζ direction
∞	free-stream quantity

Superscripts:

$*$	dimensional quantity
$'$	partial derivative in ζ (except for x', y', z')
n	iteration number
T	transpose

Abbreviations:

BL2D	boundary-layer two-dimensional program described in this report
SI	international (metric) system of units
US	U.S. customary or British system of units
VGBLP	boundary-layer program described in NASA TM-83207
s/r	subroutine

1. INTRODUCTION

This report presents the theory, formulation, and implementation of a fourth-order-accurate solution scheme for two-dimensional or axisymmetric boundary layers in speed regimes that range from low subsonic to hypersonic Mach numbers. A basic implementation of the transition zone and turbulence modeling is also included. The computer program that results from this work is available under the name BL2D. The basic formulation is based on the program VGBLP, which is described in NASA TM–83207 (ref. 1).

The code BL2D is the result of many improvements made to the VGBLP program. The changes in formulation and implementation have been substantial; as a result, the coding for BL2D has been done from scratch. Thorough validation of the code has been completed; the author is confident that the code BL2D can effectively supersede VGBLP.

The original theory and solution scheme presented in NASA TM–83207 is based on a second-order implicit scheme in the boundary layer normal direction. In contrast, the solution scheme in BL2D is based on a fourth-order-accurate compact Pade formula in the normal direction. This results in improved quality of the mean-flow profiles, which is a consideration of great importance for application to boundary-layer stability calculations. The Pade differencing scheme is discussed in detail in NASA CR–4531 (ref. 2) for three-dimensional boundary layers.

The development of BL2D was also motivated by other considerations. The VGBLP program was written for machines of limited core memory and used many nonportable constructs, such as name lists and equivalence statements. It was also written in an older version of `fortran` and was designed for optimum performance on slower machines. Modification for specific applications was cumbersome, and updating the program with new models for turbulence and transition was difficult.

The present code is written in standard `fortran77` and is portable (i.e., no machine-dependent features). The program package takes advantage of the user-friendly features of the UNIX operating system such as 'make' and file directories. Individual subroutines are now in separate files with 'include' statements that supply the common blocks. The code has been completely reprogrammed with emphasis on easy to understand and structured programming at the expense of some additional computation. An easy to use input format has been adopted. Output of solution quantities has been improved and is designed to be used for easy graphical interpretation. The code is easily modifiable to allow replacement of the built-in transition region and turbulence models with user-supplied routines in a modular form. The accuracy of the present method is independent of the normal grid distribution. With the computational speeds that are achievable today, the code can be run interactively on a desktop machine.

The BL2D code has been validated with the original VGBLP test cases. The results are summarized in this report. A user's manual is also included in this report. Sufficient details about the program have been provided in the manual so that it can be easily customized by the user for specific applications. The program package also includes the original VGBLP program files and input files for the five test cases described in reference 1. The complete program package and documentation are archived in the NASA Langley computer system and can be made available per individual request.

The author would like to request that users communicate to him any errors, omissions, or desirable modifications to the report or the computer program. An updated description of such revisions will be maintained by the author and supplied with the software and report. The e-mail address of the author is `v.iyer@larc.nasa.gov`.

2. FORMULATION

2.1 Equations in Vector Form

We start with the transformed equations given in NASA TM–83207 (ref. 1). These are equations numbered (27) through (29) (page 15 of the report). A fourth-order-accurate Pade differencing scheme is now implemented, similar to the procedure outlined in NASA CR–4531 (ref. 2). Let us use the following notations in place of the original notations used in NASA TM–83207 for the sake of simplicity, as well as for partial conformity with notations in NASA CR–4531. (See fig. 1.)

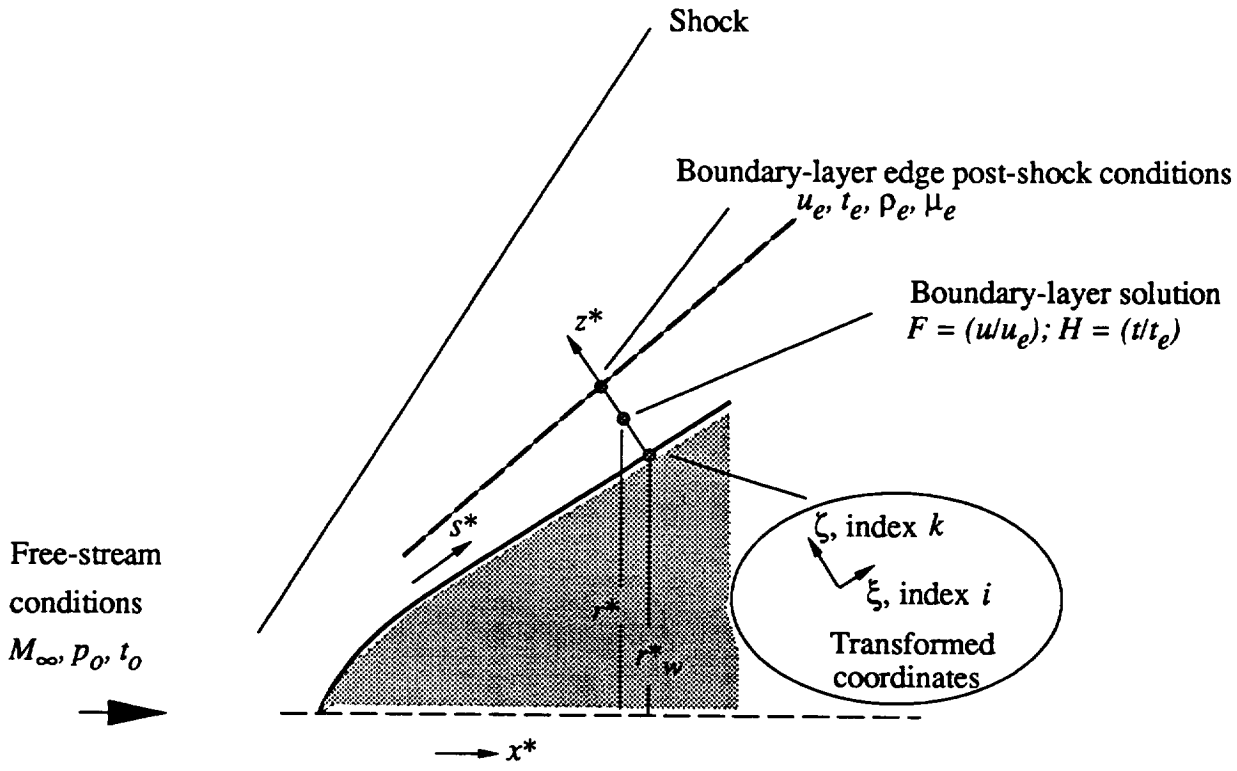

Figure 1. A sketch of notations used in boundary-layer formulation.

We use w in place of V; H in place of θ; ζ in place of η for the transformed normal coordinate; and the prime symbol $'$ for the normal derivative $(\partial/\partial\zeta)$. The subscript ξ is used to indicate the partial derivative in the ξ direction. In addition, we use the following

notations:

$$l_1 = t^{2j} l\bar{\epsilon} \tag{1}$$

$$l_2 = t^{2j} l\tilde{\epsilon} \tag{2}$$

$$L = F' \tag{3}$$

$$I = H' \tag{4}$$

The equation set can then be rewritten as

$$\begin{aligned} w' &= -F - 2\xi F_\xi \\ wF' - \left(l_1 F'\right)' &= -2\xi F F_\xi - \beta\left(F^2 - H\right) \\ wH' - \left(l_2 H'\right)' &= -2\xi F H_\xi + \alpha l_1 \left(F'\right)^2 \end{aligned} \tag{5}$$

Also note that in the equations above $j = 0$ or 1, depending on whether the flow is two-dimensional planar or axisymmetric; $l = (\rho\mu)/(\rho_e\mu_e)$; $\bar{\epsilon}$ is the eddy viscosity function $\left(1 + \frac{\epsilon}{\mu}\Gamma\right)$; $\tilde{\epsilon}$ is the eddy viscosity function $\frac{1}{N_{Pr}}\left(1 + \frac{\epsilon}{\mu}\frac{N_{Pr}}{N_{Pr,t}}\Gamma\right)$; t is the transverse curvature term r/r_w; $\beta = \frac{2\xi}{u_e}(u_e)_\xi$; and $\alpha = (\gamma - 1)M_e^2$.

To achieve a vectorial representation of the system prior to application of the fourth-order Pade differencing scheme, let us denote

$$Q = \begin{pmatrix} F \\ Fw - l_1 L \\ H \\ Hw - l_2 I \end{pmatrix} \tag{6}$$

The vector Q' can now be obtained from the system of equation set (5) as given below (with substitution for w'):

$$Q' = \begin{pmatrix} L \\ -F^2(1+\beta) - 4\xi F F_\xi + \beta H \\ I \\ -2\xi(FH)_\xi - FH + \alpha l_1 L^2 \end{pmatrix} \tag{7}$$

The element Q_2' of the equation above is obtained as

$$\begin{aligned} Q_2' &= (Fw - l_1 L)' = Fw' + wF' - (l_1 F')' = Fw' - 2\xi F F_\xi - \beta(F^2 - H) \\ &= F(-F - 2\xi F_\xi) - 2\xi F F_\xi - \beta(F^2 - H) = -F^2(1+\beta) - 4\xi F F_\xi + \beta H \end{aligned} \tag{8}$$

The element Q_4' of equation (7) is obtained as

$$\begin{aligned} Q_4' &= (Hw - l_2 I)' = Hw' + wH' - (l_2 H')' = Hw' - 2\xi F H_\xi + \alpha l_1 (F')^2 \\ &= H(-F - 2\xi F_\xi) - 2\xi F H_\xi + \alpha l_1 (F')^2 = -2\xi (FH)_\xi - FH + \alpha l_1 (F')^2 \end{aligned} \tag{9}$$

The second derivative Q'' required in the differencing scheme is

$$Q'' = \begin{pmatrix} L' \\ -2FL(1+\beta) - 4\xi(FL_\xi + LF_\xi) + \beta I \\ I' \\ -2\xi(FI + HL)_\xi - (FI + HL) + 2\alpha(l_1 LL' + L^2 l_1') \end{pmatrix} \tag{10}$$

The variables L' and I' are obtained by differentiating the second and fourth elements of equation (6) with respect to ζ and substituting for w'. The resulting expressions are

$$l_1 L' = F(2\xi F_\xi + \beta F) + L(w - l_1') - \beta H \tag{11}$$

$$l_2 I' = 2\xi F H_\xi - \alpha l_1 (F')^2 + I(w - l_2') \tag{12}$$

The final form of Q'' is, then,

$$Q'' = \begin{pmatrix} \frac{1}{l_1}[F(2\xi F_\xi + \beta F) + L(w - l_1') - \beta H] \\ -2FL(1+\beta) - 4\xi(FL_\xi + LF_\xi) + \beta I \\ \frac{1}{l_2}[2\xi F H_\xi - \alpha l_1 L^2 + I(w - l_2')] \\ -2\xi(FI + HL)_\xi - (FI + HL) + 2\alpha L[F(2\xi F_\xi + \beta F) + Lw - \beta H] \end{pmatrix} \tag{13}$$

2.2 Discretization

In accordance with the method in NASA CR-4531, we apply the fourth-order Pade differencing formula in the normal direction. This two-point compact scheme is defined in terms of the variable and its two higher derivatives. In the present case, if we assume that i

(i.e., the index in the surface direction ξ) remains constant and that k is the normal direction index, then the discretization at the midpoint of k and $(k-1)$ is written as

$$Q_k - Q_{k-1} - \frac{\Delta\zeta}{2}\left(Q'_k + Q'_{k-1}\right) + \frac{\Delta\zeta^2}{12}\left(Q''_k - Q''_{k-1}\right) + O(\Delta\zeta^5) = 0 \tag{14}$$

$$\Delta\zeta = \zeta_k - \zeta_{k-1} \tag{15}$$

The differencing in the surface direction ξ is accomplished to second order (or first order in some regions). For example, in the ξ direction, if we assume that the index k is fixed, then

$$\begin{aligned} Q_\xi &= a_1 Q_i + \{aQ\} \\ \{aQ\} &= a_2 Q_{i-1} + a_3 Q_{i-2} \end{aligned} \tag{16}$$

The values of the coefficients a_i are dependent on the location of the point in the streamwise direction. In the general case, the ξ differencing is second-order accurate. In accordance with the parabolic nature of the equations, the ξ derivative is obtained by the three-point upwind-differenced formula:

$$\begin{gathered} \left(f_\xi\right)_i = a_1 f_i + a_2 f_{i-1} + a_3 f_{i-2} \\ a_1 = \left(\Delta\xi_i^2 - \Delta\xi_{i-1}^2\right)/\Delta;\ a_2 = -\Delta\xi_i^2/\Delta;\ a_3 = \Delta\xi_{i-1}^2/\Delta \\ \Delta = \Delta\xi_i \Delta\xi_{i-1}(\Delta\xi_i + \Delta\xi_{i-1});\ \Delta\xi_i = \xi_i - \xi_{i-1};\ \Delta\xi_{i-1} = \xi_{i-1} - \xi_{i-2} \end{gathered} \tag{17}$$

When $i = 2$, the first-order formula with just two points is used, which results in the coefficients

$$a_1 = 1/\Delta\xi_2 = 1/(\xi_2 - \xi_1);\ a_2 = -a_1;\ a_3 = 0 \tag{18}$$

A linear blending of the first- and second-order formulas can also be used in a specified region. (See section 3.3 "Streamwise Gradients" for details.) Thus, the short notation $\{aQ\}$ used in equation (16) can be expanded in terms of the coefficients given above.

We define a solution vector $\{S\} = \{F, L, H, I\}^T$. Because the equations are nonlinear in $\{S\}$, Newton linearization is used to convert the system to a linear matrix inversion problem. If the superscript n denotes the current iteration stage, then we define $\{\delta S\}$ as

$$\{\delta S\} = S^n - S^{n-1} \tag{19}$$

A linear system is now set up to solve for $\{\delta S\}$ in terms of the solution at iteration level $n-1$. For example, a term that involves $(F^n)^2$ is written as

$$(F^n)^2 = \left(F^{n-1} + \delta F\right)^2 \approx \left(F^{n-1}\right)^2 + 2F^{n-1}\,\delta F \tag{20}$$

In the following equation set, the superscript $n-1$ is dropped and is taken to imply the known values of $\{S\}$ at iteration $n-1$. A few examples of the linearized formulas with this notation are given below:

$$\begin{aligned} (F^n)^2 &= F^2 + 2F\,\delta F \\ F_\xi^n &= F_\xi + a_1 \delta F \\ (FH)_\xi^n &= (FH)_\xi + a_1(H\delta F + F\delta H) \\ F^n F_\xi^n &= FF_\xi + \delta F(a_1 F + F_\xi) \end{aligned} \tag{21}$$

2.3 Linearized System

The system is explicit in ξ because of the choice of the finite-differencing scheme and is implicit in the surface-normal direction. The linearized system is represented at location i, which corresponds to the solution at iteration level n as

$$\left[\cdots\ a_{l,m}^k\ b_{l,m}^k \cdots\right] \left\{\delta S_l^k\right\} = \left\{r_l^k\right\} \tag{22}$$

where $a_{l,m}^k$ and $b_{l,m}^k$ are elements of the (4×4) blocks in the diagonal and superdiagonal locations of the linearized block-bidiagonal system. The superscript k denotes that the

discretization corresponds to the midpoint of k and $k-1$ points. The index l varies from 1 to 4, depending on which element of equation (14) is being discretized; m varies from 1 to 4, depending on which element of $\{\delta S\}$ it multiplies. The (4×4) blocks $\left[a^k_{l,m}\right]$ and $\left[b^k_{l,m}\right]$ are the only nonzero blocks in the system above because of the two-point compact scheme in the k direction. The (4×1) vector $\left\{r^k_l\right\}$ corresponds to the residual of equation (14), based on the solution $\{S\}$ at iteration $n-1$.

Let us write down the discretization of the first element of the system represented by equation (14), which can be written as

$$(F)_k - (F)_{k-1} - \frac{\Delta\zeta_k}{2}(L_k) - \frac{\Delta\zeta_k}{2}(L_{k-1}) + \frac{\Delta\zeta_k^2}{12}\left\{\frac{1}{l_1}\left[F\left(2\xi F_\xi + \beta F\right) + L(w - l_1') - \beta H\right]\right\}_k - \frac{\Delta\zeta_k^2}{12}\left\{\frac{1}{l_1}\left[F\left(2\xi F_\xi + \beta F\right) + L(w - l_1') - \beta H\right]\right\}_{k-1} = 0 \tag{23}$$

where

$$\Delta\zeta_k = \zeta_k - \zeta_{k-1} \tag{24}$$

We can now construct the elements of the blocks $\left[a^k_{l,m}\right]$, $\left[b^k_{l,m}\right]$, and $\left\{r^k_l\right\}$ for the case $l = 1$ from above by using the linearization procedure explained earlier. For example, the coefficient a^k_{11} is the coefficient of δF_{k-1} (from the first element of eq. (11)), which is discretized at $\left(k - \frac{1}{2}\right)$, and b^k_{11} is the corresponding coefficient of δF_k.

$$\begin{aligned} a_{11} &= -1 - c_{2k}(e_{11})_{k-1} \\ a_{12} &= -c_{1k} - c_{2k}(e_{12})_{k-1} \\ a_{13} &= -c_{2k}(e_{13})_{k-1} \\ a_{14} &= 0 \end{aligned} \tag{25}$$

$$
\begin{aligned}
b_{11} &= 1 + c_{2k}(e_{11})_k \\
b_{12} &= -c_{1k} + c_{2k}(e_{12})_k \\
b_{13} &= c_{2k}(e_{13})_k \\
b_{14} &= 0
\end{aligned}
\tag{26}
$$

$$
r_1 = -F_k + F_{k-1} + c_{1k}(L_k + L_{k-1}) - c_{2k}(q_{11})_k + c_{2k}(q_{11})_{k-1} \tag{27}
$$

$$
\begin{aligned}
c_{1k} &= \frac{\Delta\zeta_k}{2} \\
c_{2k} &= \frac{\Delta\zeta_k^2}{12}
\end{aligned}
\tag{28}
$$

$$
\begin{aligned}
e_{11} &= \frac{1}{l_1}\left[2\beta F + 2\xi\left(a_1 F + F_\xi\right)\right] \\
e_{12} &= \left(w - l_1'\right)/l_1 \\
e_{13} &= -\beta/l_1
\end{aligned}
\tag{29}
$$

$$
q_{11} = \frac{1}{l_1}\left[F\left(2\xi F_\xi + \beta F\right) + L\left(w - l_1'\right) - \beta H\right] \tag{30}
$$

Similar expressions can be derived from the remaining three elements of the system that are represented by equations (6)–(8). The expressions for these elements of $\left[a_{l,m}^k\right]$, $\left[b_{l,m}^k\right]$, and $\left\{r_l^k\right\}$ are given below, preceded by the corresponding discretized equations.

$$
\begin{aligned}
&(Fw - l_1 L)_k - (Fw - l_1 L)_{k-1} - \frac{\Delta\zeta_k}{2}\left\{-F^2(1+\beta) - 4\xi F F_\xi + \beta H\right\}_k \\
&\quad - \frac{\Delta\zeta_k}{2}\left\{-F^2(1+\beta) - 4\xi F F_\xi + \beta H\right\}_{k-1} \\
&\quad + \frac{\Delta\zeta_k^2}{12}\left\{-2FL(1+\beta) - 4\xi\left(FL_\xi + LF_\xi\right) + \beta I\right\}_k \\
&\quad - \frac{\Delta\zeta_k^2}{12}\left\{-2FL(1+\beta) - 4\xi\left(FL_\xi + LF_\xi\right) + \beta I\right\}_{k-1} = 0
\end{aligned}
\tag{31}
$$

$$
\begin{aligned}
a_{21} &= -w_{k-1} - c_{1k}(e_{21})_{k-1} - c_{2k}(e_{22})_{k-1} \\
a_{22} &= (l_1)_{k-1} - c_{2k}(e_{21})_{k-1} \\
a_{23} &= -c_{1k}\beta \\
a_{24} &= -c_{2k}\beta
\end{aligned}
\tag{32}
$$

$$
\begin{aligned}
b_{21} &= w_k - c_{1k}(e_{21})_k + c_{2k}(e_{22})_k \\
b_{22} &= (-l_1)_k + c_{2k}(e_{21})_k \\
b_{23} &= -c_{1k}\beta \\
b_{24} &= c_{2k}\beta
\end{aligned}
\tag{33}
$$

$$
r_2 = -(q_{21})_k + (q_{21})_{k-1} + c_{1k}(q_{22})_k + c_{1k}(q_{22})_{k-1} - c_{2k}(q_{23})_k + c_{2k}(q_{23})_{k-1} \tag{34}
$$

$$
\begin{aligned}
e_{21} &= -2F(1+\beta) - 4\xi\left(a_1 F + F_\xi\right) \\
e_{22} &= -2L(1+\beta) - 4\xi\left(a_1 L + L_\xi\right)
\end{aligned}
\tag{35}
$$

$$
\begin{aligned}
q_{21} &= Fw - l_1 L \\
q_{22} &= -F^2(1+\beta) - 4\xi F F_\xi + \beta H \\
q_{23} &= -2FL(1+\beta) - 4\xi\left(FL_\xi + LF_\xi\right) + \beta I
\end{aligned}
\tag{36}
$$

$$
\begin{aligned}
(H)_k - (H)_{k-1} - \frac{\Delta\zeta_k}{2}(I_k) - \frac{\Delta\zeta_k}{2}(I_{k-1}) + \frac{\Delta\zeta_k^2}{12}\left\{\frac{1}{l_2}\left[2\xi F H_\xi - \alpha l_1 L^2 + I(w - l_2')\right]\right\}_k \\
- \frac{\Delta\zeta_k^2}{12}\left\{\frac{1}{l_2}\left[2\xi F H_\xi - \alpha l_1 L^2 + I(w - l_2')\right]\right\}_{k-1} = 0
\end{aligned}
\tag{37}
$$

$$
\begin{aligned}
a_{31} &= -c_{2k}(e_{31})_{k-1} \\
a_{32} &= -c_{2k}(e_{32})_{k-1} \\
a_{33} &= -1 - c_{2k}(e_{33})_{k-1} \\
a_{34} &= -c_{1k} - c_{2k}(e_{34})_{k-1}
\end{aligned}
\tag{38}
$$

$$
\begin{aligned}
b_{31} &= c_{2k}(e_{31})_k \\
b_{32} &= c_{2k}(e_{32})_k \\
b_{33} &= 1 + c_{2k}(e_{33})_k \\
b_{34} &= -c_{1k} + c_{2k}(e_{34})_k
\end{aligned}
\tag{39}
$$

$$
r_3 = -H_k + H_{k-1} + c_{1k}(I_k + I_{k-1}) - c_{2k}(q_{31})_k + c_{2k}(q_{31})_{k-1} \tag{40}
$$

$$
\begin{aligned}
e_{31} &= \frac{1}{l_2}\left[2\xi H_\xi\right] \\
e_{32} &= \frac{1}{l_2}[-2\alpha l_1 L] \\
e_{33} &= \frac{1}{l_2}[2\xi F a_1] \\
e_{34} &= \left(w - l_2'\right)/l_2
\end{aligned}
\tag{41}
$$

$$
q_{31} = \frac{1}{l_2}\left[2\xi F H_\xi - \alpha l_1 L^2 + I\left(w - l_2'\right)\right] \tag{42}
$$

$$
\begin{aligned}
&(Hw - l_2 I)_k - (Hw - l_2 I)_{k-1} \\
&- \frac{\Delta\zeta_k}{2}\Big\{-2\xi(FH)_\xi - FH + \alpha l_1 L^2\Big\}_k - \frac{\Delta\zeta_k}{2}\Big\{-2\xi(FH)_\xi - FH + \alpha l_1 L^2\Big\}_{k-1} \\
&+ \frac{\Delta^2\zeta_k}{12}\Big\{-2\xi(FI + HL)_\xi - (FI + HL) + 2\alpha L\big[F\big(2\xi F_\xi + \beta F\big) + Lw - \beta H\big]\Big\}_k \\
&- \frac{\Delta^2\zeta_k}{12}\Big\{-2\xi(FI + HL)_\xi - (FI + HL) + 2\alpha L\big[F\big(2\xi F_\xi + \beta F\big) + Lw - \beta H\big]\Big\}_{k-1} \\
&= 0
\end{aligned}
\tag{43}
$$

$$
\begin{aligned}
a_{41} &= -c_{1k}(e_{41})_{k-1} - c_{2k}(e_{42})_{k-1} \\
a_{42} &= -c_{1k}(e_{43})_{k-1} - c_{2k}(e_{44})_{k-1} \\
a_{43} &= -w_{k-1} - c_{1k}(e_{45})_{k-1} - c_{2k}(e_{46})_{k-1} \\
a_{44} &= (l_2)_{k-1} - c_{2k}(e_{45})_{k-1}
\end{aligned}
\tag{44}
$$

$$
\begin{aligned}
b_{41} &= -c_{1k}(e_{41})_k + c_{2k}(e_{42})_k \\
b_{42} &= -c_{1k}(e_{43})_k + c_{2k}(e_{44})_k \\
b_{43} &= w_k - c_{1k}(e_{45})_k + c_{2k}(e_{46})_k \\
b_{44} &= (-l_2)_k + c_{2k}(e_{45})_k
\end{aligned}
\tag{45}
$$

$$
r_4 = -(q_{41})_k + (q_{41})_{k-1} + c_{1k}\{q_{42}\}_k + c_{1k}\{q_{42}\}_{k-1} - c_{2k}\{q_{43}\}_k + c_{2k}\{q_{43}\}_{k-1} \tag{46}
$$

$$
\begin{aligned}
e_{41} &= -2\xi\left(H_\xi + Ha_1\right) - H \\
e_{42} &= -2\xi\left(I_\xi + Ia_1\right) - I + 2\alpha L\left[2\xi\left(a_1 F + F_\xi\right) + 2\beta F\right] \\
e_{43} &= 2\alpha l_1 L \\
e_{44} &= -2\xi\left(H_\xi + Ha_1\right) - H + 4\alpha wL + 2\alpha\left[F\left(2\xi F_\xi + \beta F\right) - \beta H\right] \\
e_{45} &= -2\xi\left(F_\xi + Fa_1\right) - F \\
e_{46} &= -2\xi\left(L_\xi + La_1\right) - L - 2\alpha\beta L
\end{aligned}
\tag{47}
$$

$$
\begin{aligned}
q_{41} &= Hw - l_2 I \\
q_{42} &= -2\xi(FH)_\xi - FH + \alpha l_1 L^2 \\
q_{43} &= -2\xi(FI + HL)_\xi - (FI + HL) + 2\alpha L\left[F\left(2\xi F_\xi + \beta F\right) + Lw - \beta H\right]
\end{aligned}
\tag{48}
$$

The resulting system is block tridiagonal of the order $(4 \times ke \times ke)$, where ke is the total number of points in the normal direction. The system is block tridiagonal because of the shift of rows that results from the implementation of the boundary conditions, as explained in references 2 and 3. Each row of the system at level k can be written as shown:

$$
\left[\cdots \begin{pmatrix} a_{11}^k & a_{12}^k & a_{13}^k & a_{14}^k \\ a_{21}^k & a_{22}^k & a_{23}^k & a_{24}^k \\ 0 & 0 & 0 & 0 \\ 0 & 0 & 0 & 0 \end{pmatrix} \begin{pmatrix} b_{11}^k & b_{12}^k & b_{13}^k & b_{14}^k \\ b_{21}^k & b_{22}^k & b_{23}^k & b_{24}^k \\ a_{31}^{k+1} & a_{32}^{k+1} & a_{33}^{k+1} & a_{34}^{k+1} \\ a_{41}^{k+1} & a_{42}^{k+1} & a_{43}^{k+1} & a_{44}^{k+1} \end{pmatrix} \begin{pmatrix} 0 & 0 & 0 & 0 \\ 0 & 0 & 0 & 0 \\ b_{31}^{k+1} & b_{32}^{k+1} & b_{33}^{k+1} & b_{34}^{k+1} \\ b_{41}^{k+1} & b_{42}^{k+1} & b_{43}^{k+1} & b_{44}^{k+1} \end{pmatrix} \cdots \right]
$$

$$
\vdots \qquad\qquad \vdots
$$

$$
\begin{Bmatrix} \delta F_k \\ \delta L_k \\ \delta H_k \\ \delta I_k \end{Bmatrix} = \begin{Bmatrix} r_1^k \\ r_2^k \\ r_3^{k+1} \\ r_4^{k+1} \end{Bmatrix}
$$

$$
\vdots \qquad\qquad \vdots
\tag{49}
$$

The boundary conditions imposed at the wall and the boundary-layer edge modify the system. For the adiabatic wall condition, the first row of the block tridiagonal system is modified as

$$\left[\begin{pmatrix} 1 & 0 & 0 & 0 \\ 0 & 0 & 0 & 1 \\ a^2_{31} & a^2_{32} & a^2_{33} & a^2_{34} \\ a^2_{41} & a^2_{42} & a^2_{43} & a^2_{44} \end{pmatrix} \begin{pmatrix} 0 & 0 & 0 & 0 \\ 0 & 0 & 0 & 0 \\ b^2_{31} & b^2_{32} & b^2_{33} & b^2_{34} \\ b^2_{41} & b^2_{42} & b^2_{43} & b^2_{44} \end{pmatrix} \cdots \right] \begin{Bmatrix} \delta F_1 \\ \delta L_1 \\ \delta H_1 \\ \delta I_1 \\ \vdots \end{Bmatrix} = \begin{Bmatrix} 0 \\ 0 \\ r^2_3 \\ r^2_4 \\ \vdots \end{Bmatrix} \tag{50}$$

Similarly, at the boundary-layer edge, the edge velocity and temperature are prescribed; this modifies the last row of the system as shown below:

$$\left[\cdots \begin{pmatrix} a^{ke}_{11} & a^{ke}_{12} & a^{ke}_{13} & a^{ke}_{14} \\ a^{ke}_{21} & a^{ke}_{22} & a^{ke}_{23} & a^{ke}_{24} \\ 0 & 0 & 0 & 0 \\ 0 & 0 & 0 & 0 \end{pmatrix} \begin{pmatrix} b^{ke}_{11} & b^{ke}_{12} & b^{ke}_{13} & b^{ke}_{14} \\ b^{ke}_{21} & b^{ke}_{22} & b^{ke}_{23} & b^{ke}_{24} \\ 1 & 0 & 0 & 0 \\ 0 & 0 & 1 & 0 \end{pmatrix} \right] \begin{Bmatrix} \vdots \\ \delta F_{ke} \\ \delta L_{ke} \\ \delta H_{ke} \\ \delta I_{ke} \end{Bmatrix} = \begin{Bmatrix} \vdots \\ r^{ke}_1 \\ r^{ke}_2 \\ 0 \\ 0 \end{Bmatrix} \tag{51}$$

2.4 Inversion of the System

At any location i, assume that we have an initial estimate of the solution profiles F and H as a function of ζ and their derivatives F' and H'. Also assume that we have an estimate of the transformed values of w and the viscosity ratios l, l_1, l_2 and assume that the edge conditions are known. With the knowledge of the upstream profiles, the system described by equation (49) is defined. Inversion of this block-tridiagonal system by standard routines yields the solution $\delta F, \delta L, \delta H$ and δI. However, this solution is based on the linearized formula. The solution is updated, and the calculation is repeated until convergence is achieved.

Subsequent to convergence at a given station, the solution is advanced to the next step in the ξ direction. The solution profiles at two upstream stations are saved at any given streamwise station. Lack of convergence is indicative of incipient boundary-layer separation. This can be confirmed by looking at the upstream history of $C_{f,e}$.

3. PROGRAM DESCRIPTION

3.1 Edge Conditions from Inviscid Inputs

The program can be run in SI or US units. The basic free-stream inputs are M_∞, P_0, and T_0 or M_∞, P_∞, and T_∞. The isentropic formula

$$\left(\frac{T_0}{T_\infty}\right) = \left(1 + \frac{\gamma - 1}{2} M_\infty^2\right); \quad \left(\frac{P_0}{P_\infty}\right) = \left(\frac{T_0}{T_\infty}\right)^{\left(\frac{1}{\gamma - 1}\right)} \tag{52}$$

supplies the missing quantities. The normalized pressure quantities are

$$p_0 = \frac{P_0}{\rho_\infty U_\infty^2}; \quad p_\infty = \frac{P_\infty}{\rho_\infty U_\infty^2} \tag{53}$$

Note that pressure quantities are normalized by $\rho_\infty U_\infty^2$ and that normalized quantities are indicated by lower case. The gas properties N_{Pr} and γ and the gas constant R are input. The reference temperature is defined as

$$T_{\text{ref}} = \frac{U_\infty^2}{[\gamma/(\gamma - 1)]R} \tag{54}$$

The normalized total pressure and temperature values are, then,

$$t_0 = \frac{1}{2} + \frac{1}{(\gamma - 1)M_\infty^2}; \quad t_\infty = \frac{1}{(\gamma - 1)M_\infty^2} \tag{55}$$

To calculate boundary-layer edge velocity, the conditions on body surface must be calculated. If no shock is present between the free stream and the body, the normalized total pressure at the boundary-layer edge p_{10} is equal to p_0. If a shock is present, the condition behind the shock is calculated from the oblique shock-wave formula, based on the input shock-wave angle. If we assume for now that no shock curvature is present (hence, no variable entropy effects are present), then the computation requires the value of the shock

wave-angle θ_s as an input quantity. With M_θ defined as $M_\infty^2 \sin^2 \theta_s$, the normalized total pressure behind the shock is evaluated from

$$p_{10} = p_0 \left\{ \frac{(\gamma+1)M_\theta}{(\gamma-1)M_\theta + 2} \right\}^{\frac{\gamma}{\gamma-1}} \left\{ \frac{(\gamma+1)}{2\gamma M_\theta - (\gamma-1)} \right\}^{\frac{1}{\gamma-1}} \tag{56}$$

The edge velocity normalized by the free-stream velocity is obtained as

$$u_e = \sqrt{2t_0 \left\{ 1 - \left(\frac{p_e}{p_{10}} \right)^{\frac{\gamma-1}{\gamma}} \right\}} \tag{57}$$

where p_e is the input normalized boundary-layer edge pressure. The normalized edge temperature is then

$$t_e = t_0 - \frac{1}{2} u_e^2 \tag{58}$$

The edge density becomes

$$\rho_e = \frac{\gamma p_e}{(\gamma-1)t_e} \tag{59}$$

The edge viscosity μ_e (normalized by the reference viscosity μ^*_{ref} evaluated at T_{ref}) is calculated as a function of t_e by using either the Sutherland law

$$\begin{gathered} \mu_e = \frac{\mu_e^*}{\mu_{\text{ref}}^*} = t_e^{1.5} \left(\frac{1+t_r}{t_e+t_r} \right) \\ \mu_{\text{ref}}^* = 1.458 \times 10^{-6} \frac{T_{\text{ref}}^{1.5}}{T_{\text{ref}} + T_r} \ \text{Pa} \cdot \text{sec} \quad \text{or} \\ \mu_{\text{ref}}^* = 2.27 \times 10^{-8} \frac{T_{\text{ref}}^{1.5}}{T_{\text{ref}} + T_r} \left(\frac{\text{lb} \cdot \text{sec}}{\text{ft}^2} \right) \\ t_r = T_r / T_{\text{ref}}; \quad T_r = 110.33 \text{ K or } 198.6^\circ\text{R} \end{gathered} \tag{60}$$

or the power law

$$\begin{gathered} \mu_e = t_e^{c_2} \\ \mu_{\text{ref}}^* = c_1 T_{\text{ref}}^{c_2} \end{gathered} \tag{61}$$

$$c_1 = 5.0231 \times 10^{-7} \text{ (SI units)}; \quad c_1 = 7.1738 \times 10^{-9} \text{ (US units)}; \quad c_2 = 0.647$$

The program input is in the form of dimensional edge-pressure distribution at surface locations not necessarily coincident with the actual computation locations. The input quantities are interpolated to the required locations with a piecewise polynomial fit.

3.2 Normal Grid Distribution

Because the Pade formula is a compact scheme that is based on the solution variables and their derivatives at the two points that span the local cell center, a stretched grid can be employed without degradation of the fourth-order accuracy of the method. For laminar flows, no stretching is required in the transformed plane. However, for turbulent flows the large velocity gradients in the inner layer and relatively smaller gradients in the outer portion of the boundary layer require that some form of boundary-layer stretching be employed.

The original code employed an exponential stretching in the normal direction such that the ratio k_s is a constant.

$$\frac{\Delta\zeta_{k+1}}{\Delta\zeta_k} = \frac{\zeta_{k+1} - \zeta_k}{\zeta_k - \zeta_{k-1}} = k_s \tag{62}$$

The normal grid distribution is then obtained as

$$\zeta_k = \zeta_{ke}\left(\frac{k_s^{k-1} - 1}{k_s^{ke-1} - 1}\right) \qquad (k_s > 1) \tag{63}$$

The input options to generate the normal grid in VGBLP were: specify k_s, ζ_{ke}, and ke (`IGEOM = 1` in the program) or specify $\Delta\zeta_2 = \zeta_2 - \zeta_1$, ζ_{ke}, and ke (`IGEOM = 2` in the program). This type of exponential distribution sometimes results in inadequate resolution near the edge of turbulent boundary layers because of the large ζ values required. This inadequate resolution in turn produces large truncation errors, especially when points are added in the normal direction to account for boundary-layer growth.

In the program BL2D, a two-part mesh distribution is implemented. (See fig. 2.) The mesh distribution in the inner part (delineated by $0 \leq \zeta \leq \zeta_i$; $1 \leq k \leq ki$) follows the same exponential distribution as in VGBLP (eq. (63)). The input parameters are ζ_i, k_s, and ki (computer variable names `ZI`, `AK`, and `NZI`). The mesh distribution in the outer part is uniform in ζ, based on ζ_e, ζ_i, and $(ke - ki)$ (computer variable names `ZMAX`, `ZI`, and `(NZ-NZI)`). Obviously, the five input quantities (k_s, ζ_i, ki, ζ_e, and ke) must be carefully chosen to avoid abrupt changes in the mesh step size at $k = ki$. The program `gridcheck.f` can be used to arrive at the optimum distribution before running the boundary-layer program. To set a single exponential stretching for the entire region, set $\zeta_i = \zeta_e$ and $ke = ki$. The advantage of this two-part distribution is evident when points must be added to accommodate boundary-layer growth.

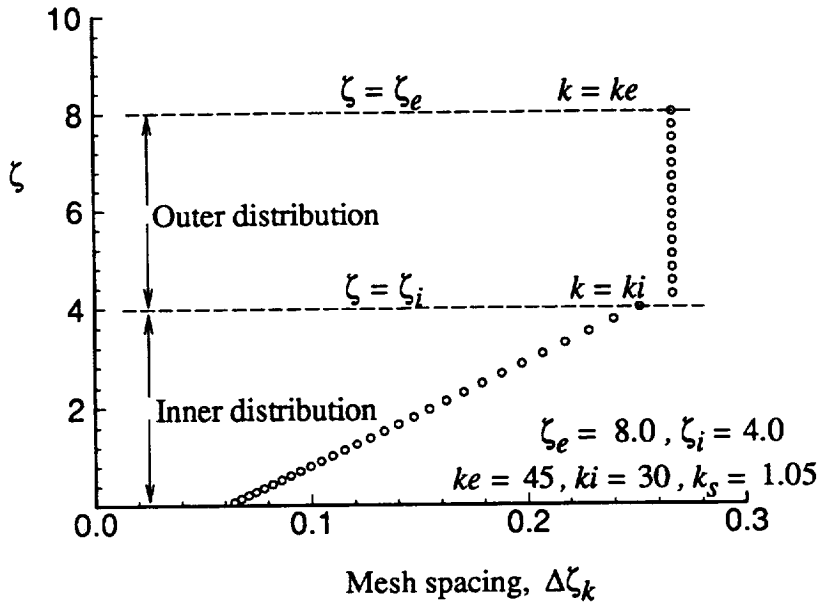

Figure 2. Two-part mesh distribution used in program.

In the event that the user wants to implement a different normal grid distribution, this can be set up easily in `subroutine grid`. The addition of points to cover boundary-layer

growth is done in `subroutine add`. This addition of points is also easily modifiable if the user wants to change the present logic (i.e., each new point is added at a constant step size).

3.3 Streamwise Gradients

The streamwise grid distribution is specified in the input by means of the number of steps and the corresponding step sizes Δs^*. The streamwise gradient is calculated based on a second-order formula that can be blended into a first-order formula for a certain region. The transformed streamwise coordinate ξ is

$$\xi = \int_0^s \rho_e u_e \mu_e (r_w)^{2j} \, ds \tag{64}$$

The ξ derivative from a three-point upwind-differenced formula (valid for `i` $\geq$ `iord2`) is

$$\begin{gathered} (f_\xi)_i = a_1 f_i + a_2 f_{i-1} + a_3 f_{i-2} \\ a_1 = (\Delta\xi_i^2 - \Delta\xi_{i-1}^2)/\Delta; \; a_2 = -\Delta\xi_i^2/\Delta; \; a_3 = \Delta\xi_{i-1}^2/\Delta \\ \Delta = \Delta\xi_i \Delta\xi_{i-1}(\Delta\xi_i + \Delta\xi_{i-1}); \; \Delta\xi_i = \xi_i - \xi_{i-1}; \; \Delta\xi_{i-1} = \xi_{i-1} - \xi_{i-2} \end{gathered} \tag{65}$$

When $i \leq$ `iord1`, the first-order formula with just two points is used, which results in the coefficients

$$a_1 = 1/\Delta\xi_2 = 1/(\xi_2 - \xi_1); \; a_2 = -a_1; \; a_3 = 0 \tag{66}$$

For `iord1` $\leq i \leq$ `iord2`, the first-order formula is blended to the second-order formula with a linear variation.

3.4 Starting Solutions

Depending on the geometry, the starting solution is generated from the similarity assumption (for a body with a sharp tip or leading edge) or from the equations that are valid for a two-dimensional stagnation point (for a body with a blunt tip or leading edge).

The similarity solution is obtained by dropping all streamwise gradient terms. In the program, this step is done by setting the coefficients a_1, a_2, and a_3 to 0.

3.5 Implementation of Boundary Conditions

Mass injection or suction at the wall is input into the code in the form of the normal momentum $\rho_w^* w_w^*$ (in dimensional units, (Pa·s)/m or (lb·s)/ft^3). These values are first interpolated to the boundary-layer grid locations from the input distribution. The value of the transformed normal velocity w at the wall is obtained from the relation

$$w_1 = \frac{\sqrt{2\xi}(\rho_w^* w_w^*)\sqrt{Re_{\text{ref}}}}{\mu_e r_w^{*j}(\rho_e^* u_e^*)} \tag{67}$$

The continuity equation (eq. 5, line 1) is integrated with the trapezoidal rule; the initial value is specified as shown above. A negative value for $\rho_w^* w_w^*$ indicates suction.

The energy boundary condition at the wall is specified in the input by selection of the variable `iwall`. A value of 0 indicates adiabatic wall conditions, and a value of 1 indicates that the wall temperature T_w is to be specified. A value of 2 indicates that the dimensional heat flux at the wall $\dot{q_w}^*$ in dimensional units (W/m^2 or Btu/ft^2·sec) is to be specified. In this case, the temperature gradient at the wall is specified in terms of the transformed variable $H_w{}'$ as

$$\frac{\dot{q}_w^*}{(U_\infty^2 \mu_{\text{ref}}^*)} = \dot{q}_w = -\frac{\rho_e \mu_e u_e t_e r_w^{*j}}{\sqrt{Re_{\text{ref}}}\sqrt{2\xi} N_{Pr}} l_w H_w' \tag{68}$$

Note that the input and output of heat flux in US units is in Btu/ft^2·sec. Within the program, the units of lb/(ft·sec) is used (1 Btu/ft^2·sec = 778.26 lb/(ft·sec)).

3.6 Variable Entropy Formulation

In the case of highly curved shocks in front of blunt bodies in high-speed flow, the change in edge conditions that results from the entropy layer may need to be taken into account.

A detailed discussion of the approach followed here is given in references 4 and 5. Briefly, this step involves an initial complete boundary-layer calculation that neglects this effect. Subsequently, from the boundary-layer solution information a mass balance is performed at each streamwise station to compute the radius of the corresponding stream tube at the shock location. The local shock angle and the corresponding post-shock edge conditions are computed from this calculation. The boundary-layer calculations are then repeated with the new edge conditions until the variable entropy convergence criterion is satisfied.

3.7 Transition Zone Modeling

The location of transition is either explicitly specified or calculated from the stability index parameter reaching a specified value. For details, refer to reference 3. This simple representation of transition onset can be replaced by a user-supplied model. The extent of the transition zone is calculated in the program by using a simple correlation that is based on the local Reynolds number or it can be explicitly specified. See references 1 and 4 for a complete description. The intermittency function Γ is used to characterize the transition zone and is calculated as a function of ξ. A Γ value of 1 signifies the beginning of the fully turbulent zone.

3.8 Turbulence Modeling

The algebraic turbulence models used in BL2D are described in references 1 and 4. Two choices are available: a general mixing length model (`KODVIS = 1`); or a two-layer eddy-viscosity model (`KODVIS = 2`). The intermittency factor, Γ, is multiplied by the ϵ/μ values and used to model the transitional zone. The program is designed to allow a user to implement any desired model, for example, two-equation closure models.

3.9 Internal Flows

These flows are treated in the same manner as external flows. The curvature terms will,

however, involve a change in the sign. If curvature terms are neglected, then the solution is identical to the external flow. If the curvature terms become significant, this indicates that the boundary-layer thickness values are significant enough to alter the inviscid pressures for an internal flow. This in turn indicates significant viscous-inviscid interaction. In view of this, for internal flow cases, computation should be done neglecting the curvature terms.

3.10 Output of Physical Quantities

The output of wall quantities and boundary-layer integrated parameters are determined based on user-selected codes. Solution profiles at any station can be output by enabling the corresponding flags. Details are given in chapter 5, entitled "User's Manual."

4. VALIDATION

Five cases are presented here to validate BL2D with VGBLP. These cases are identical to those presented in reference 1. Most capabilities of the code are covered between these cases. Because the results compare well, the author is confident that BL2D can effectively supersede VGBLP.

4.1 Case 1: Flow Past a Flat Plate at Mach 2.8

A sketch and description of the flow case and conditions are given in figure 3 and table 1. As indicated in the sketch, the flow has laminar, transitional, and turbulent regions. The thermal boundary condition at the wall is adiabatic.

The input boundary-layer edge conditions are constant and are specified in terms of two data points. The step size is variable and the solution is obtained at 62 stations.

The results from BL2D are compared with the VGBLP results for identical input conditions in figures 4–9. Figure 4 is a comparison of the skin-friction coefficient based on the edge conditions ($C_{f,e}$), 99.5–percent boundary-layer thickness (t^*), and displacement thickness (δ^*). Figure 5 is a close-up of the same results around the transition region $0 < x^* < 0.04$ m. These parameters are dependent on the wall gradients and the shape of the profiles. Excellent agreement has been obtained.

Figure 6 shows a comparison of the wall temperature ratio (T_w/T_0) and the streamwise intermittency parameter. Figures 7–9 are comparisons of the solution profiles F, H, and w at six locations in the flow (four in the turbulent region and one each in the laminar and transitional regions). Again, excellent agreement has been demonstrated.

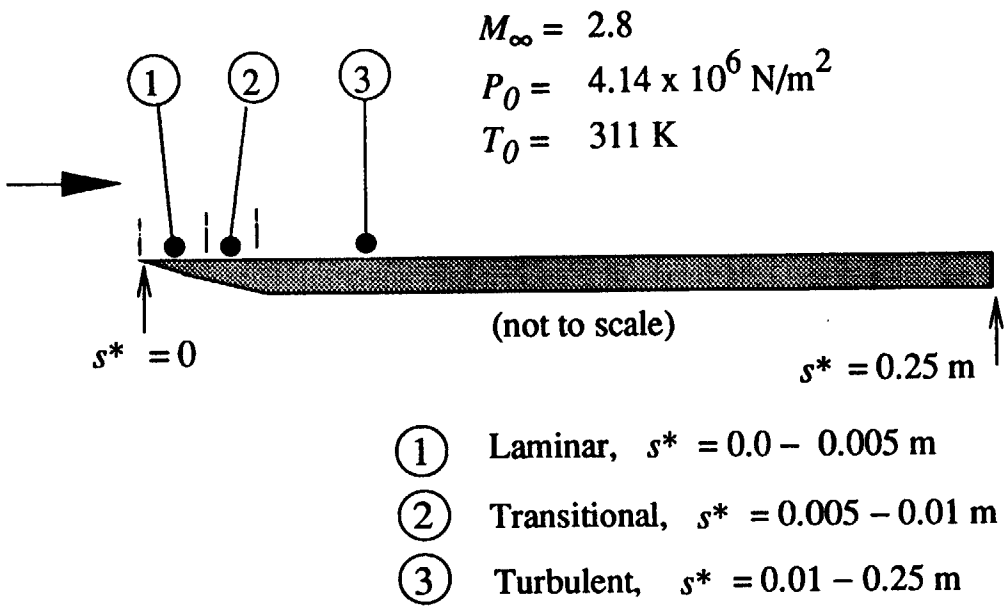

Figure 3. Case 1: geometry and conditions.

Table 1. Case 1: Description and Input Summary

```
Description
-----------

Case 1: Supersonic Flow over Flat Plate

Free-stream conditions
----------------------

M-inf = 2.8
P-tot = 4.14 x 10^6 N/m2
T-tot = 311 deg K

Wall conditions
---------------

Adiabatic wall (IWALL = 0)
No mass injection

Flow type
---------

No shock (WAVE = 0 deg)
2D (J = 0)
No stagnation point (IBODY = 2)
Constant entropy (IENTRO = 1)

Viscous terms
-------------

Laminar
Transitional (SMXTR = 2400); for s > 0.005 m
Turbulent (TLNGTH = 2); for s > 0.01 m

Other
-----

Body opening angle PHII = 0
Solution for 0 < s < 0.25 m at 62 stations
```

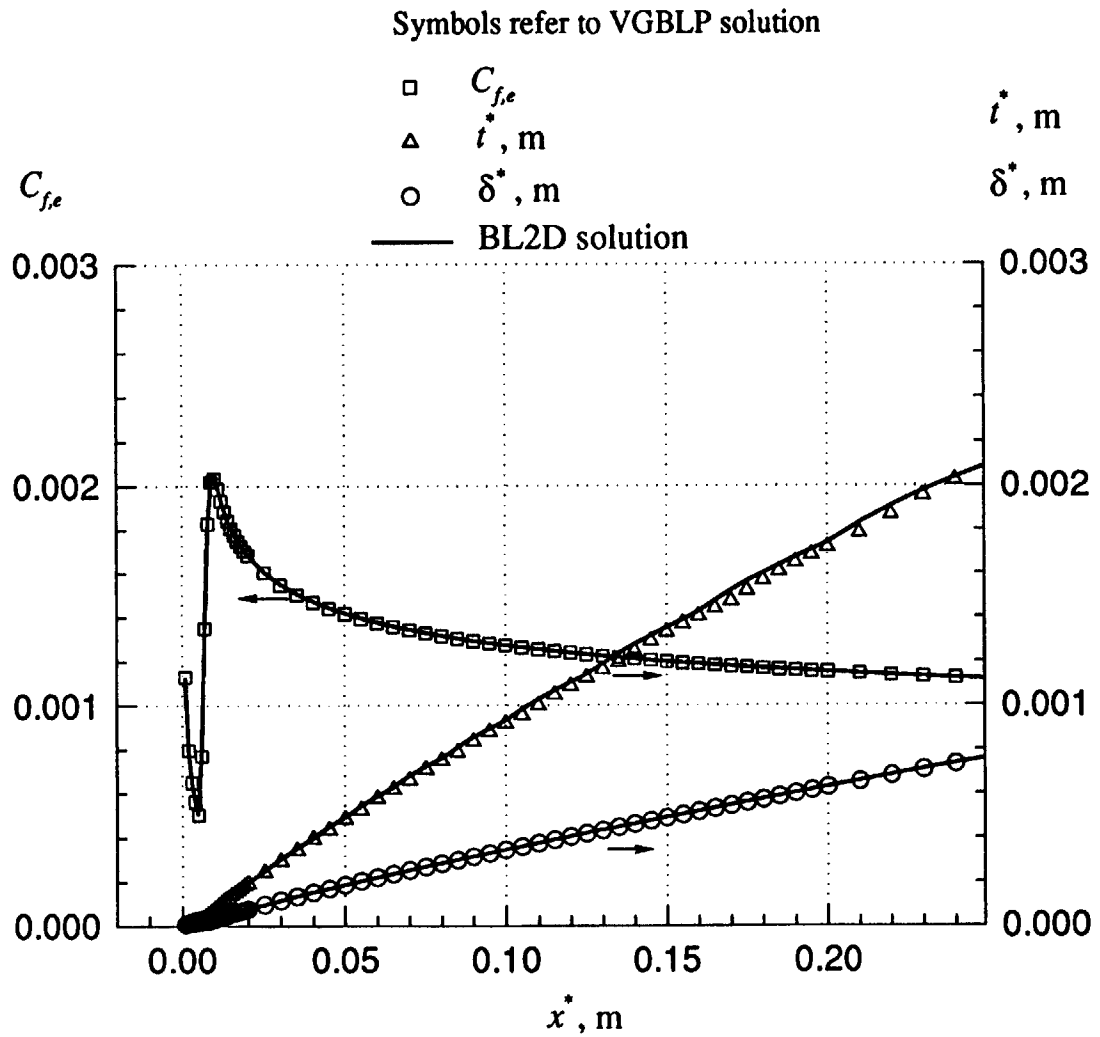

Figure 4. Case 1: comparison of BL2D and VGBLP solutions ($C_{f,e}$, t^*, δ^*).

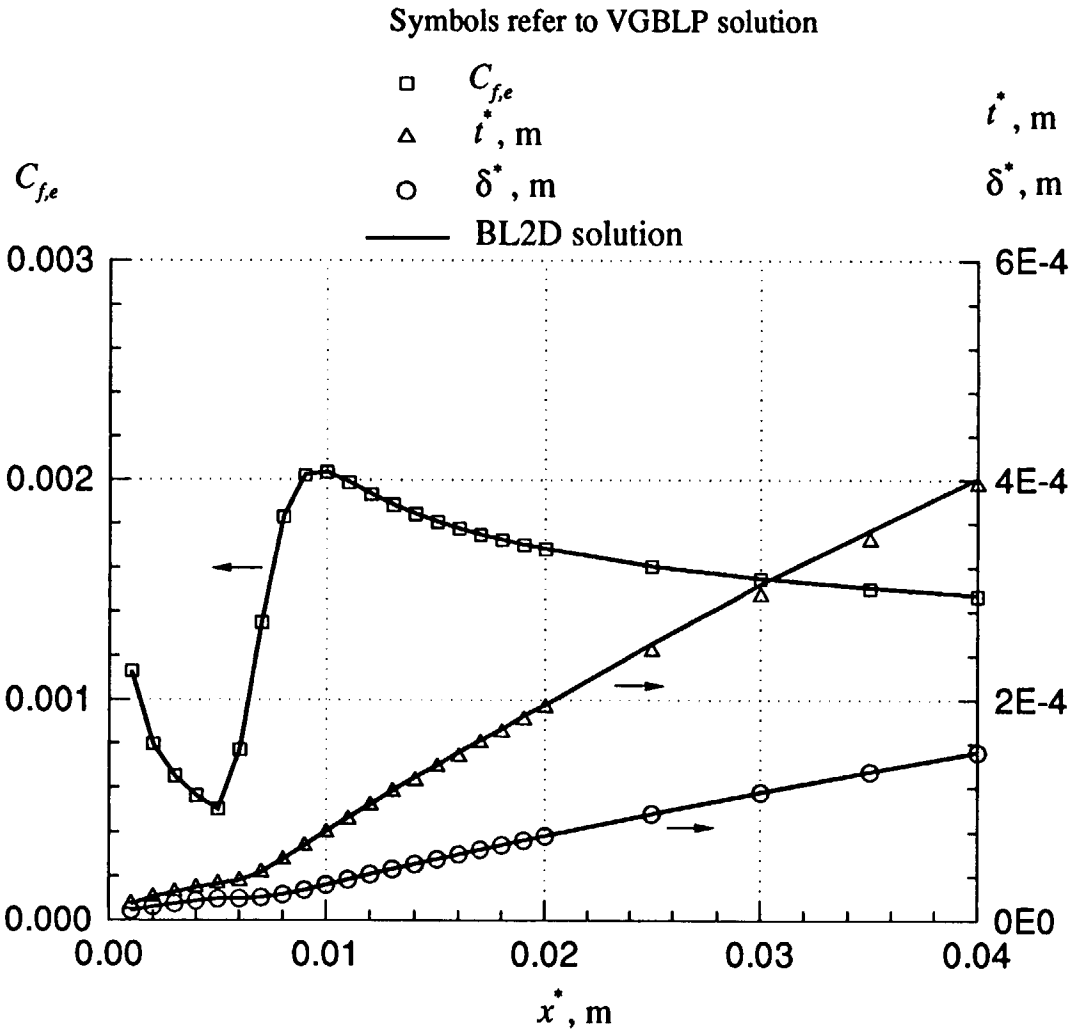

Figure 5. Case 1: comparison of BL2D and VGBLP solutions ($C_{f,e}$, t^*, δ^* (for $x^* < 0.04$)).

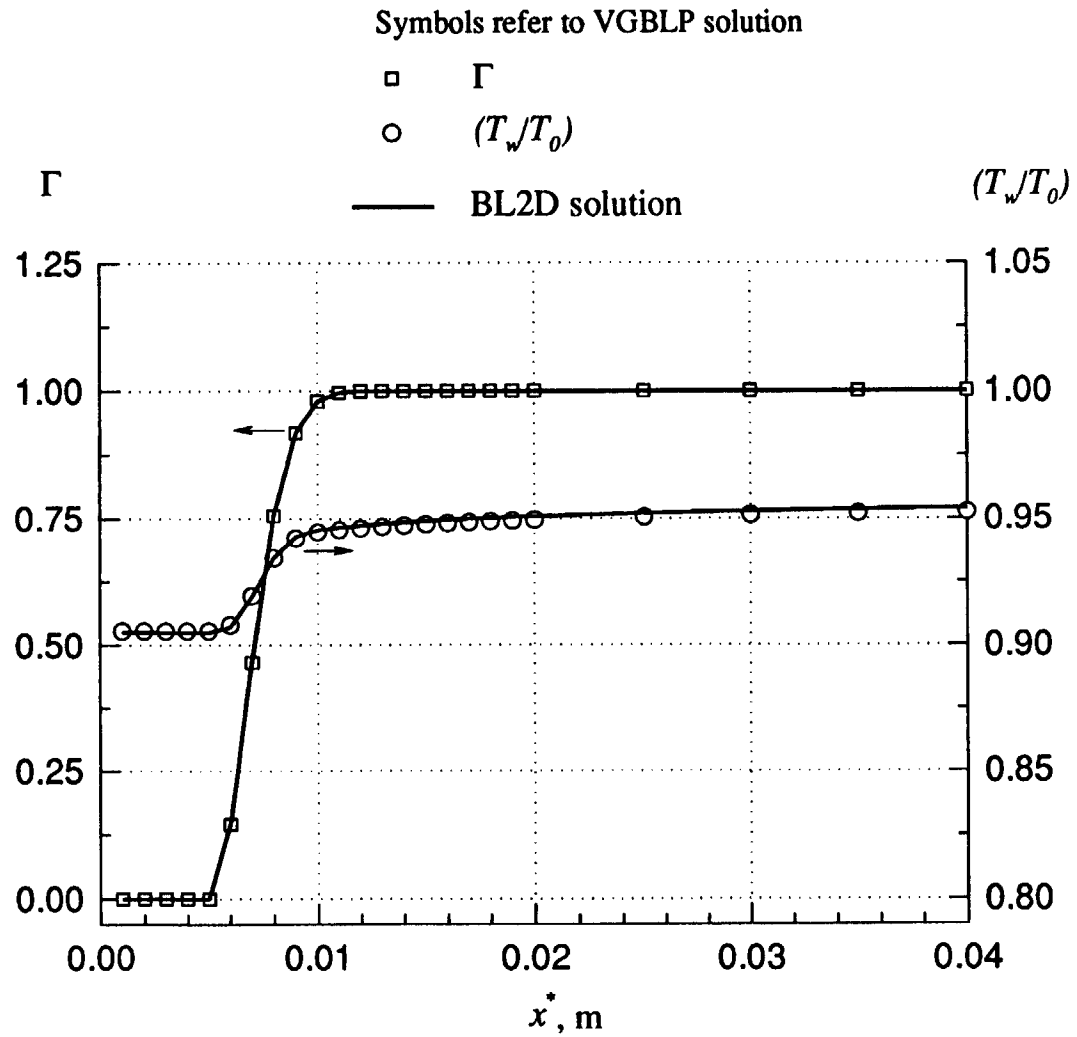

Figure 6. Case 1: comparison of BL2D and VGBLP solutions (Γ, (T_w/T_0)).

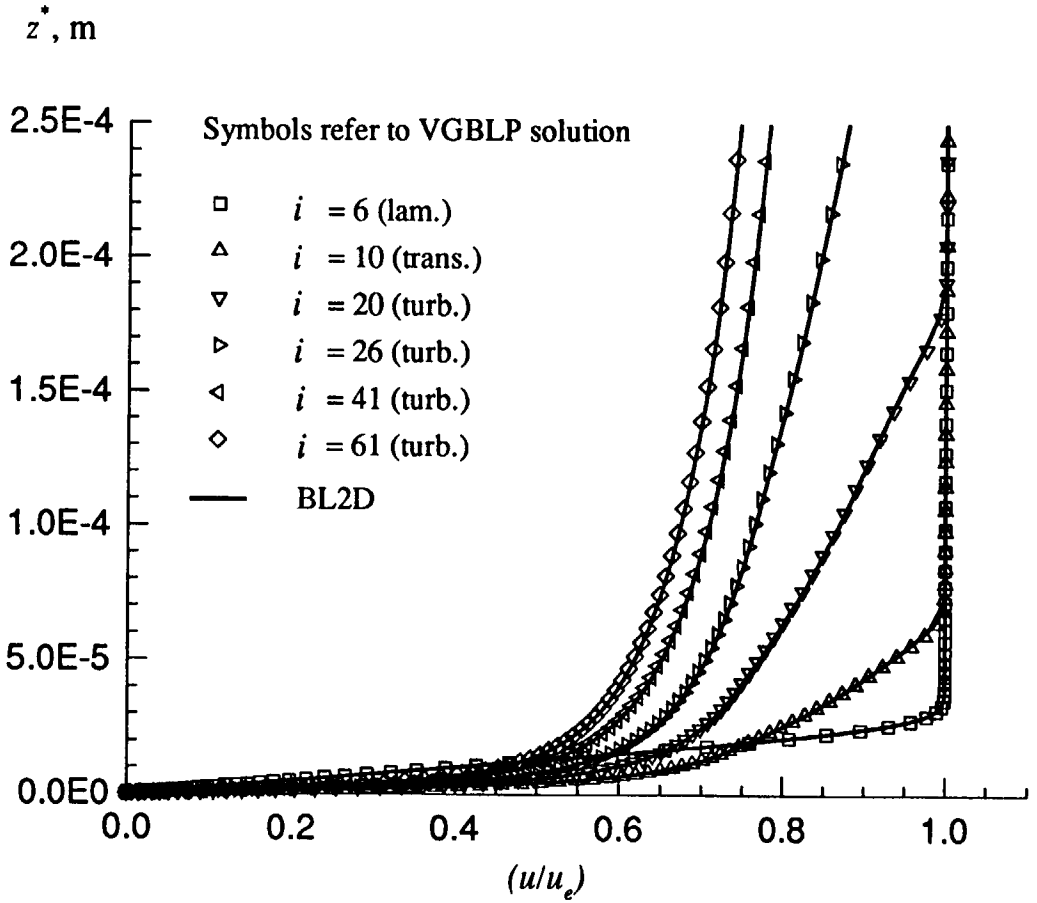

Figure 7. Case 1: comparison of BL2D and VGBLP solution profiles (u/u_e).

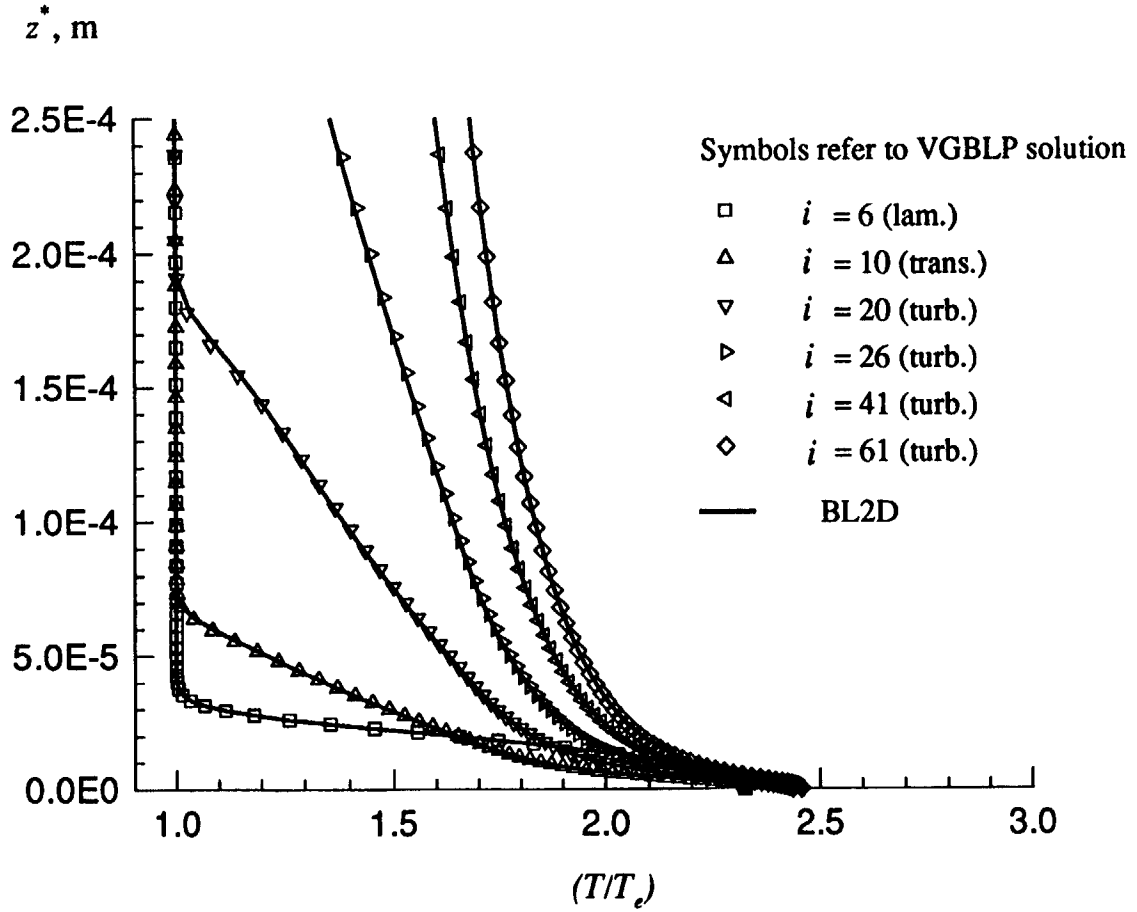

Figure 8. Case 1: comparison of BL2D and VGBLP solution profiles (T/T_e).

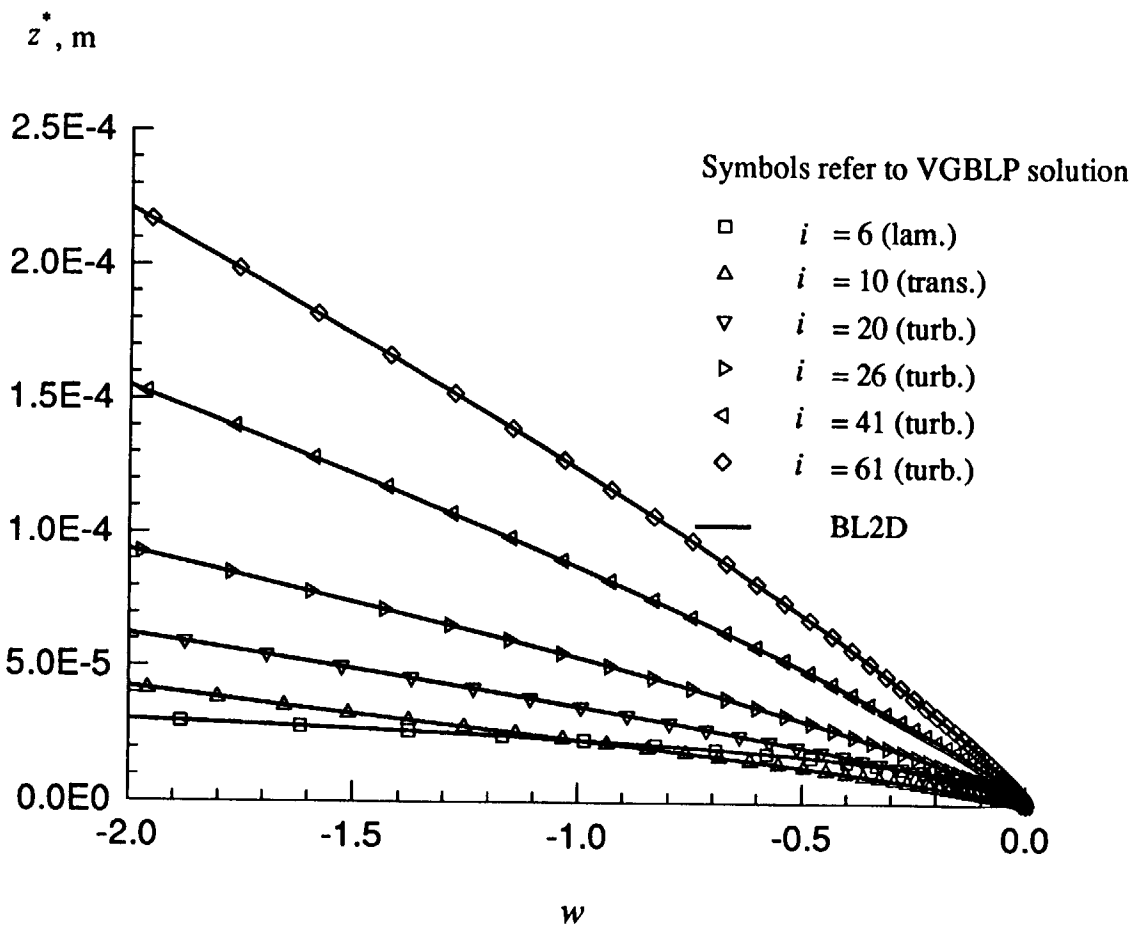

Figure 9. Case 1: comparison of BL2D and VGBLP solution profiles *(w)*.

4.2 Case 2: Flow Past a Waisted Body at Mach 1.7

This case involves a flow with an oblique shock that results from a sharp-tipped axisymmetric body; the resulting boundary layer has a pressure gradient of varying sign and magnitude. Figure 10 shows a sketch of the body and the variation of the surface pressure. The body has a short laminar region followed by a short transition region. The onset and the extent of transition are explicitly specified. Table 2 presents the flow and input details.

Figure 11 shows a comparison of the skin-friction coefficient based on edge conditions ($C_{f,e}$), 99.5–percent boundary-layer thickness (t^*), and displacement thickness (δ^*). Figure 12 shows a comparison of the wall temperature ratio (T_w/T_0) and the streamwise intermittency parameter. Figures 13–15 are comparisons of the solution profiles F, H, and w at five locations in the flow (four in the turbulent region and one in the laminar region). Again, excellent agreement has been obtained.

For this slender axisymmetric body with appreciable boundary-layer thickness values in comparison with the body radius, the curvature terms are likely to be significant. The results presented above include this effect by enabling the curvature terms in the equation (option `IW = 1`). The results of a run made with the curvature terms disabled (`IW = 0`) are shown in figure 16. Previous results with the curvature effects included are also shown for comparison. A noticeable difference is evident in the solution, especially at downstream locations at which the boundary-layer thickness is significant. The present results also compare well with the VGBLP results obtained with the curvature terms zeroed out.

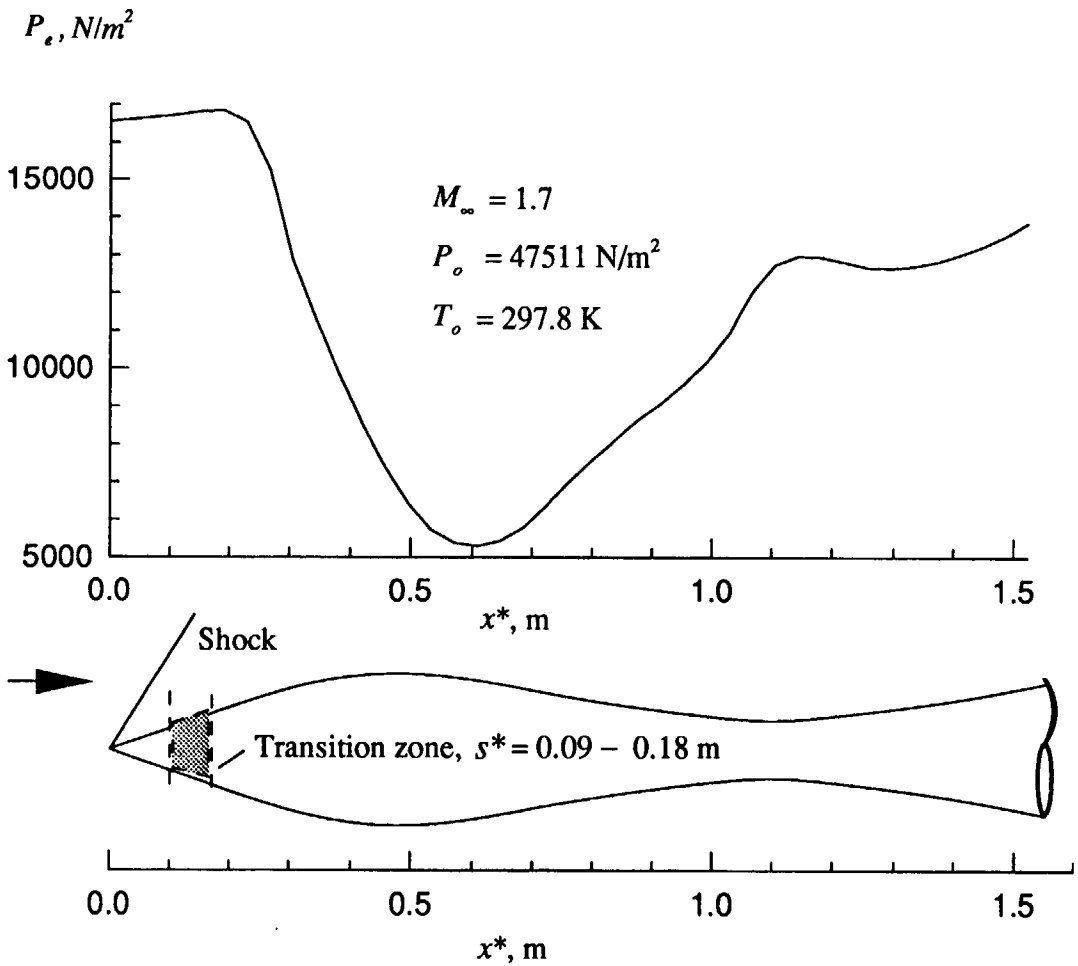

Figure 10. Case 2: geometry and conditions.

Table 2. Case 2: Description and Input Summary

```
Description
-----------

Case 2: Supersonic Flow over Waisted Afterbody

Free-stream conditions
----------------------

M-inf = 1.7
P-tot = 47511 N/m2
T-tot = 297.8 deg K

Wall conditions
---------------

Adiabatic wall (IWALL = 0)
No mass injection

Flow type
---------

Oblique shock (WAVE = 43.523 deg)
Axisymmetric (J = 1)
No stagnation point (IBODY = 2)
Constant entropy (IENTRO = 1)

Viscous terms
-------------

Laminar
Transitional (SST = 0.0901); for s > 0.09 m
Turbulent (TLNGTH = 2); for s > 0.18 m

Other
-----

Body opening angle PHII = 20
Solution for 0 < s < 1.53 m at 165 stations
Curvature term on or off (IW = 1 or IW = 0)
```

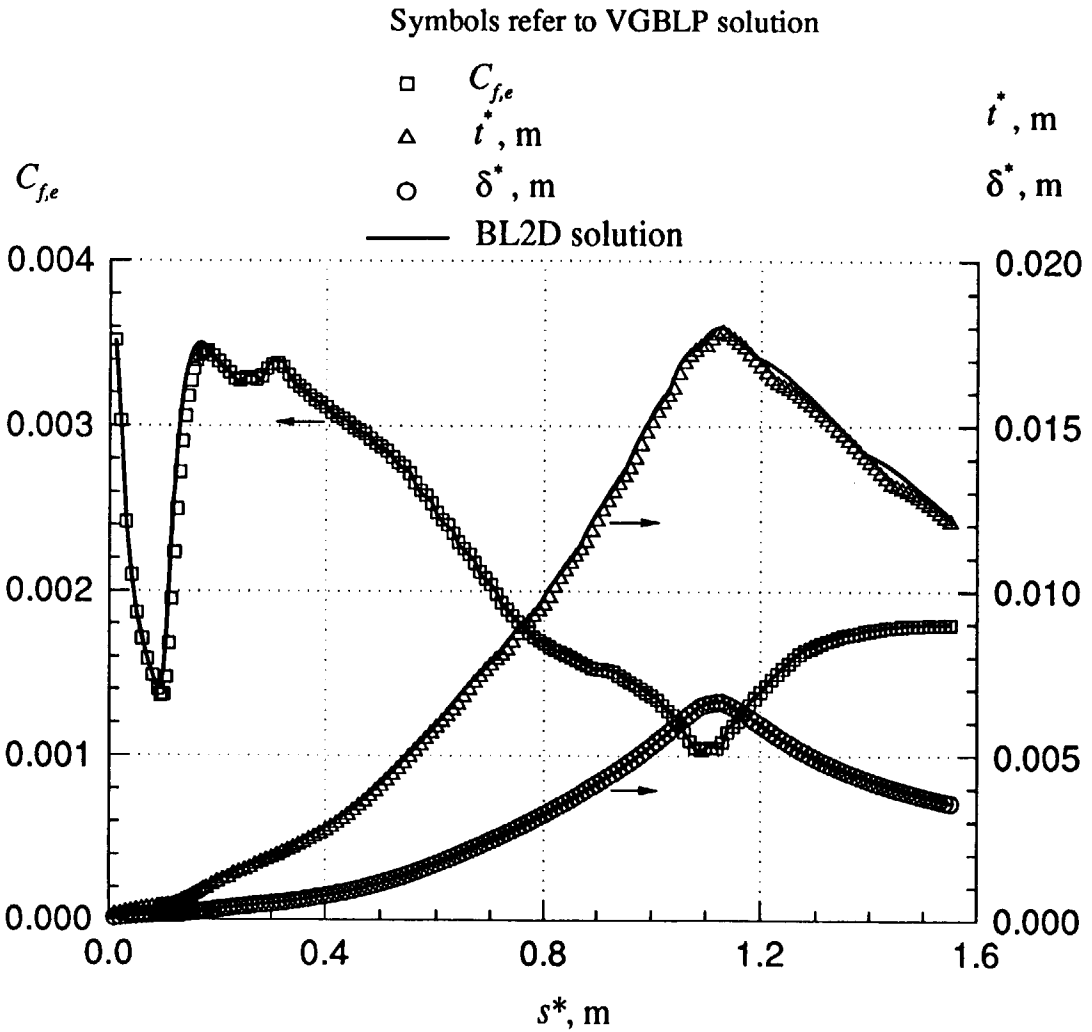

Figure 11. Case 2: comparison of BL2D and VGBLP solutions ($C_{f,e}$, t^*, δ^*).

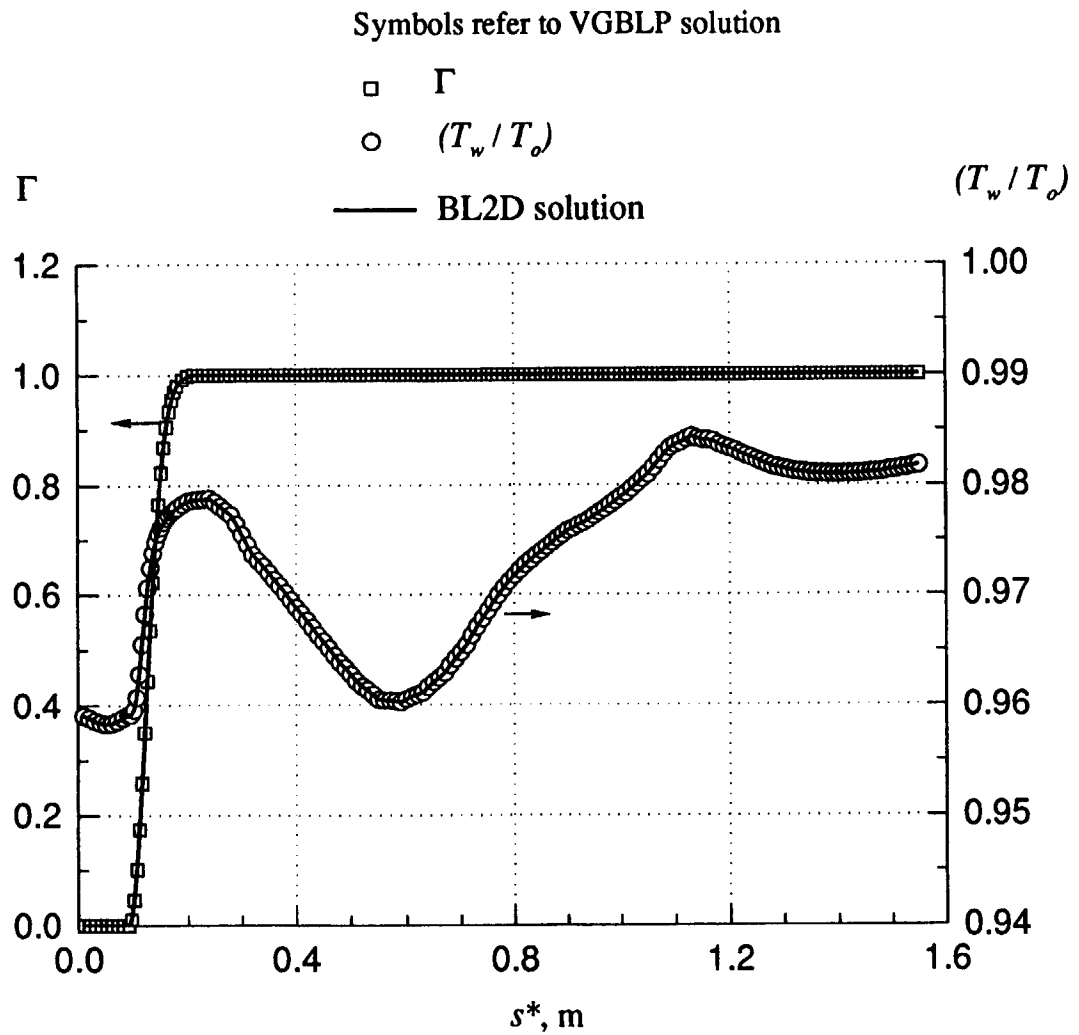

Figure 12. Case 2: comparison of BL2D and VGBLP solutions $(\Gamma, (T_w/T_o))$.

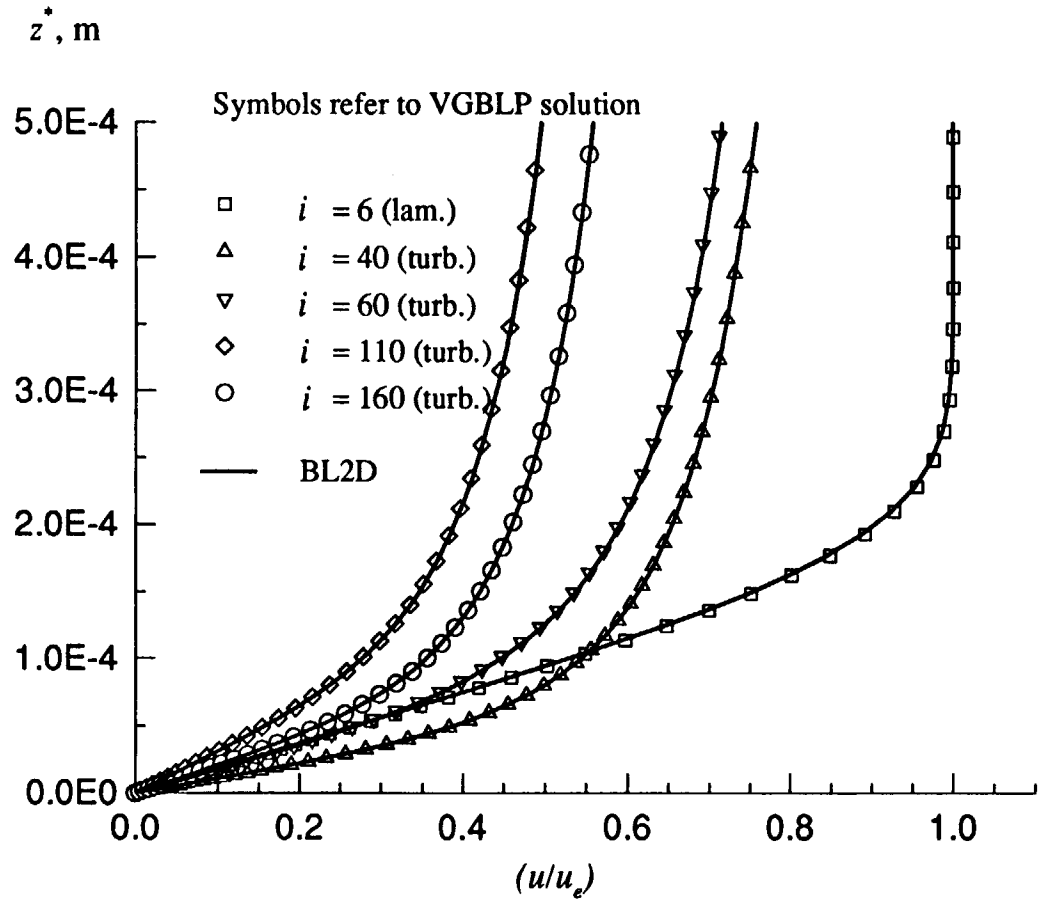

Figure 13. Case 2: comparison of BL2D and VGBLP solution profiles (u/u_e).

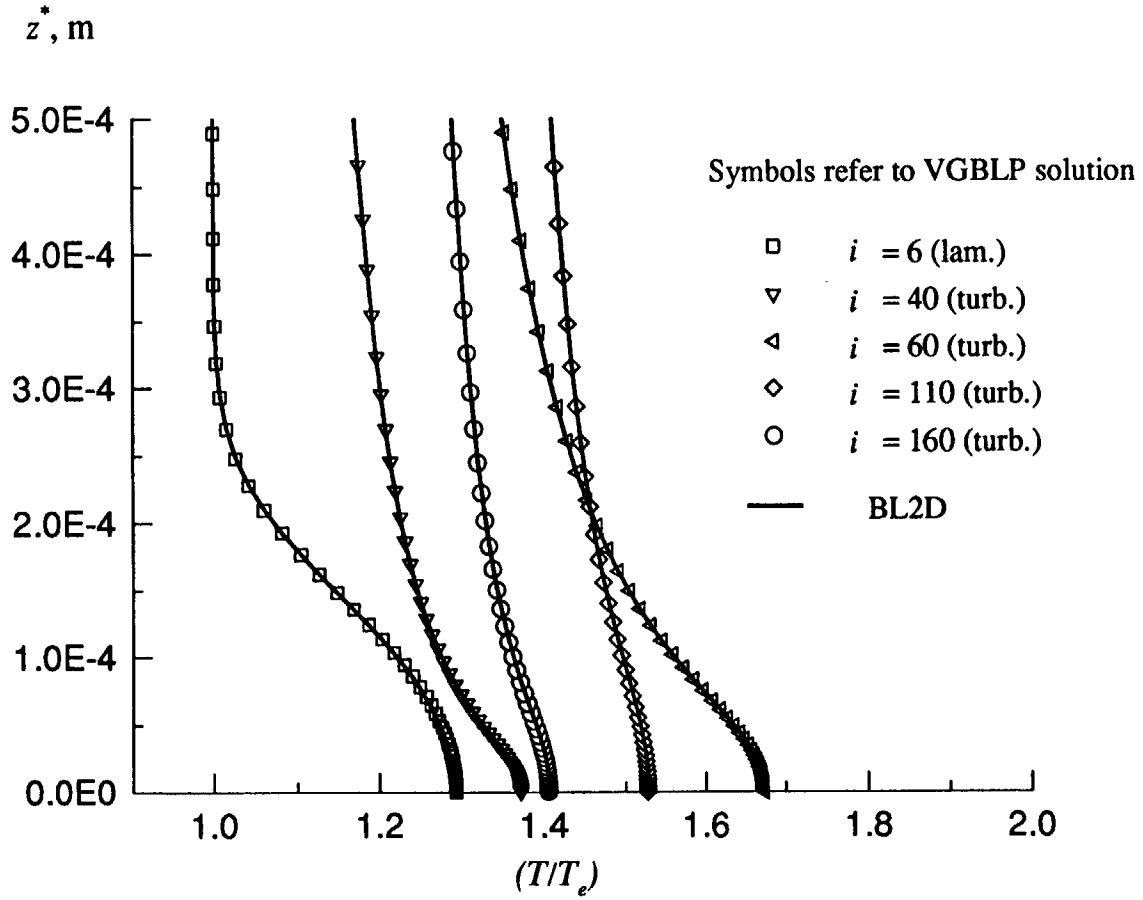

Figure 14. Case 2: comparison of BL2D and VGBLP solution profiles (T/T_e).

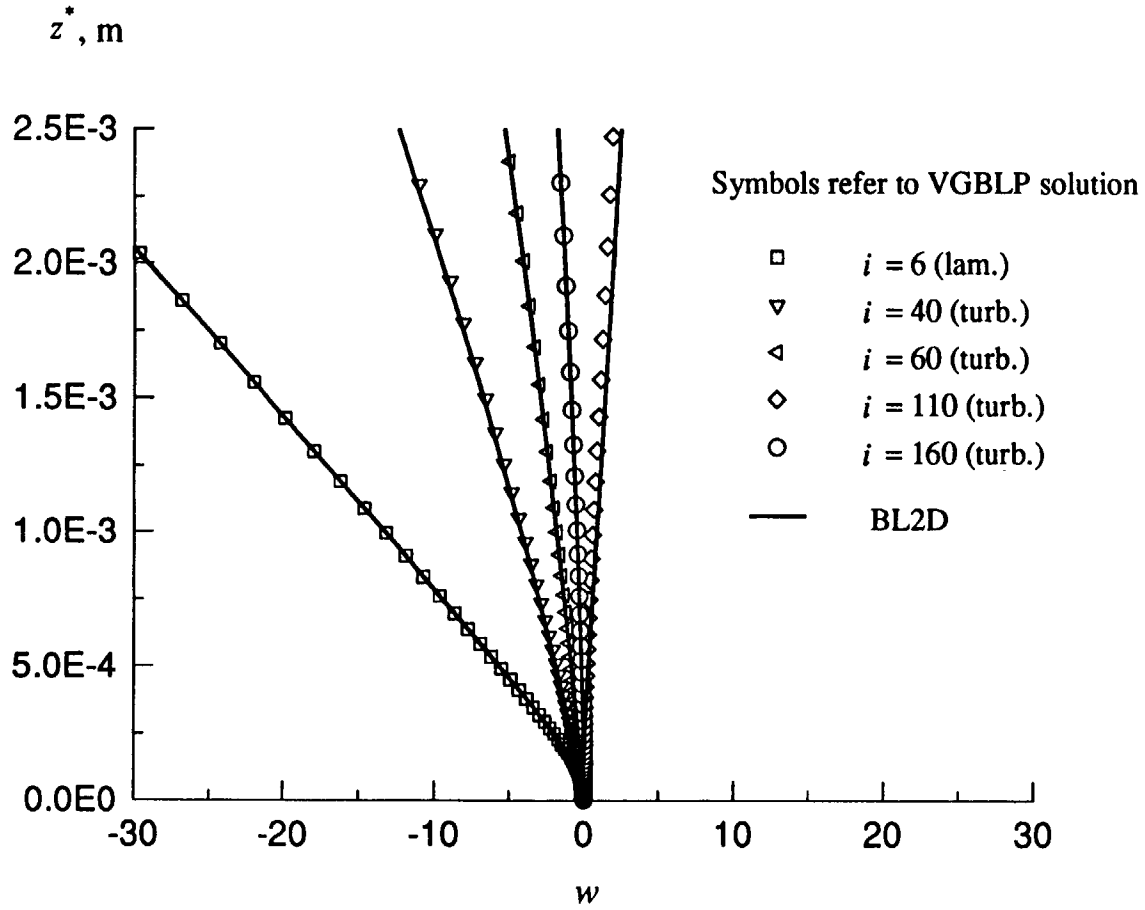

Figure 15. Case 2: comparison of BL2D and VGBLP solution profiles *(w)*.

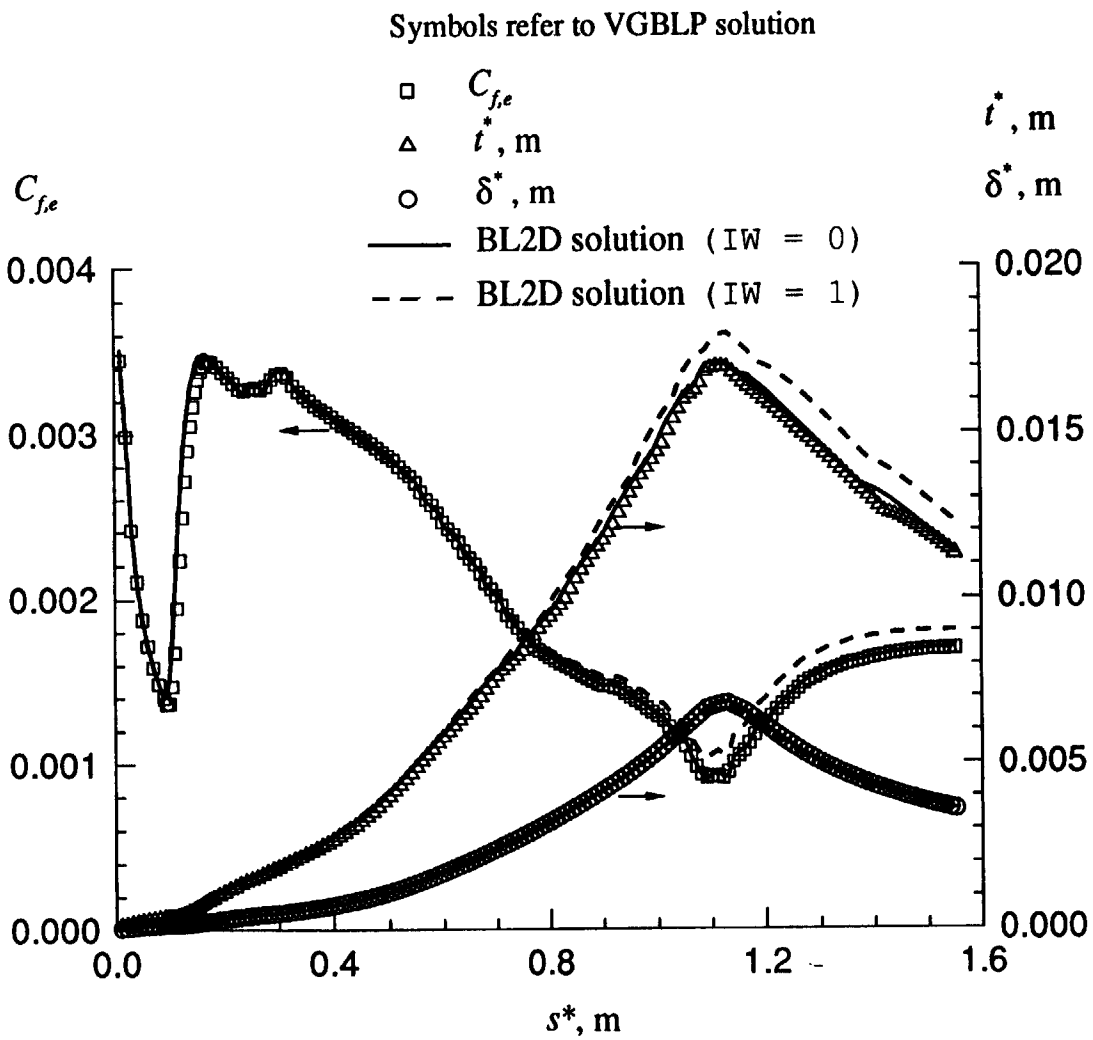

Figure 16. Case 2: comparison of BL2D and VGBLP solutions ($C_{f,e}$, t^*, δ^*) with effect of zeroing out curvature term (IW = 0).

4.3 Case 3: Flow Past a Sharp Cone at Mach 7.4

This case involves a sharp cone with a half angle of 5° and a cooled wall. This case demonstrates the use of the wall boundary conditions in the code. Three subcases correspond to the prescribed conditions of no suction, suction, and blowing (cases 3.1, 3.2, and 3.3, respectively). The boundary-layer grid is clustered near the region in which the wall mass transfer has a step change. In all three runs, the wall temperature is a constant value. The flow is laminar. Details of the geometry and the input conditions are given in figure 17 and table 3.

Case 3.1: No Suction. Figure 18 shows a comparison of the skin-friction coefficient based on edge conditions ($C_{f,e}$), 99.5–percent boundary-layer thickness (t^*), and displacement thickness (δ^*). Figure 19 shows a comparison of the wall heat transfer rate $\dot{q}_w^*$ and the Stanton number based on the edge conditions. Figures 20−21 are comparisons of the solution profiles F and H at five locations in the flow. The BL2D profiles are slightly fuller than the VGBLP profiles, probably due to the different numerics of the differencing schemes.

Case 3.2: Boundary-Layer Suction. A constant suction rate of −0.090117 Pa·s/m is applied for $s^* > 0.096012$ m. The resulting variations of $C_{f,e}$, t^*, and δ^* are shown in figure 22. The variation of $\dot{q}_w^*$ and the Stanton number are shown in figure 23. The agreement between VGBLP and BL2D is good. The profiles of u/u_e and T/T_e are shown in figures 24−25. The profiles are fuller as a result of suction.

Case 3.3: Boundary-Layer Blowing. A constant blowing rate of 0.090117 Pa·s/m is applied for $s^* > 0.096012$ m. The boundary layer separates at around $s^* = 0.11$ m. The resulting variations of $C_{f,e}$, t^*, and δ^* are shown in figure 26. The profiles of u/u_e and T/T_e at three locations are shown in figures 27−28. Because of its proximity to the separation point, profiles at the third location of BL2D and VGBLP are slightly different.

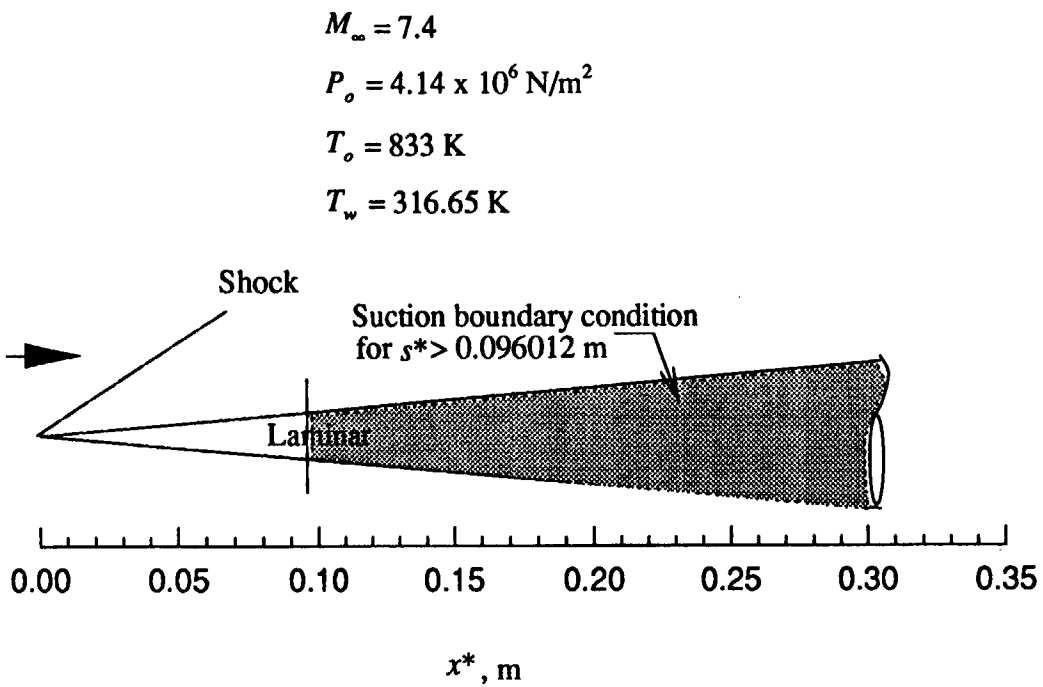

Figure 17. Case 3: geometry and conditions.

Table 3. Case 3: Description and Input Summary

```
Description
-----------

Case 3: Hypersonic Flow over Sharp Cone

Free-stream conditions
----------------------

M-inf = 7.4
P-tot = 4.14 x 10^6 N/m2
T-tot = 833 deg K

Wall conditions
---------------

Wall temperature specified (IWALL = 1)
No mass injection  (Case 3.1)
Prescribed suction (Case 3.2)
Prescribed blowing (Case 3.3)

Flow type
---------

Oblique shock (WAVE = 9.214 deg)
Axisymmetric (J = 1)
No stagnation point (IBODY = 2)
Constant entropy (IENTRO = 1)

Viscous terms
-------------

Laminar

Other
-----

Body opening angle PHII = 5
Solution for 0 < s < 0.3 m at 85 stations
```

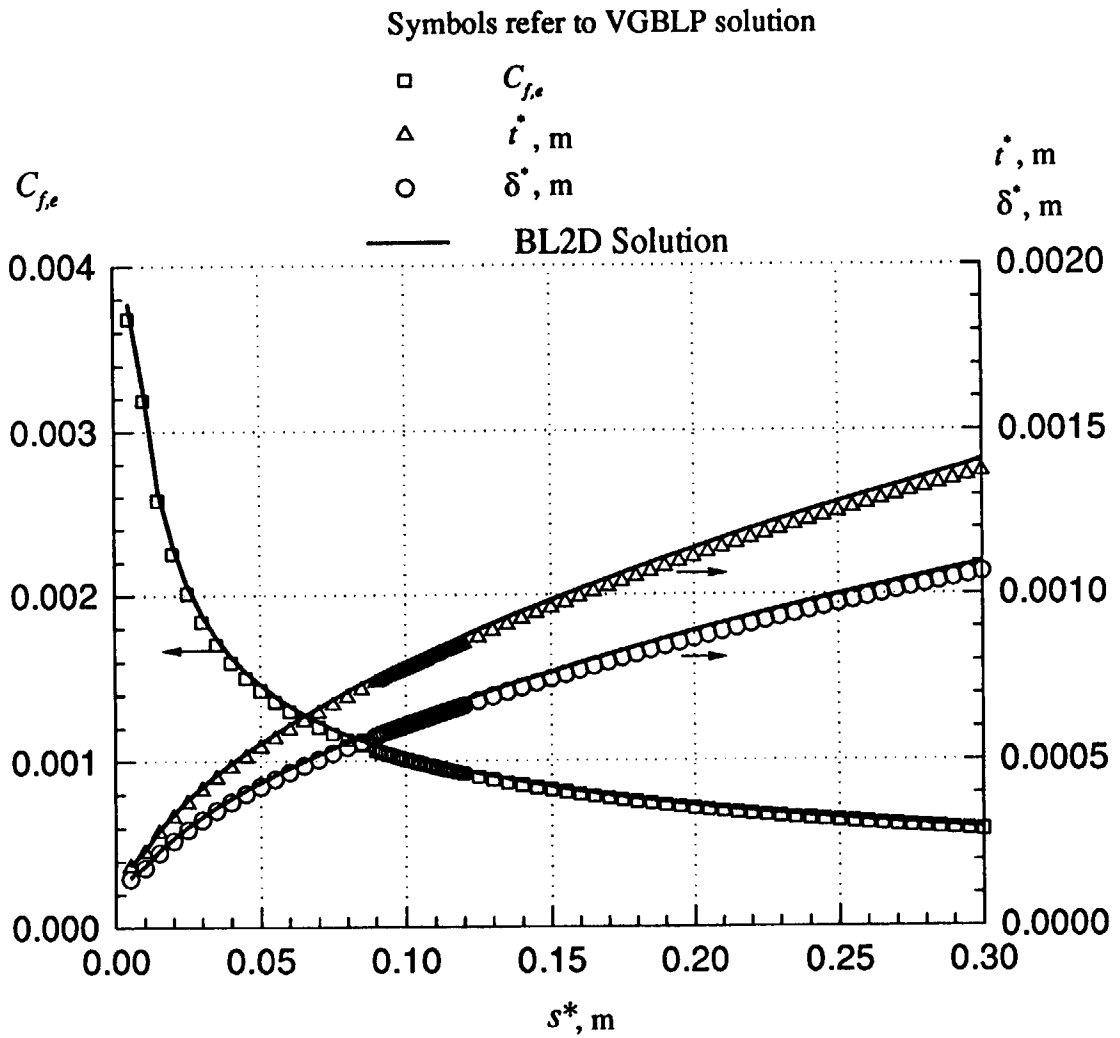

Figure 18. Case 3.1: comparison of BL2D and VGBLP solutions ($C_{f,e}$, t^*, δ^*).

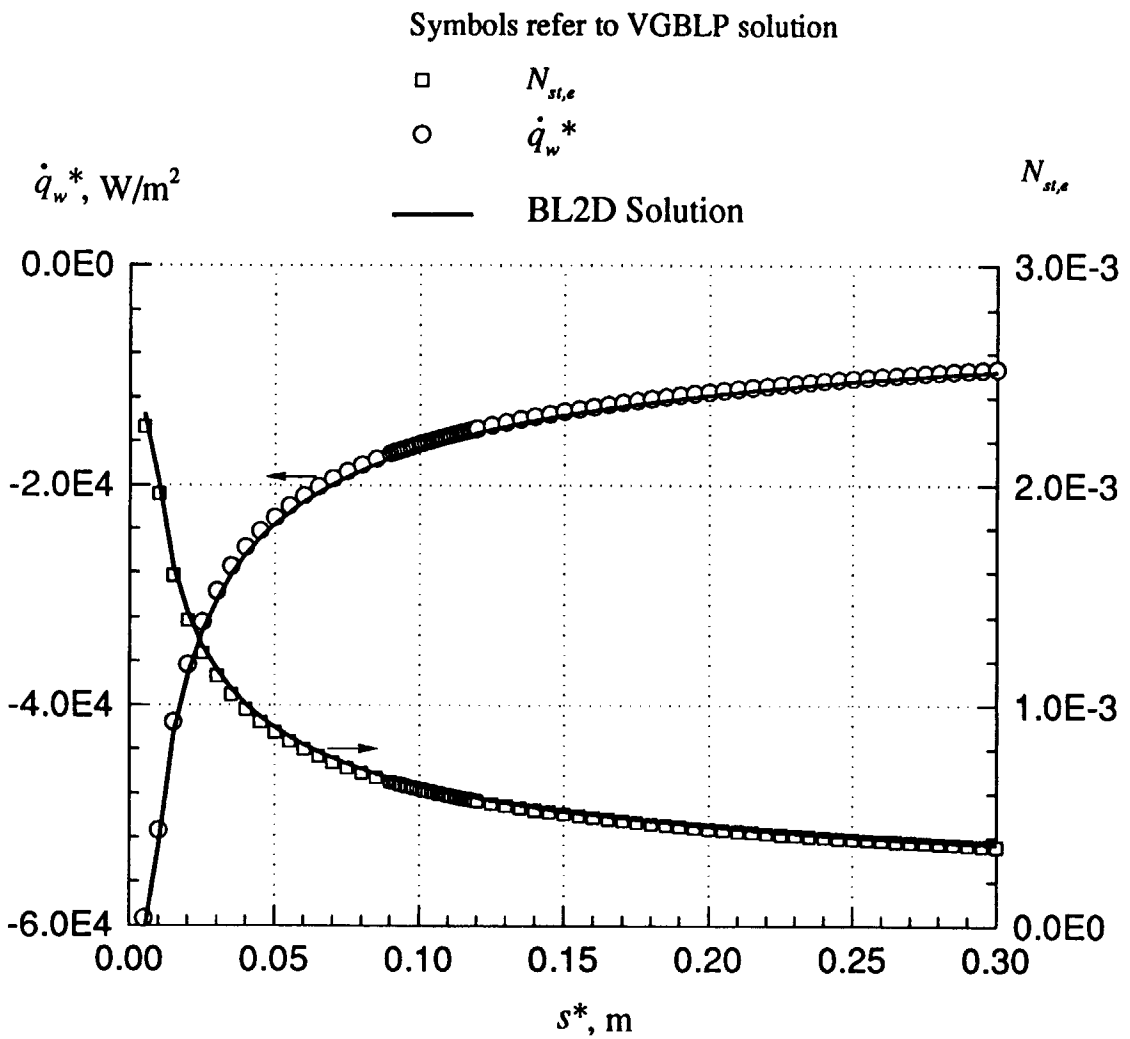

Figure 19. Case 3.1: comparison of BL2D and VGBLP solutions ($\dot{q}_w$*, $N_{st,e}$).

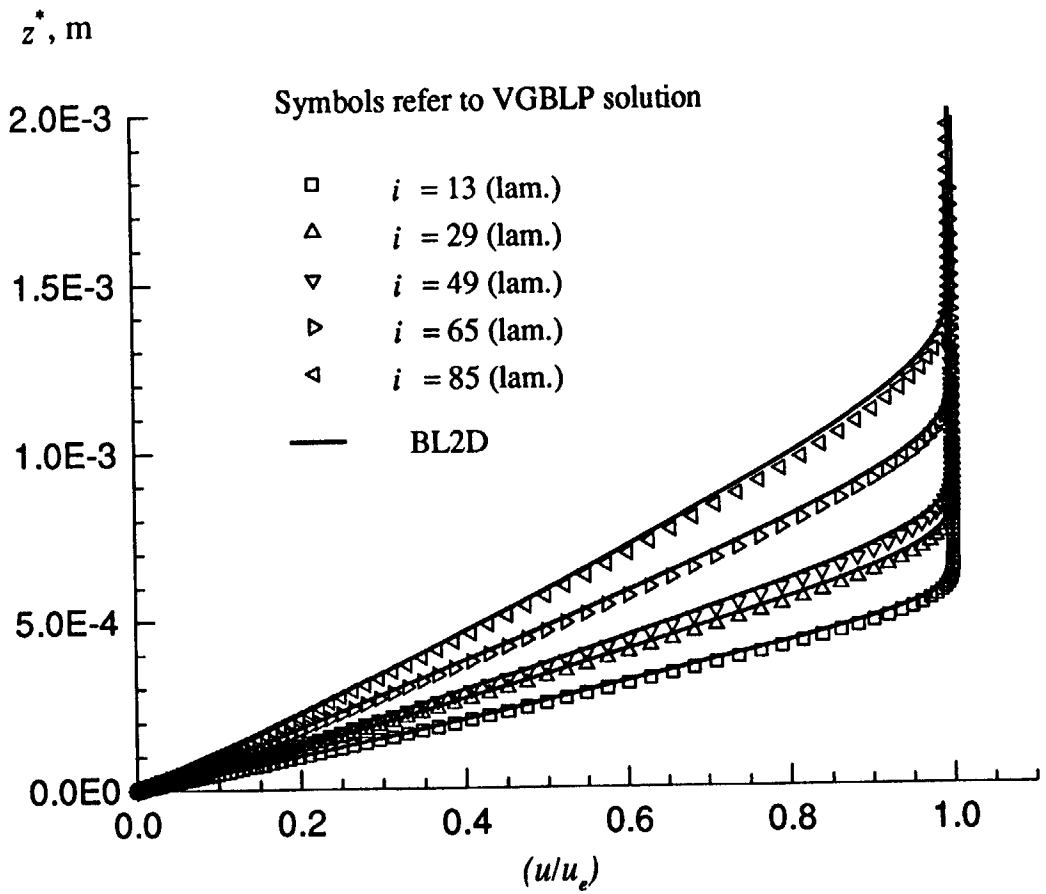

Figure 20. Case 3.1: comparison of BL2D and VGBLP solution profiles (u/u_e).

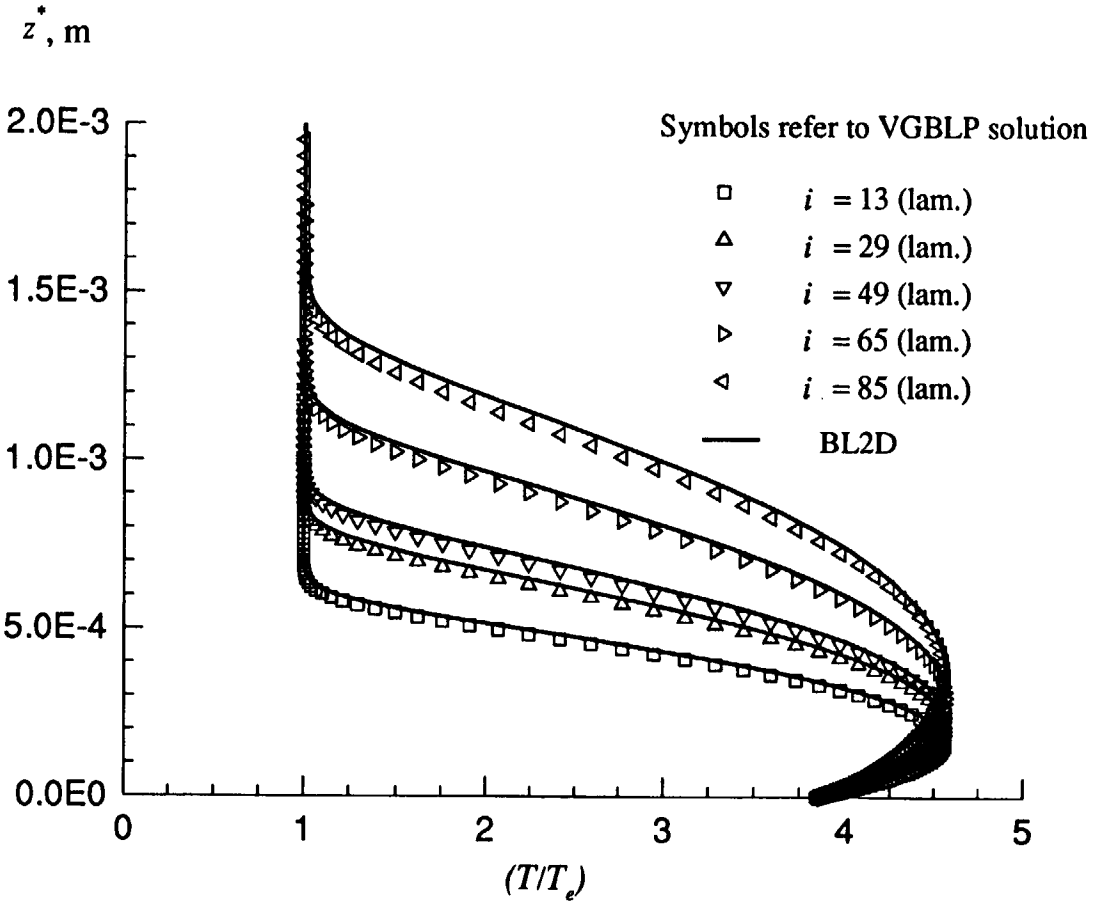

Figure 21. Case 3.1: comparison of BL2D and VGBLP solution profiles (T/T_e).

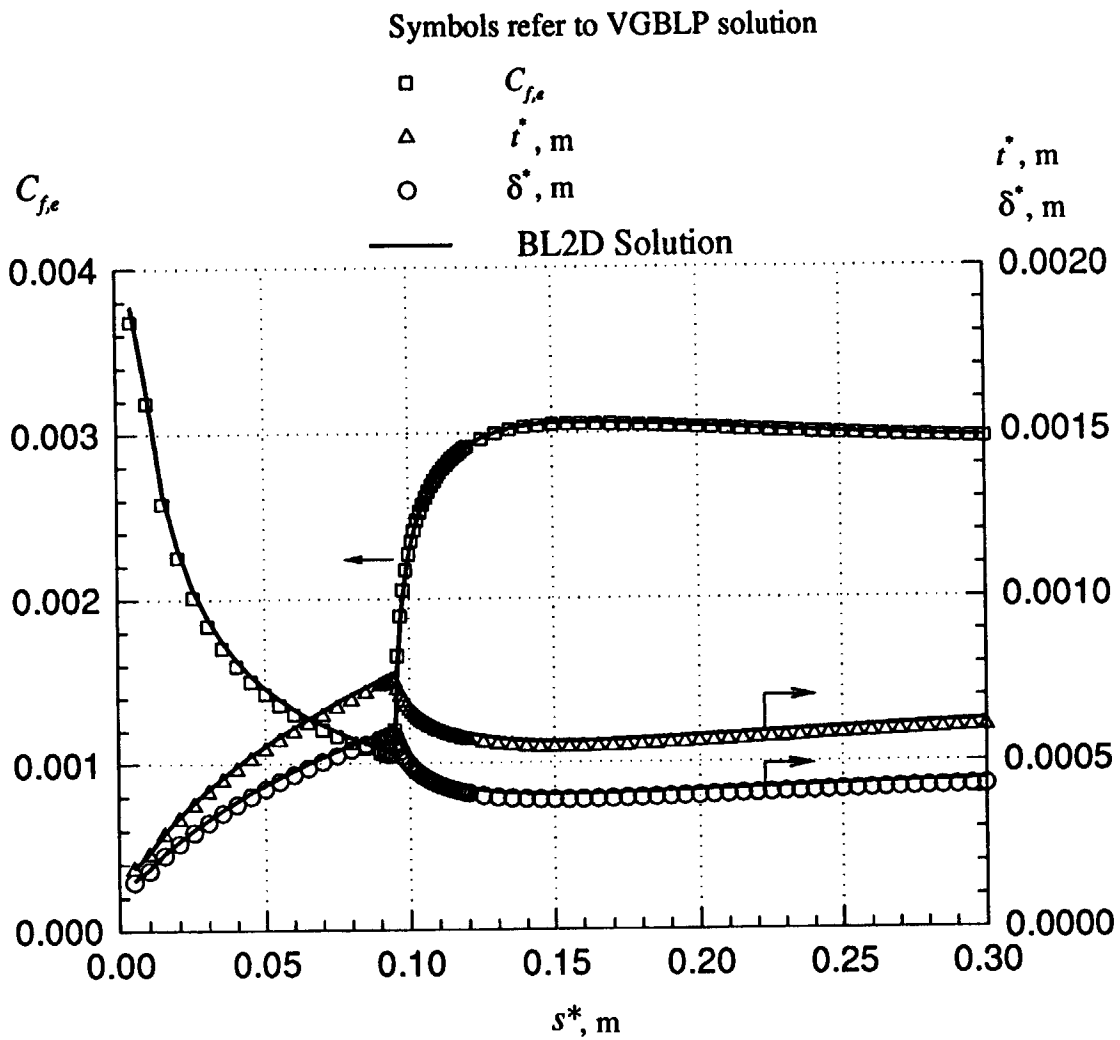

Figure 22. Case 3.2: comparison of BL2D and VGBLP solutions ($C_{f,e}$, t^*, δ^*).

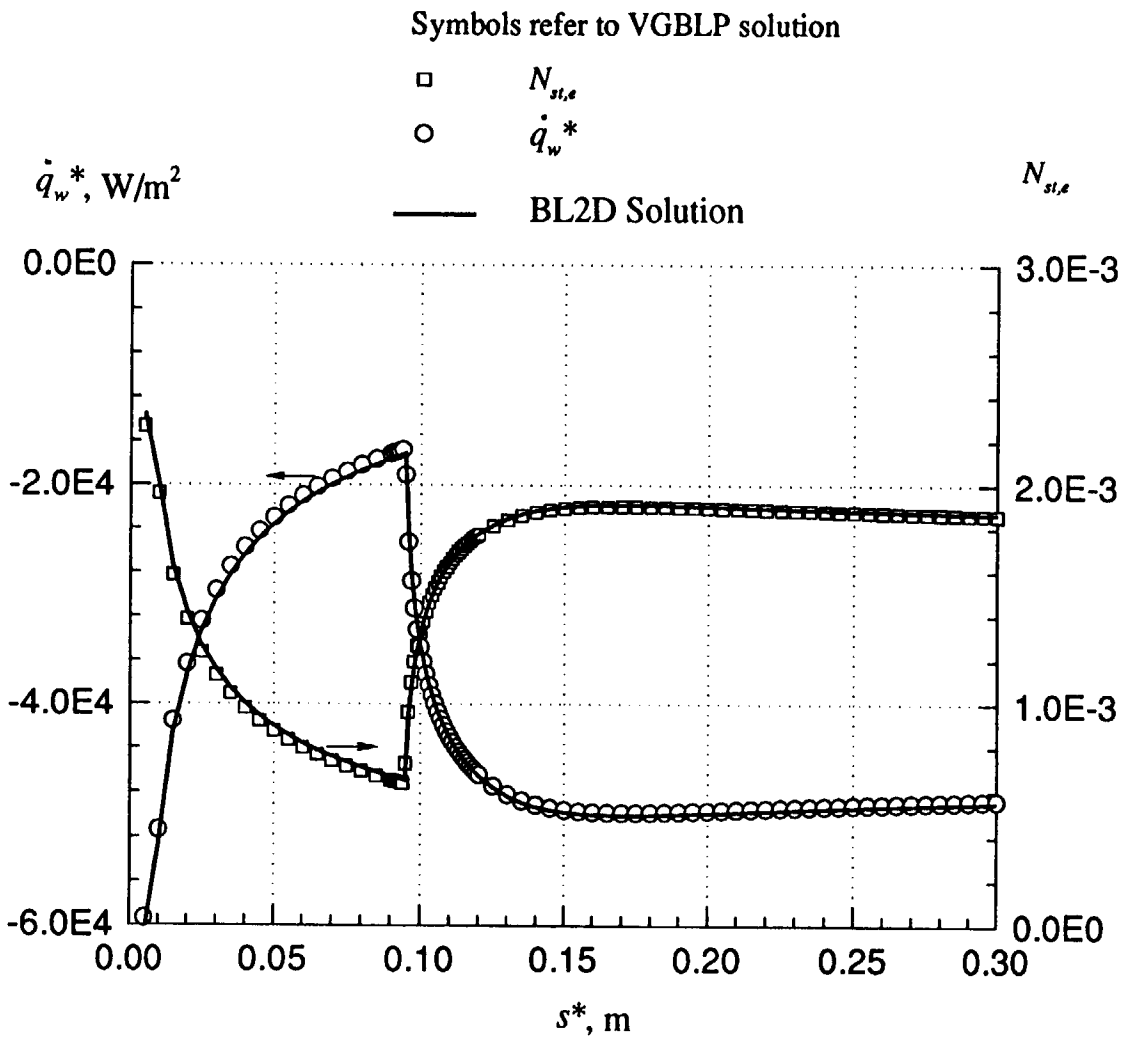

Figure 23. Case 3.2: comparison of BL2D and VGBLP solutions ($\dot{q}_w$*, $N_{st,e}$).

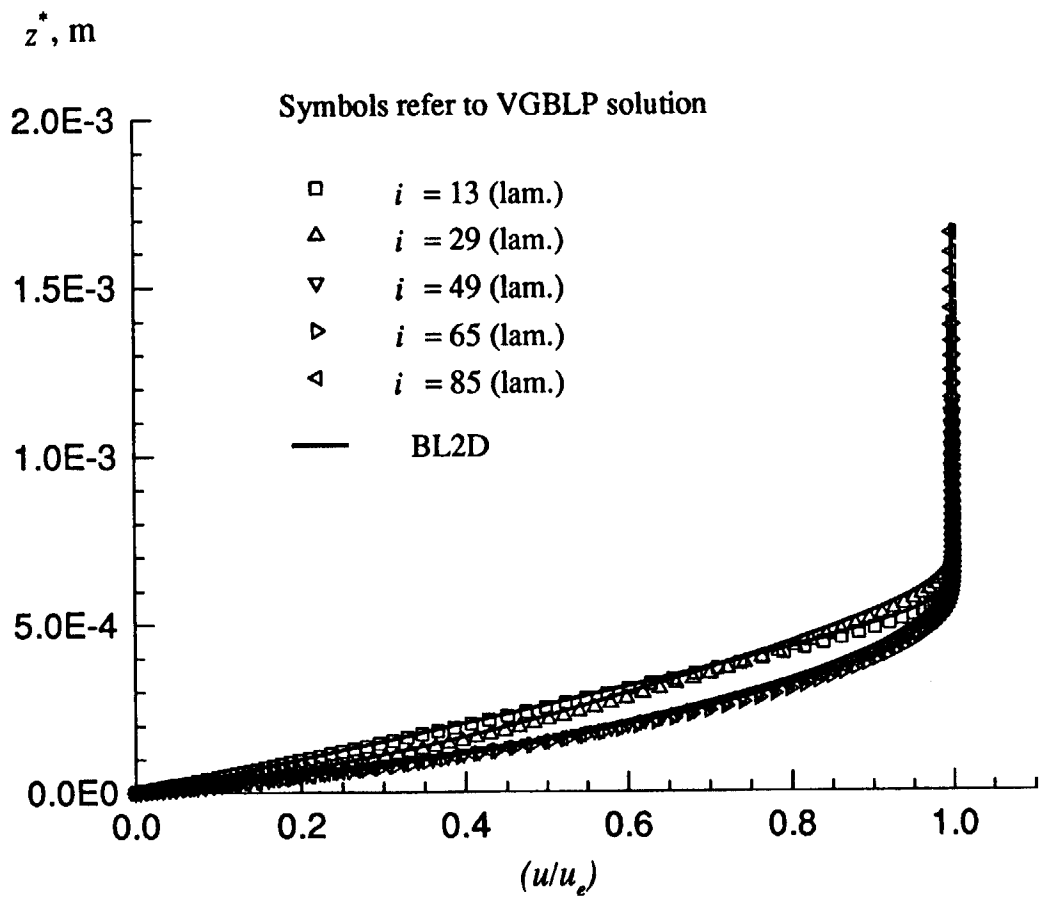

Figure 24. Case 3.2: comparison of BL2D and VGBLP solution profiles (u/u_e).

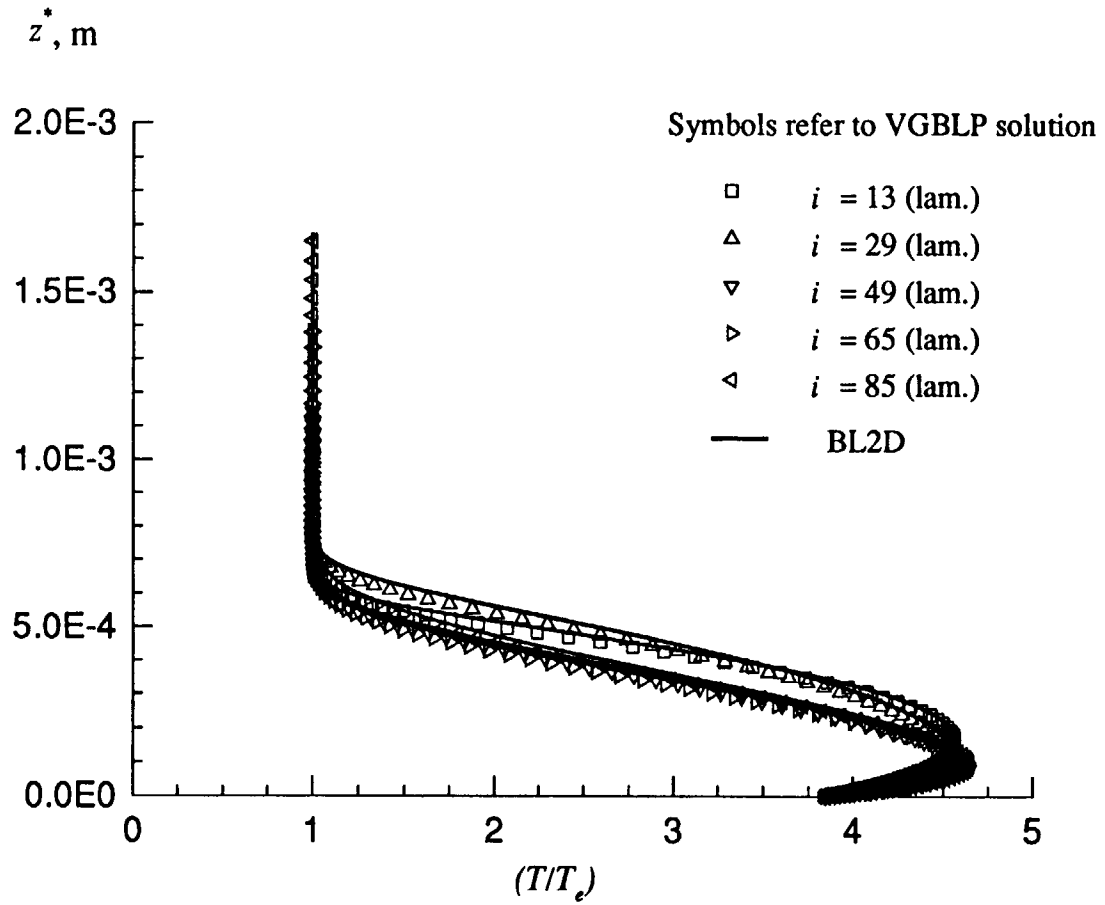

Figure 25. Case 3.2: comparison of BL2D and VGBLP solution profiles (T/T_e).

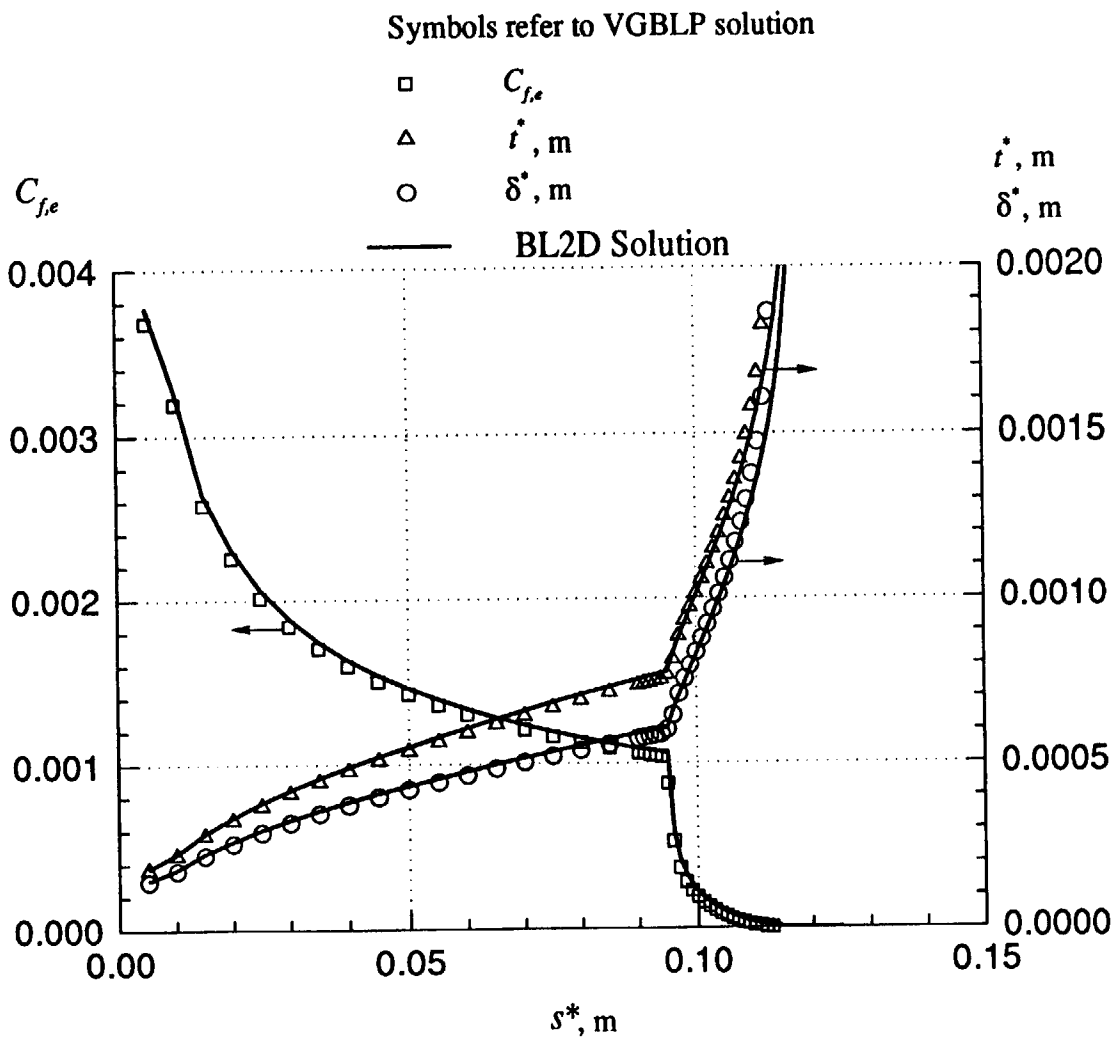

Figure 26. Case 3.3: comparison of BL2D and VGBLP solutions $(C_{f,e}, t^*, \delta^*)$.

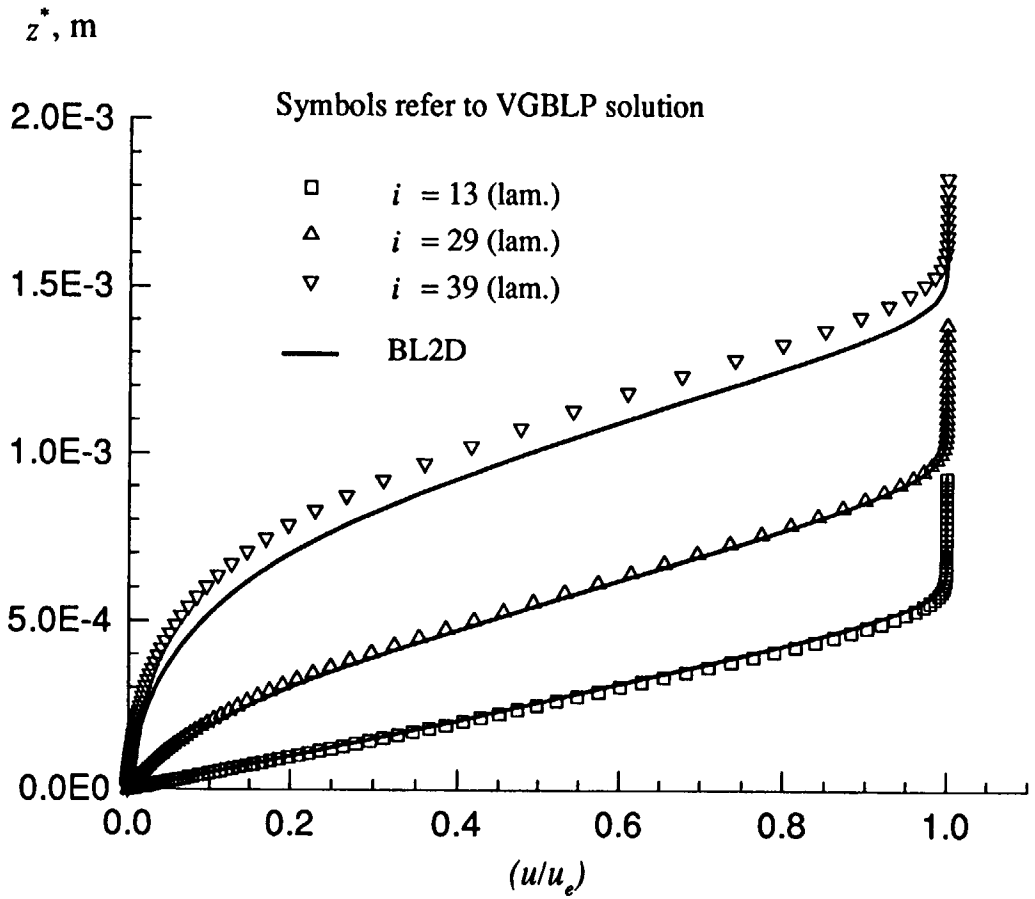

Figure 27. Case 3.3: comparison of BL2D and VGBLP solution profiles (u/u_e).

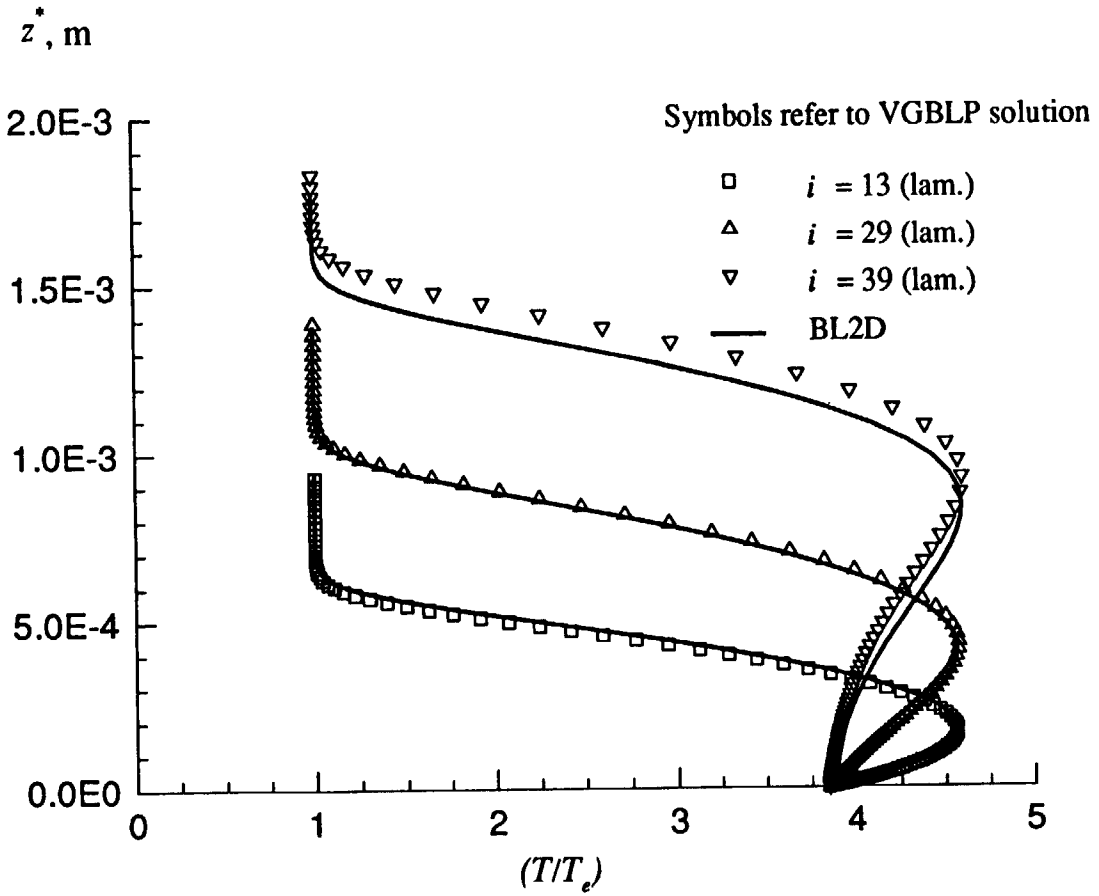

Figure 28. Case 3.3: comparison of BL2D and VGBLP solution profiles (T/T_e).

4.4 Case 4: Hypersonic Flow Past a Blunt Cone

Here, we look at the flow past a blunt cone at a Mach number of 20.3 in Helium gas (in which γ, R, and N_{Pr} are different from those in air). Further, the shock curvature in this problem indicates the need to use the variable entropy option `IENTRO = 2` in the code. Figure 29 and table 4 give a description of the flow and input conditions.

Figure 30 presents the results from BL2D and VGBLP that correspond to the first pass in the variable entropy iteration (`ITE = 1`). This computation is equivalent to running the code with no variable entropy iteration (`IENTRO = 1`). Good agreement is obtained for $C_{f,e}$, t^*, and δ^*. Note that in this case the BL2D computation uses first-order streamwise derivatives because the edge conditions are not smooth.

Figure 31 shows the same results at the end of the variable entropy iteration convergence (`ITE = 3` in this case for both codes). Note that the calculation now involves the shock curvature determined locally from the slope of the shock front. Because the original shock shape and gradient data from reference 1 are not smooth, a spline smoothing was done (external to the program), and the smoothed coordinates and slopes were used in the BL2D and VGBLP computations. Results in figure 31 show that the variable entropy has a significant effect on the results. The two codes agree fairly well in the variable entropy mode; the slight difference in results near the stagnation point was traced to an error in initialization for `ITE > 1` in VGBLP. Figure 32 shows a comparison of the heating rate at the wall. The rough edge data and the nearly separated boundary layer for $s^* > 0.02$ m cause the slight difference in the results.

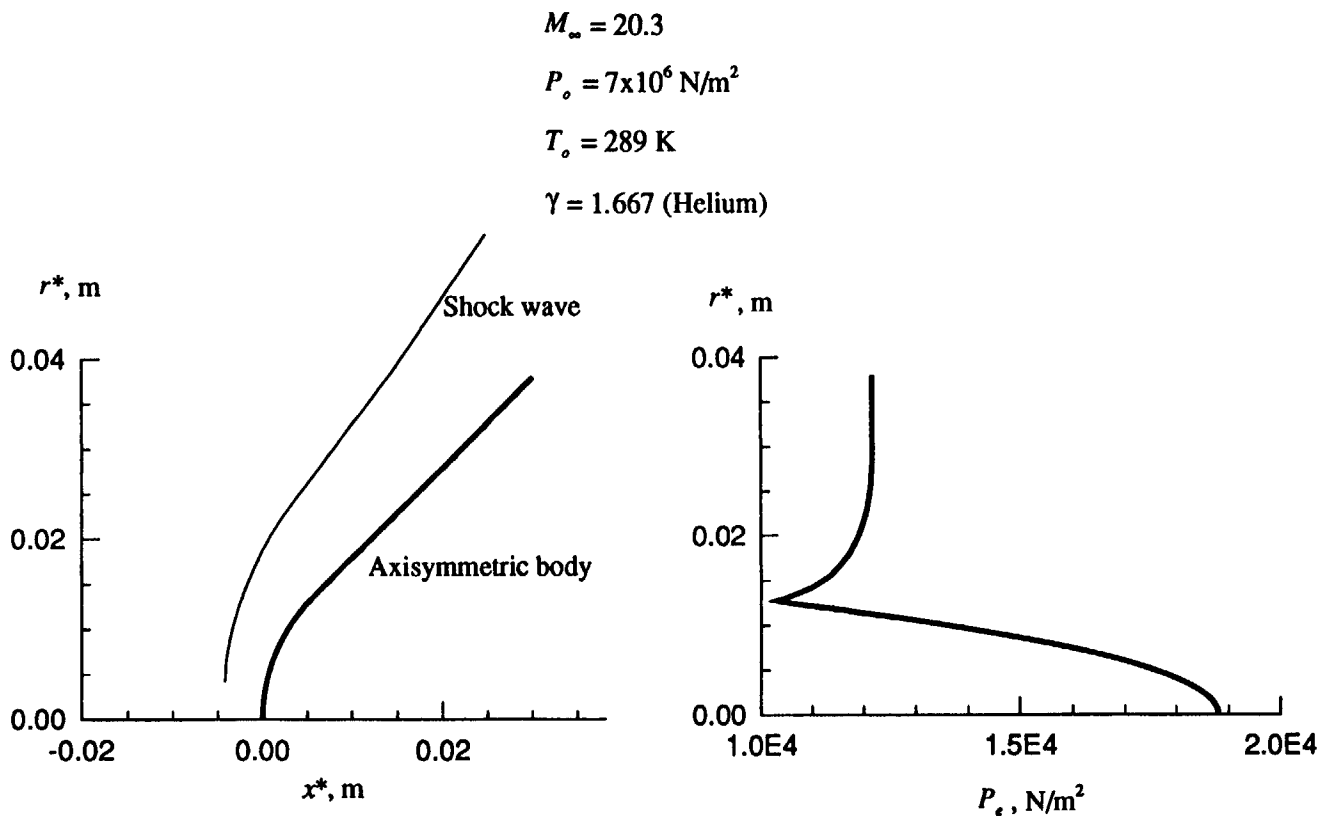

Figure 29. Case 4: geometry and conditions.

Table 4. Case 4: Description and Input Summary

```
Description
-----------

Case 4: Hypersonic Flow over Blunt Body


Free-stream conditions
----------------------

M-inf = 20.3
P-tot = 7 x 10^6 N/m2
T-tot = 289 deg K

Wall conditions
---------------

Wall temperature specified (IWALL = 1)
No mass injection

Flow type
---------

Curved shock, normal at stagnation point (WAVE = 90 deg)
Axisymmetric (J = 1)
Stagnation point (IBODY = 1)
Variable entropy (IENTRO = 2)

Viscous terms
-------------

Laminar, power law for viscosity

Other
-----

Body opening angle PHII = 90
Solution for 0 < s < 0.03 m at 121 stations
Helium gas (PRL = 0.688, GAM = 1.6667, RSTAR = 2079.0 m^2/(sec^2 degK)
Shock wave coordinates input for variable entropy calculation
```

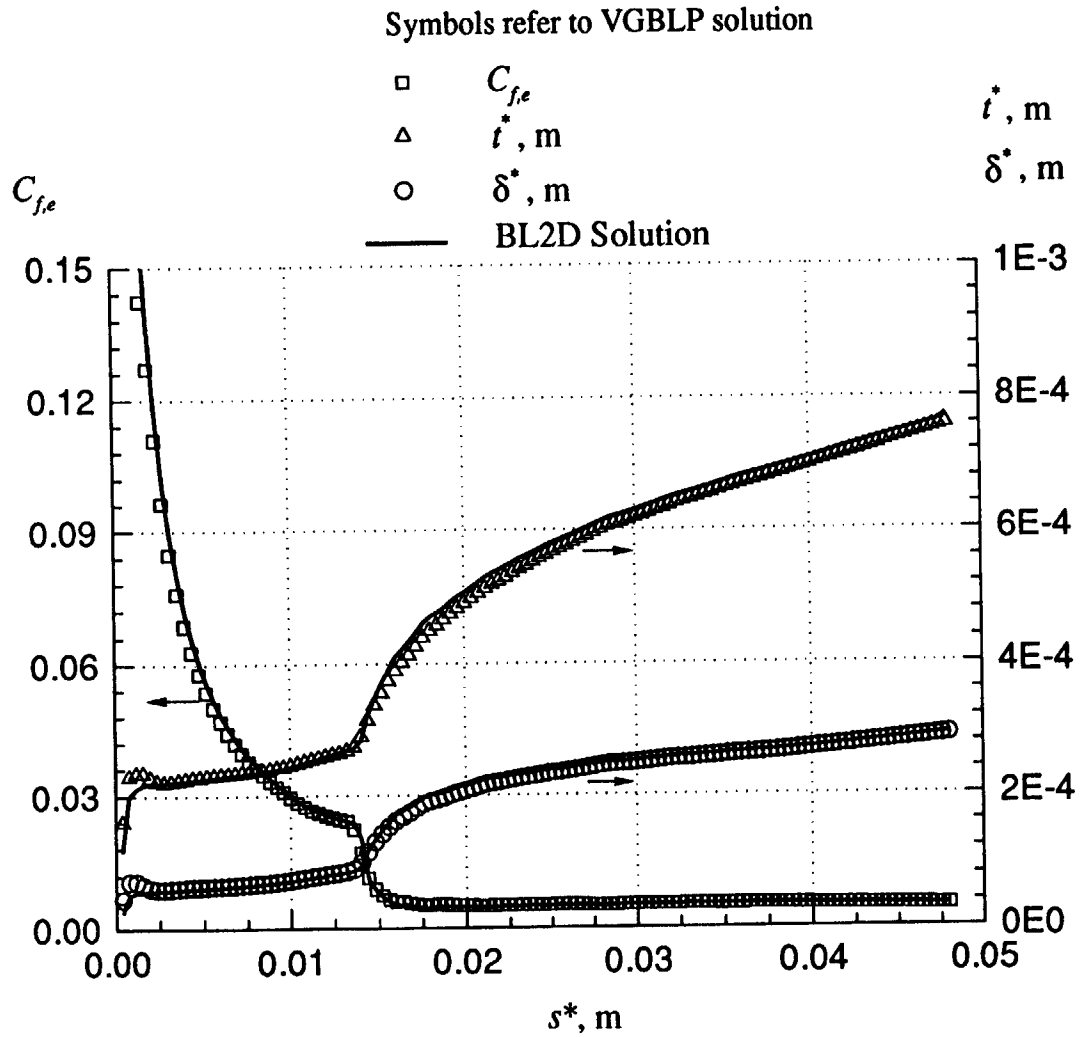

Figure 30. Case 4: comparison of BL2D and VGBLP solutions ($C_{f,e}$, t^*, δ^*); variable-entropy results for iteration 1.

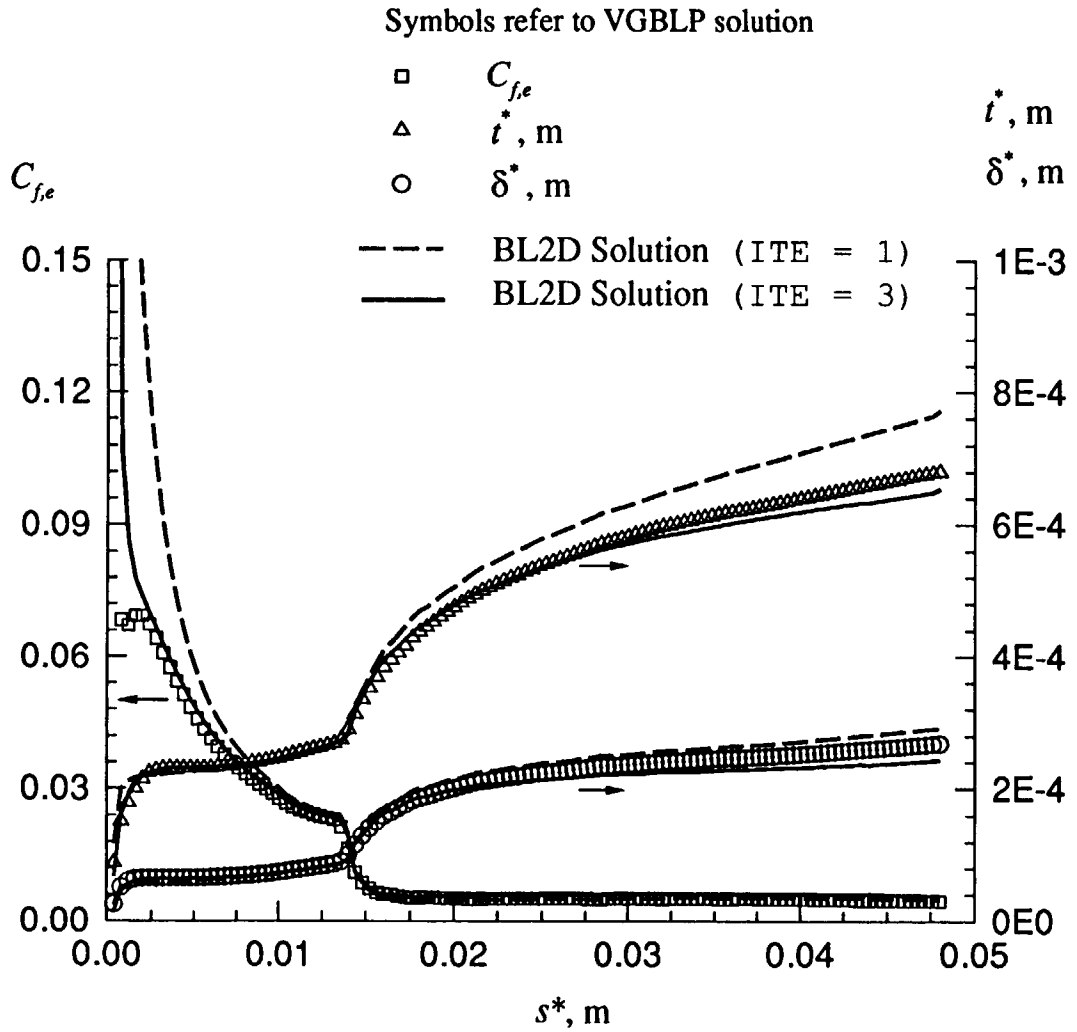

Figure 31. Case 4: comparison of BL2D and VGBLP solutions ($C_{f,e}$, t*, δ*); variable-entropy results for iteration 1 and 3.

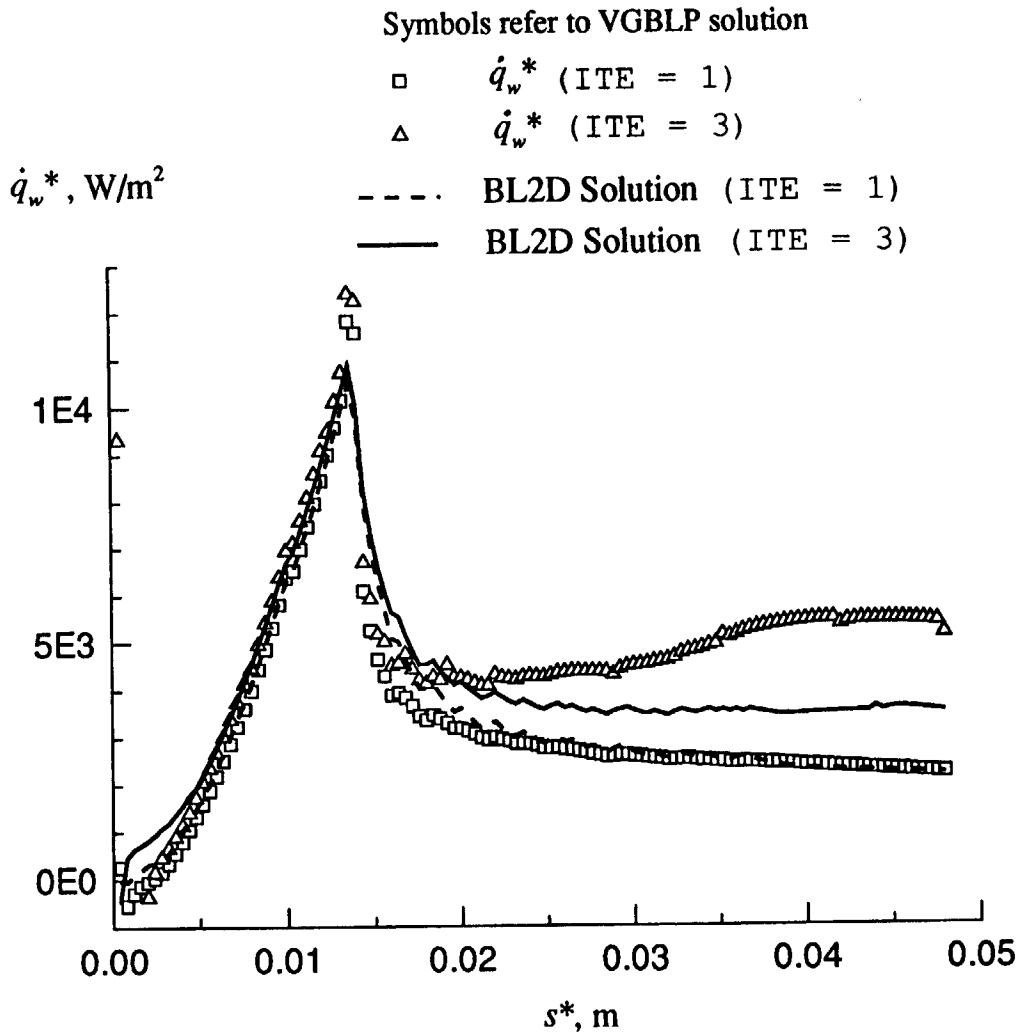

Figure 32. Case 4: comparison of wall heat flux (with variable entropy iteration enabled).

4.5 Case 5: Turbulent Flow in a Convergent-Divergent Nozzle

The free-stream or inflow Mach number here is 0.012058; the flow is rapidly expanded in the nozzle to an exit plane Mach number of 5. The flow is turbulent almost from the beginning. The flow and geometry parameters are given in figure 33 and table 5.

A comparison of the displacement-thickness values from BL2D and VGBLP is given in figure 34. A log scale is used for δ^* because of its exponential growth in the divergent portion of the nozzle. Figure 35 shows the standard plot of $C_{f,e}$, t^*, and δ^* as a function of s^*.

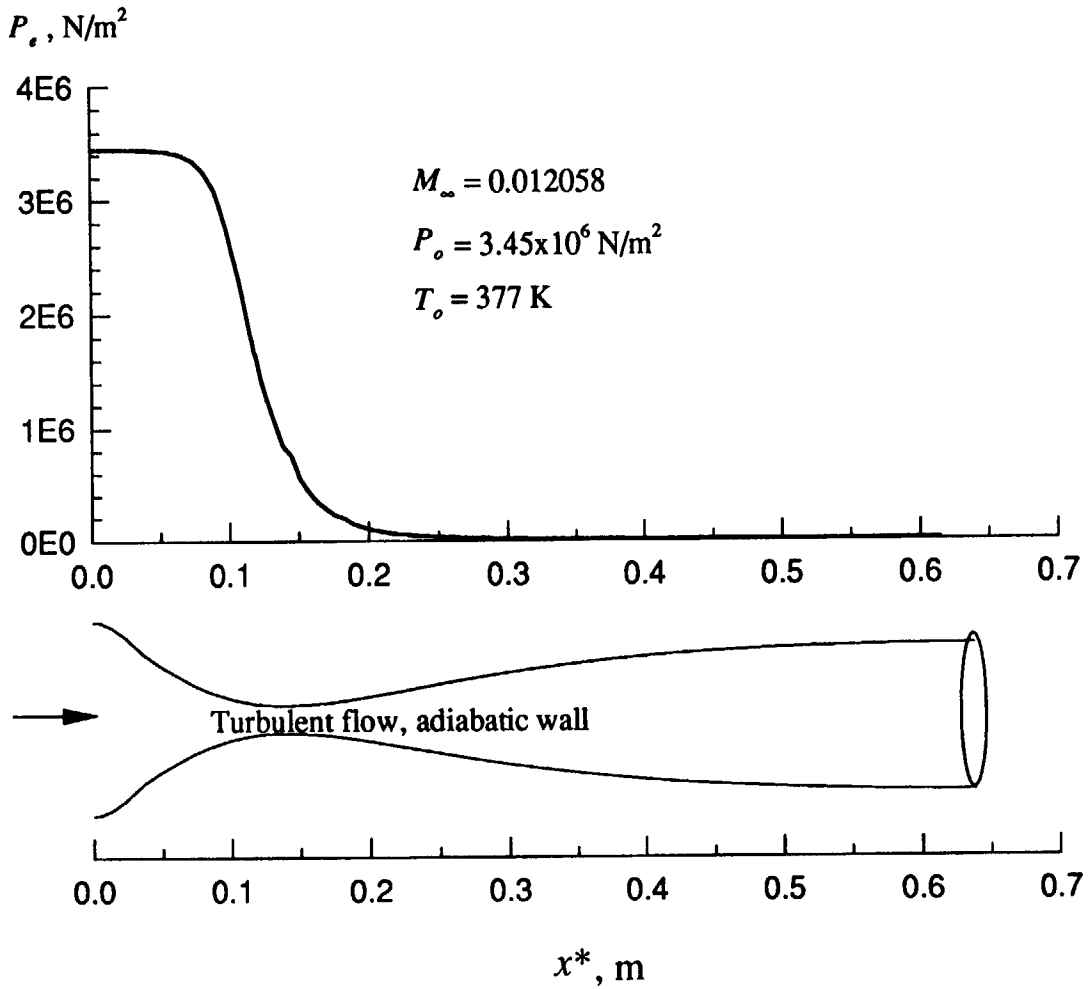

Figure 33. Case 5: geometry and conditions.

Table 5. Case 5: Description and Input Summary

```
Description
-----------

Case 5:  Flow in a Convergent-Divergent Nozzle

Free-stream conditions
----------------------

M-inf = 0.012058
P-tot = 3.45 x 10^6 N/m2
T-tot = 377 deg K

Wall conditions
---------------

Adiabatic wall (IWALL = 0)
No mass injection

Flow type
---------

No shock
Axisymmetric (J = 1)
No stagnation point (IBODY = 2)

Viscous terms
-------------

Turbulent

Other
-----

Body opening angle PHII = 0
Solution for 0 < s < 0.62 m at 101 stations
```

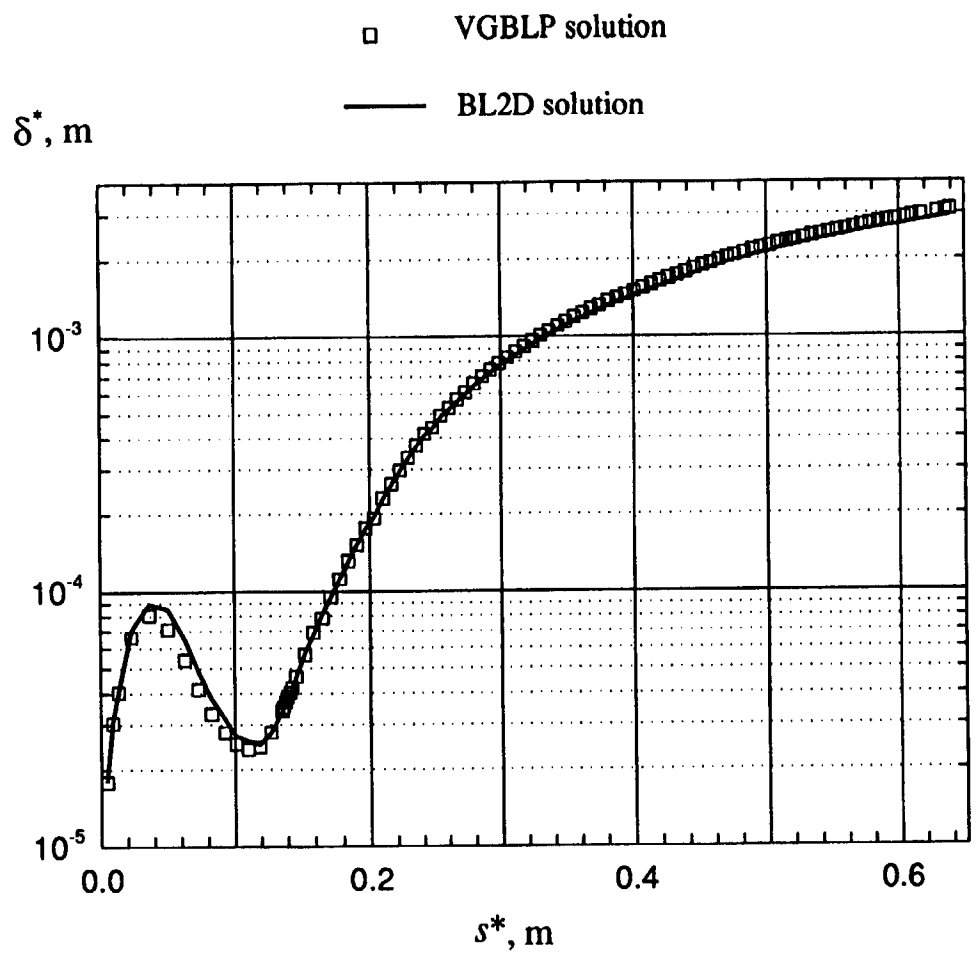

Figure 34. Case 5 Results: comparison of displacement thickness values.

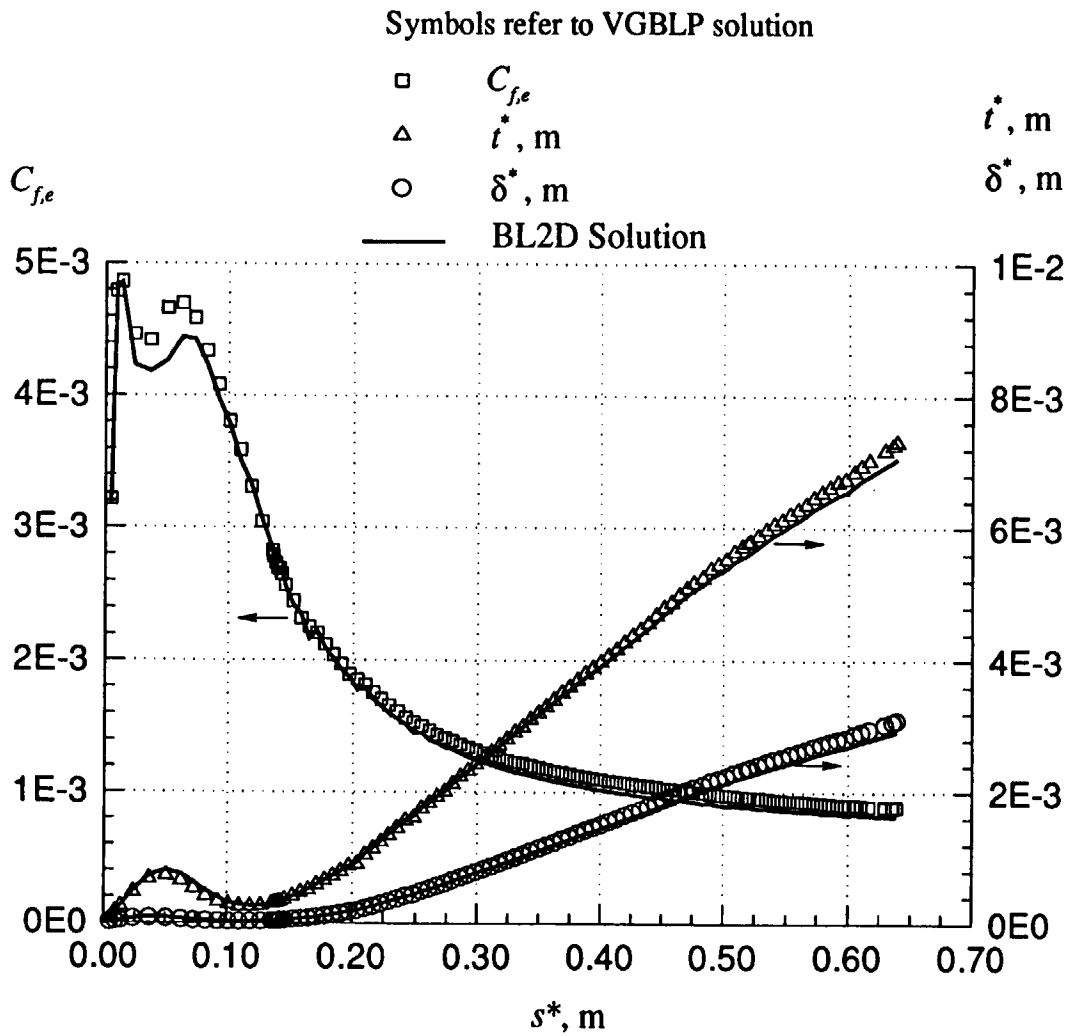

Figure 35. Case 5: comparison of BL2D and VGBLP solutions ($C_{f,e}$, t^*, δ^*).

5. USER'S MANUAL

5.1 BL2D Program Structure

The program is located in several directories. Please refer to figure 36 for the locations of various files in the program package.

The subdirectory `bl2d/source` contains the Fortran files that correspond to the subroutines of BL2D. Herein can also be found a `Makefile` to automatically compile the required subroutines and create the executable code. Details for running the program are given in section 5.3, "Running the Program BL2D".

The subdirectory `bl2d/inputs` contains input files for the five test cases used in validation. (See chapter 4, entitled "Validation".) This subdirectory also contains versions of the `include` files used for the test cases. These files contain the common blocks used in the source routines. Array dimensions are set with `parameter` statements.

The subdirectory `bl2d/lib` contains some useful programs for the input check. Please refer to the `Readme` file in this subdirectory for further details.

The subdirectory `bl2d/vgblp` contains a version of VGBLP used in the validation runs, along with corresponding input files. Many modifications have been incorporated in the original program to run on UNIX machines with a `fortran77` compiler. Note that the original program statements are in upper case and the modifications that are incorporated are in lower case. The `Readme` file in this subdirectory explains how to run the test cases.

The subdirectory `bl2d/doc` contains documentation on BL2D. Future updates will also be documented in this area in an `Update.info` file.

A synopsis of the call sequence of various routines in BL2D and the solution logic is given in appendix A. Appendix A also contains a brief description of the purpose of each subroutine.

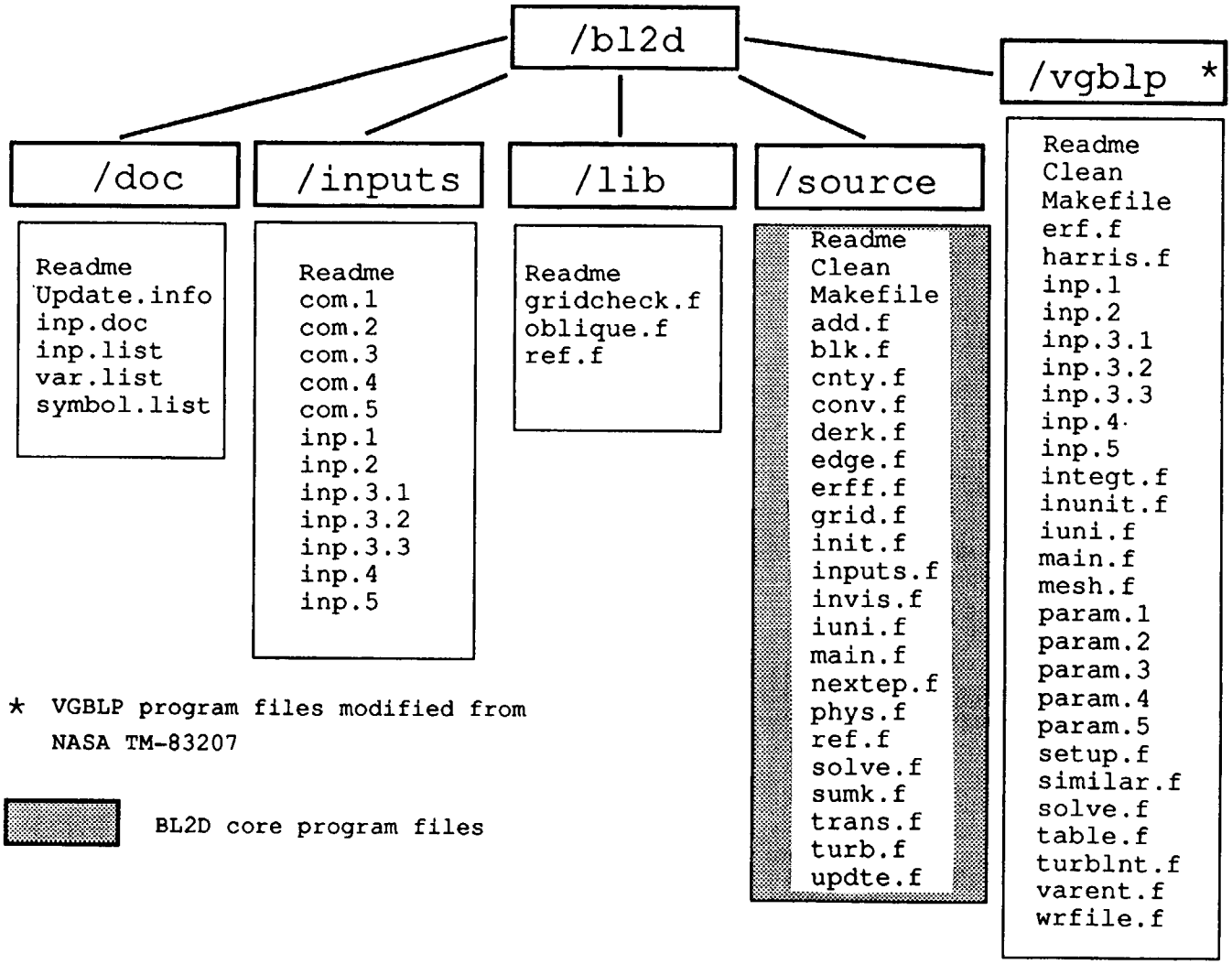

Figure 36. Program files structure.

5.2 Description of Input File for BL2D

A sample input file for BL2D (for Case 1) is shown below. This input file is the same as `bl2d/inputs/inp.1` included in the BL2D program package.

```
VALIDATION OF BL2D WITH VGBLP CASE 1 MACH 2.8 FLAT PLATE, X=0.0 to 0.25
IUNIT           AMACH           PTS or PFS      TTS or TFS      IFS(- for FS)
1               2.8             0.414e7         311.0           1
GAM             IGAS            IWALL           J               IFT
1.4             1               0               0               1
IBODY           WAVE            PHII            IENTRO          CONVE
2               0.0             0.0             1               1.e-02
ZMAX            ZI              NZI             AK              N2
40.0            40.00           81              1.10            81
DFPTOL          DHPTOL          IACC            ITMAX           IW
1.e-03          1.e-03          4               100             0
DFE             DHE             IADD            VELEDG          NX1
0.0001          0.0001          0               0.995           61
IYINT           KODAMP          KODPRT          KODVIS          KTCOD
2               2               1               2               2
SMXTR           SST             TLNGTH          PRT             NXLIM
2400.0          1.e8            2.0             0.95            62
RSTAR           IORD1           IORD2           ITEMAX          PRL
286.96          2               3               1               0.72
STEP SIZES (NX1 VALUES)
.001    .001    .001    .001    .001
.001    .001    .001    .001    .001
.001    .001    .001    .001    .001
.001    .001    .001    .001    .001
.005    .005    .005    .005    .005
.005    .005    .005    .005    .005
.005    .005    .005    .005    .005
.005    .005    .005    .005    .005
.005    .005    .005    .005    .005
.005    .005    .005    .005    .005
.005    .005    .005    .005    .005
.005    .010    .010    .010    .010
.010
WALL OR PROFILE PRINT FLAGS (0,1 or 2), NX1 VALUES
1       1       1       1       2
1       1       1       2       1
1       1       1       1       1
1       1       1       2       1
1       1       1       1       2
1       1       1       1       1
1       1       1       1       1
1       1       1       1       2
1       1       1       1       1
1       1       1       1       1
1       1       1       1       1
1       1       1       1       2
1
OUTPUT FOR PLOTS, NUMBER OF VARIABLES FOLLOWED BY VARIABLE NUMBER CODES
8       34      2       25      46      4       39      45      40
NUMBER          L (INVISCID INPUTS)
2               1
XE      RADE    SE      PESE    TWSE    QESE    WWSE
0.000   1.0     0.0     152552. 0.0     0.0     0.0
1.000   1.0     0.100   152552. 0.0     0.0     0.0
```

Most of the input parameters correspond to VGBLP. (In most cases, the same variable names are used.) However, the input format has been improved. The `namelist` input format is no longer used. Line headers are used in the input file to facilitate input in

an unambiguous and error-free manner. Common input errors, such as improper array dimensions and incompatible values, are trapped in the program.

The input files for running the five validation cases are available in the `bl2d/inputs` subdirectory. These input files may be useful to the user in the selection of appropriate input parameters for a new case.

A detailed description of the input file format is given in appendix B. (The same information is also available in the file `bl2d/doc/inp.doc`.) An alphabetical list of BL2D input variables with a short description is given in appendix C. In this section, some of the new features in the input are described.

The free-stream conditions can be specified in terms of stagnation or static values (i.e., `(PTS,TTS)` or `(PFS,TFS)`). The choice is indicated by the input variable, `IFS`; a negative value indicates that static values are to be input.

As given previously, the normal grid distribution is input such that an inner and an outer distribution can be specified; a single exponential distribution can also be specified, as in VGBLP. See section 3.2 entitled, "Normal Grid Distribution" for more details. Also note that the program `gridcheck.f` in the subdirectory `bl2d/lib` can be used to arrive at the optimum distribution before the boundary-layer program is run.

In BL2D, the solution convergence is tested on the maximum values of both $\partial F'$ and $\partial H'$. The corresponding tolerance values are input. If the convergence tolerances are not met in `ITMAX` iterations, then a warning of no adequate convergence is issued and the solution march is continued.

The flag `iadd` is a new feature by which the normal grid extent and dimension can be increased to accommodate the growth of the boundary layer in transformed variable space, if needed. Normal grid points are presently added at equal increments. If no more points

can be added due to a limit on the array dimensions, an error message will be printed. The criterion for adding normal grid points is based on sum of the gradient F' at the 10 outermost grid points. If this sum exceeds the input tolerance value DFE and if iadd = 1, the program adds points automatically. A similar test is done on the temperature profile gradient, based on the input value of DHE.

The input of nxlim $\leq$ nx enables the solution march to be stopped at an earlier step for diagnostic runs.

Wall parameters or solution profiles are printed via flags. A value of 0 indicates no print, 1 indicates that the wall parameters will print, and 2 indicates that both the wall parameters and the profiles will print. This flag is specified at the end of each marching step. A flag of 1 at the 10th location indicates that wall parameters at i = 11 (i.e., end of step 10) will be printed. Wall parameters are output to fort.2, and profiles are output to fort.8. In addition, up to 49 wall parameters can be output to file fort.7 at all i locations (i > 1) for plotting purposes. A number code which ranges from 1 to 49 is used for the variables that can be output. The list of these variables is given in appendix D. Up to 10 variables can be output at a time per run.

5.3 Running the Program BL2D

The BL2D program is run in the subdirectory bl2d/source. The program expects input under the file name inp.dat and an include file that contains common blocks under the file name com. The maximum dimensions of the array are set in the file com via parameter statements. The array dimensions are as follows:

```
nzm = maximum value of normal grid points

nxm = maximum value of streamwise grid points
```

```
   nmax = greater of (nzm,nxm)

   num = number of inviscid data points

   nsm = number of points that define the curved shock

         set to 1, if variable entropy option not used

   numblm = number of points that define PRTAR array, 1 if kodprt
= 1 or 2

   Case 1 example:

   parameter(nzm = 81,nxm = 62,nmax = 81,num = 2,nsm = 1,numblm = 1)
```

To run Case 1, for example, copy `com.1` and `inp.1` (from subdirectory `bl2d/inputs`) to `com` and `inp.dat`, respectively; remove all `.o` files (only if a new `com` file is being used, as in this example); type `make` to create the executable code; and type `a.out` to run the program. Detailed output is written to the file `fort.2`. Other outputs are written to `fort.7` and `fort.8`. The input and `include` files for other cases are available as `inp.`*n* and `com.`*n* in the subdirectory `bl2d/inputs` (where *n* refers to the case number).

5.4 Modifying the Code

Inevitably, modifications must be added to the code for specific applications. The modular structure of the code enables the user to perform this easily. Most often, additional output statements are added or some new parameters are computed. New transition zone models and turbulence models can also be easily added. The modifications can be incorporated in `main.f` by additional call statements or write statements. To assist the user in possible modifications, a list of the main variables used in the program and their definitions are given in appendix E.

Finally, the author requests that he be kept informed of details of errors, omissions, and suggested modifications to the report or the computer program, if any. An updated description of such revisions will be maintained by the author and supplied with the software and report (file `bl2d/doc/Update.info`). The e-mail address of the author is, `v.iyer@larc.nasa.gov`.

ACKNOWLEDGEMENTS

This research was supported by the Laminar Flow Control Project Team, Fluid Mechanics and Acoustics Division, NASA Langley Research Center, Hampton, VA under contract no. NAS1–19672. The author is grateful to Dr. Julius E. Harris of NASA Langley Research Center for many helpful suggestions and discussions. Thanks are due to Ms. Jonay A. Campbell for her help in the technical editing of this report.

REFERENCES

[1] Harris, J. E.; and Blanchard, D. K.: *Computer Program for Solving Laminar, Transitional, or Turbulent Compressible Boundary-Layer Equations for Two-Dimensional and Axisymmetric Flow.* NASA TM–83207, 1982.

[2] Iyer, V: *Three-Dimensional Boundary-Layer Program (BL3D) for Swept Subsonic or Supersonic Wings With Application to Laminar Flow Control.* NASA CR–4531, 1993.

[3] Iyer, V: *Computation of Three-Dimensional Compressible Boundary Layers to Fourth-Order Accuracy on Wings and Fuselages.* NASA CR–4269, 1990.

[4] Harris, J. E.: *Numerical Solution of the Compressible Laminar, Transitional, and Turbulent Boundary Layer Equations With Comparisons to Experimental Data.* Ph.D. Thesis, Virginia Polytechnic Institute, May 1970.

[5] Price, J. M.; and Harris, J. E.: *Computer Program for Solving Nonsimilar-Boundary-Layer Equations for Laminar, Transitional, or Turbulent Flows of a Perfect Gas.* NASA TMX-2458, 1972.

APPENDIX A. BL2D PROGRAM LOGIC

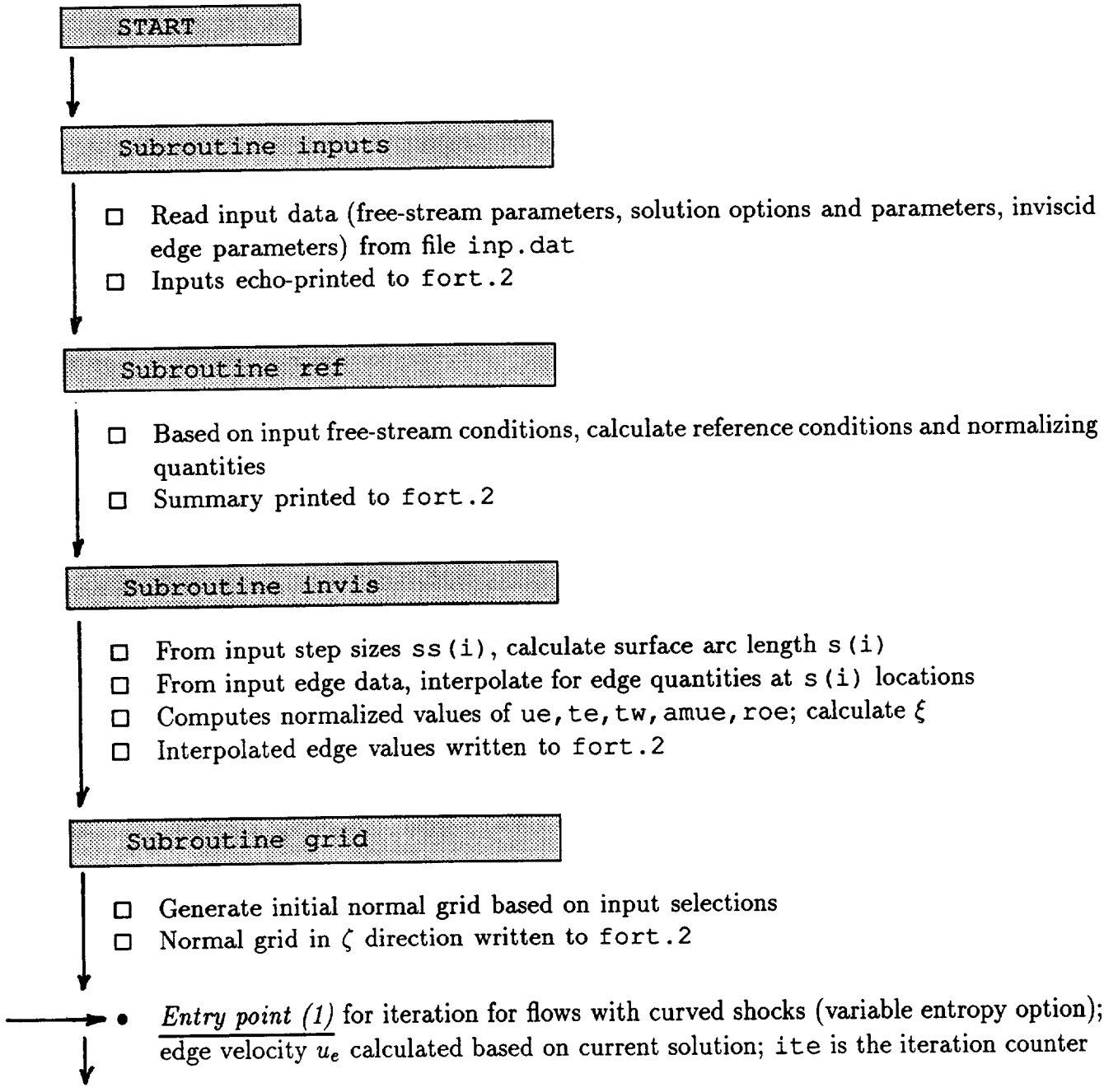

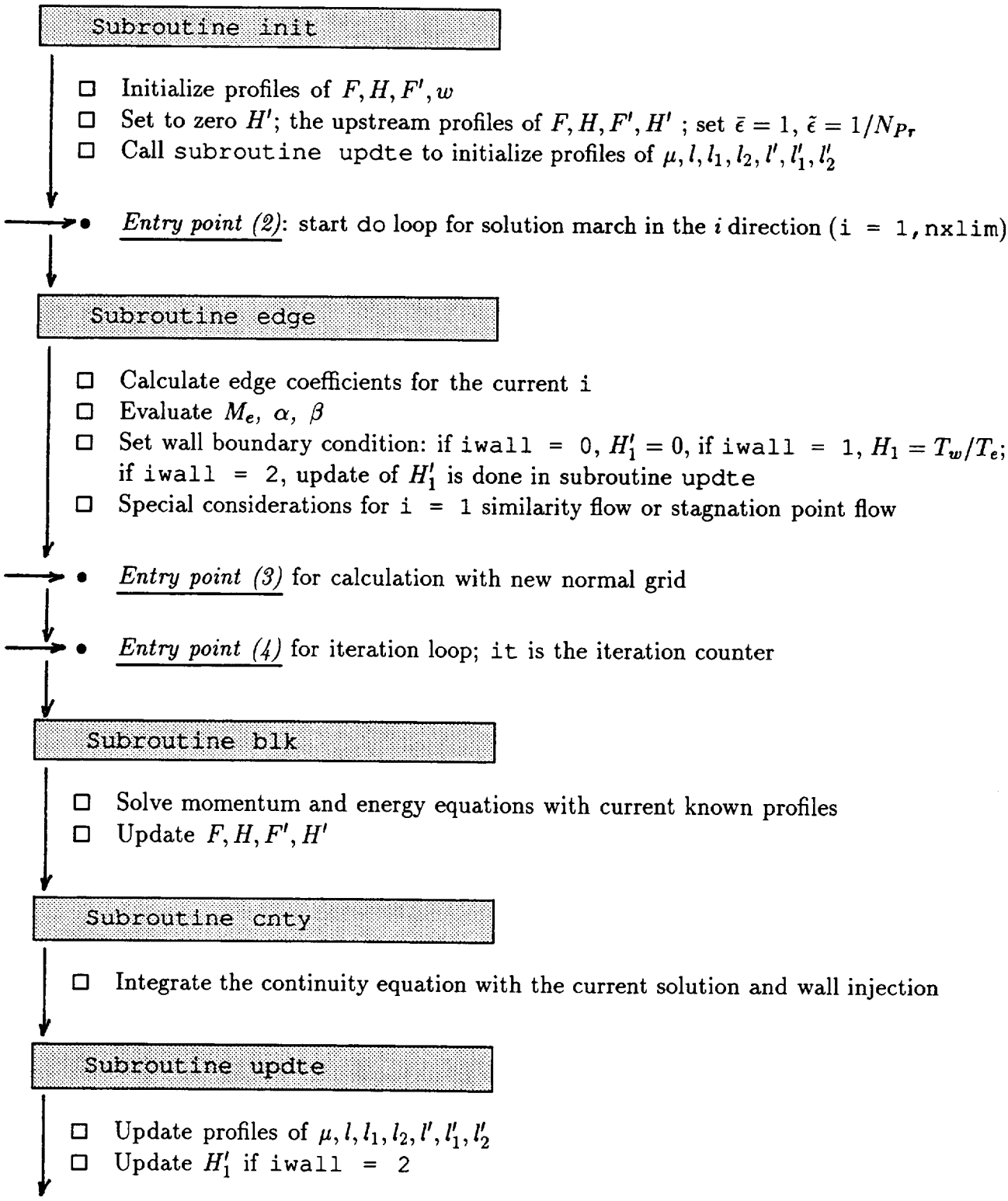
Subroutine init
Initialize profiles of F, H, F', w
Set to zero H'; the upstream profiles of F, H, F', H' ; set $\bar{\epsilon} = 1$, $\tilde{\epsilon} = 1/N_{Pr}$
Call subroutine updte to initialize profiles of $\mu, l, l_1, l_2, l', l'_1, l'_2$
Entry point (2): start do loop for solution march in the i direction (i = 1,nxlim)
Subroutine edge
Calculate edge coefficients for the current i
Evaluate M_e, α, β
Set wall boundary condition: if iwall = 0, $H'_1 = 0$, if iwall = 1, $H_1 = T_w/T_e$; if iwall = 2, update of H'_1 is done in subroutine updte
Special considerations for i = 1 similarity flow or stagnation point flow
Entry point (3) for calculation with new normal grid
Entry point (4) for iteration loop; it is the iteration counter
Subroutine blk
Solve momentum and energy equations with current known profiles
Update F, H, F', H'
Subroutine cnty
Integrate the continuity equation with the current solution and wall injection
Subroutine updte
Update profiles of $\mu, l, l_1, l_2, l', l'_1, l'_2$
Update H'_1 if iwall = 2

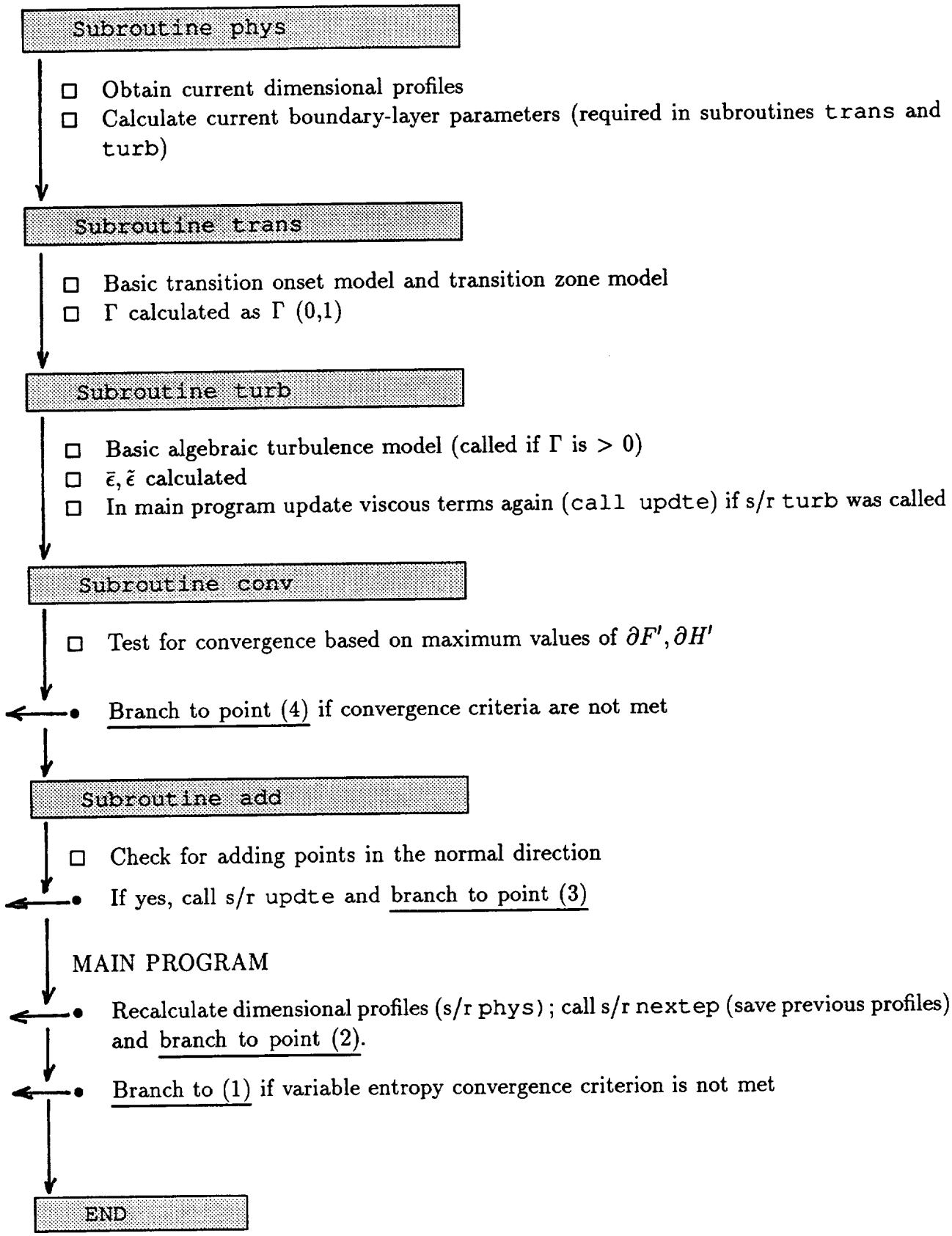
Subroutine phys
Obtain current dimensional profiles
Calculate current boundary-layer parameters (required in subroutines trans and turb)
Subroutine trans
Basic transition onset model and transition zone model
Γ calculated as Γ (0,1)
Subroutine turb
Basic algebraic turbulence model (called if Γ is > 0)
$\bar{\epsilon}, \tilde{\epsilon}$ calculated
In main program update viscous terms again (call updte) if s/r turb was called
Subroutine conv
Test for convergence based on maximum values of $\partial F', \partial H'$
Branch to point (4) if convergence criteria are not met
Subroutine add
Check for adding points in the normal direction
If yes, call s/r updte and branch to point (3)
MAIN PROGRAM
Recalculate dimensional profiles (s/r phys); call s/r nextep (save previous profiles) and branch to point (2).
Branch to (1) if variable entropy convergence criterion is not met
END

APPENDIX B. INPUT FILE FORMAT FOR BL2D

```
Line 1 -------
TITLE (no more than 79 characters long)

Line 2 -------
IUNIT          AMACH          PTS or PFS      TTS or TFS      IFS

Line 3 -------
Values corresponding to line headings above
IUNIT   0 for British units
        1 for SI units
AMACH   mach number
PTS     free-stream total pressure (lb/ft2 or N/m2)
PFS     free-stream static pressure (lb/ft2 or N/m2)
TTS     free-stream total temperature (deg R or deg K)
TFS     free-stream static temperature (deg R or deg K)
IFS     negative value indicates that input values are PFS and TFS
        positive value indicates that input values are PTS and TTS

Line 4 -------
GAM             IGAS            IWALL           J               IFT

Line 5 -------
Values corresponding to line headings above
GAM     ratio of specific heats
IGAS    1 for Sutherland law for viscosity
        2 for Power law
        default values for the corresponding coefficients
        (vis1c1,vis1c2 for igas=1; vis2c1,vis2c2 for igas=2)
        are specified in s/r ref
IWALL   wall boundary condition;
        0 for adiabatic
        1 for wall temperature specification
        2 for wall heat flux specification (if other than zero)
J       0 for 2-D
        1 for axisymmetric
IFT     0 for locally similar solution (for checking purposes)
        1 non-similar solution (recommended)
Line 6 -------
IBODY           WAVE            PHII            IENTRO          CONVE

Line 7 -------
Values corresponding to line headings above
IBODY   1 for flow with a stagnation point
        2 for flow without stagnation point
WAVE    shock wave angle at x=0 (input 0 if no shock)
PHII    opening angle of body at x=0, deg.
IENTRO  1 for constant entropy
        2 for variable entropy
CONVE   convergence criterion for variable entropy iteration
```

```
Line 8 -------
ZMAX            ZI              NZI             AK              NZ

Line 9 -------
Values corresponding to line headings above (normal grid parameters)
ZMAX    the maximum value of the transformed normal co-ordinate
ZI      normal co-ordinate value at the end of inner distribution
NZI     number of mesh points in the inner distribution
AK      stretching parameter for inner distribution (AK=1 for equal spacing)
NZ      total number of normal grid points

Line 10 ------
DFPTOL          DHPTOL          IACC            ITMAX           IW

Line 11 ------
Values corresponding to line headings above
DFPTOL  convergence criterion for delta-F-prime
DHPTOL  convergence criterion for delta-H-prime
IACC    order of accuracy, 2 or 4
ITMAX   maximum number of iterations
IW      0 to neglect transverse curvature
        1 to include transverse curvature

Line 12 ------
DFE             DHE             IADD            VELEDG          NX1

Line 13 ------
Values corresponding to line headings above
DFE     criterion on F at BL edge for adding points (if IADD=1)
DHE     criterion on H at BL edge for adding points (if IADD=1)
IADD    0 --> do not check to see if addition of normal grid points is required
        1 --> add normal grid points if required (test based on DFE, DHE)
VELEDG  value of F to be used in defining edge of BL
NX1     no. of steps (= NX-1, where NX is the total number of streamwise points)

Line 14 ------
IYINT           KODAMP          KODPRT          KODVIS          KTCOD

Line 15 ------
Values corresponding to line headings above (for transition/turbulence model)
IYINT   1 --> normal intermittency function set to 1
        2 --> normal intermittency function from an equation
KODAMP  1 --> local values used in equation for damping
        2 --> wall values used in equation for damping
KODPRT  1 --> constant PRT
        2 --> Rotta distribution for PRT
        3 --> tabular input for PRT
KODVIS  1 --> mixing length model
        2 --> two-layer eddy viscosity model
KTKOD   1 --> transition extent from equation
        2 --> transition extent from specified TLNGTH
```

```
Line 16 ------
SMXTR           SST             TLNGTH          PRT             NXLIM

Line 17 ------
Values corresponding to line headings above (for transition/turbulence model)
SMXTR   critical vorticity Reynolds number for transition onset estimation
SST     x-location of transition (either one of SMXTR or SST will take effect)
TLNGTH  ratio of x at transition zone end to x at transition zone beginning
PRT     turb. Prandtl number
NXLIM   --> stop march at I=NXLIM (NXLIM<or=NX)

Line 18 ------
RSTAR           IORD1           IORD2           ITEMAX          PRL

Line 19 -----
Values corresponding to line headings above
RSTAR   gas constant, dimensional
        for air RSTAR=1716 ft^2/sec^2 degR or 286.96 m^2/sec^2 K
IORD1   locations i.LE.iord1 will have first order streamwise gradients
IORD2   locations i.GE.iord2 will have second order streamwise gradients;
        the intermediate locations will have first-order/second-order blend
        program checks for IORD1 > 1; IORD2  > IORD1
ITEMAX  maximum number variable entropy iterations
PRL     Prandtl number, laminar value

Line 20 ------
STEP SIZES (NX1 VALUES)

Line 21 ------
NX1 values of step sizes, (SS(I),I=1,NX1); values separated by a space or comma

Line aa ------
WALL OR PROFILE PRINT FLAGS (0,1 or 2), NX1 VALUES

Lines aa+1, aa+2, ... ------
Print flags corresponding to each step, NX1 values separated by space or comma
        0 --> no wall or profile print
        1 --> wall print
        2 --> wall and profile print

Line bb ------
OUTPUT FOR PLOTS, NUMBER OF VARIABLES FOLLOWED BY VARIABLE NUMBER CODES

Lines bb+1, bb+2, ... ------
number codes for variables to be output, see list below of variables
that can be output; maximum 10 number codes only; first value is the
number (IVL) of variables to be output, followed by IVL number of
variable number codes separated by a space or comma
```

```
Line cc ------
NUMBER          L (INVISCID INPUTS)

Line cc+1 ------
Values corresponding to line headings above
NUMBER  no. of points of inviscid data
L       order of interpolation, 1 for linear, 2 for quadratic, etc.

Line cc+2 ------
XE      RADE    SE      PESE    TWSE    QESE    WWSE

Lines cc+3, cc+4, ... ------
values corresponding to line headings above (NUMBER number of lines)
XE      axial length, m (ft)
RADE    body radius, m (ft)
SE      body surface arc length, m (ft)
PESE    BL edge pressure, Pa (lb/ft2)
TWSE    wall temperature, deg K (deg R), used if IWALL=1
QESE    wall heat flux, W/m2 (Btu/ft2-s), used if IWALL=2
WWSE    wall mass flux, Pa-s/m (lb-s/ft3)

Line dd *** lines below required only if KODPRT=3 ***
NUMB1

Line dd+1 ------
number of values to be read in for GLAR,PRTAR table (NASA TM-83207 for details)

Line dd+2 ------
GLAR    PRTAR

Lines dd+3, dd+4, ... ------
NUMB1 values of (GLAR,PRTAR) pairs, one pair to a line
        *** lines above required only if KODPRT=3 ***

Line ee *** lines below required only if IENTRO=2 ***
NS (NO. OF CURVED SHOCK COORDINATES FOR VARIABLE ENTROPY CALCULATION)

Line ee+1 ------
Value corresponding to line heading above (number of curved shock co-ordinates)

Line ee+2 ------
RRS          ZZS          DRSDZS

Lines ee+3, ee+4, ... ------
NS values of groups of (RRS,ZZS,DRSDZS), one group to a line
describing the shape of the shock line defined as below:
RRS     radial location of a point on the shock curve, dimensional
ZZS     axial location of a point on the shock curve, dimensional
DRSDZS  derivative of RRS with respect to ZZS
        *** lines above required only if IENTRO=2 ***
```

APPENDIX C. INPUT PARAMETERS FOR BL2D

AK	stretching parameter k_s for inner distribution of normal grid; $k_s > 1$
AMACH	mach number, M_∞
CONVE	convergence criterion on u_e for variable entropy iteration
DFE	criterion on F' at boundary-layer edge for adding points (used only if IADD=1)
DFPTOL	convergence criterion on $\delta F'$
DHE	criterion on H' at boundary-layer edge for adding points (used only if IADD=1)
DHPTOL	convergence criterion on $\delta H'$
DRDZS	derivative of shock curve radius with respect to axial length
GAM	ratio of specific heats, γ
GLAR	array (z/δ) that corresponds to PRTAR array (see NASA TM-83207 for details)
IACC	order of accuracy, 2 or 4
IADD	0, no addition of normal grid points; 1, add if required
IBODY	1 for flow with a stagnation point; 2 for flow without stagnation point
IENTRO	1 for constant entropy; 2 for variable entropy
IFS	1 for input of PTS, TTS; -1 for input of PFS, TFS
IFT	0 for locally similar solution; 1 for non-similar solution (recommended)
IGAS	1 for Sutherland law for viscosity; 2 for power law; if IGAS is 2, check power law coefficients vis2c1, vis2c2 in s/r ref
IORD1	value such that when I.LE.IORD1, streamwise gradients are computed to first order; IORD1 > 1
IORD2	value such that when I.GE.IORD2, streamwise gradients are computed to second order; IORD2 > IORD1
ITMAX	maximum number of iterations
ITEMAX	maximum number of iterations in the variable entropy loop
IUNIT	0 for British units; 1 for SI units
IVL	number of variables to be output from list in appendix D
IW	0 to neglect transverse curvature; 1 to include transverse curvature; select 0 for internal flows
IWALL	wall bounday condition: 0 for adiabatic; 1 for temperature specified; 2 for heat flux specified
IYINT	1, normal intermittency function set to 1; 2, function from equation (see NASA TM-83207 for details)
J	0 for two-dimensional; 1 for axisymmetric
KODAMP	1, local values used in equation for damping; 2, wall values used
KODPRT	1, constant PRT; 2, Rotta distribution for PRT; 3, table input for PRT
KODVIS	1, mixing length model; 2, two-layer eddy viscosity model
KTCOD	1, transition extent from equation; 2, from specified TLNGTH
L	order of interpolation: 1 for linear; 2 for quadratic, etc.
NS	number of points that define the shock curve (used only if IENTRO = 2)

NUMBER	number of input points that define the boundary-layer edge conditions
NUMB1	number of values of (GLAR, PRTAR) pairs
NX1	number of steps (= NX - 1, where NX is the total number of streamwise points)
NXLIM	stop march at I = NXLIM (NXLIM.LE.NX)
NZ	total number of normal grid points, ke
NZI	number of mesh points in the inner distribution, ki
PESE	boundary-layer edge pressure, P_e (N/m^2 or lb/ft^2)
PFS	free-stream static pressure, P_∞ (N/m^2 or lb/ft^2)
PHII	opening angle of body at $s^* = 0$, deg
PRL	Prandtl number, N_{Pr}, laminar value
PRT	Prandtl number $N_{Pr,t}$, turbulent value
PRTAR	array of PRT values input in tabular form (for KODPRT = 3)
PTS	free-stream total pressure, P_0 (N/m^2 or lb/ft^2)
QESE	wall heat flux $\dot{q}_w^*$; used if IWALL = 2 (W/m^2 or $Btu/ft^2 \cdot sec$)
RADE	body radius (m or ft)
RRS	shock curve radius (m or ft)
RSTAR	gas constant ($m^2/(sec^2K)$ or $ft^2/(sec^2{}^\circ R)$); for air RSTAR = 286.96 or 1716.0
SE	body surface arc length; s^* at input data points (m or ft)
SMXTR	critical vorticity Reynolds number for transition onset estimation
SS	array of length NX1 containing step size values
SST	s^* location of transition (to be set as a large value if SMXTR criterion is to be used)
TFS	free-stream static temperature, T_∞ (K or °R)
TLNGTH	ratio of s^* at end of transition zone to s^* at beginning of transition zone (for KTKOD = 2)
TTS	free-stream stagnation temperature, T_0 (K or °R)
TWSE	wall temperature, used if IWALL = 1 (K or °R)
VELEDG	value of F to be used to define edge of boundary layer
WAVE	shock-wave angle at $s^* = 0$ (input 0 if no shock)
WWSE	wall mass flux $w_w{}^*$ ($Pa \cdot s/m$ or $lb \cdot s/ft^3$)
XE	axial length (m or ft)
ZI	normal coordinate value at the end of inner distribution, ζ_i
ZMAX	the maximum value of the transformed normal coordinate, ζ_e
ZZS	shock curve axial location (m or ft)

APPENDIX D. NUMBER CODES FOR OUTPUT OF VARIABLES IN BL2D

Number code	BL2D variable	Description of the output variable (output to file `fort.7`)
1	`betah`	pressure gradient parameter, $2\xi\frac{\partial u_e^*}{\partial \xi}$
2	`cfe`	skin-friction coefficient based on edge conditions, $C_{f,e}$
3	`cfw`	skin-friction coefficient based on wall conditions, $C_{f,w}$
4	`disp`	displacement thickness, δ^* (m or ft)
5	`dpeds`	pressure gradient, $\partial/\partial s^*$ of P_e
6	`dsmxo`	$\partial/\partial s^*$ of maximum vorticity Reynolds number
7	`dteds`	temperature gradient, $\partial/\partial s^*$ of T_e
8	`dueds`	velocity gradient, $\partial/\partial s^*$ of u_e^*
9	`error`	convergence parameter, $\partial F'/F'$ at the wall
10	`form`	ratio of displacement thickness to momentum thickness
11	`hd`	heat transfer coefficient, h
12	`itro`	number of variable entropy iterations
13	`ame`	edge Mach number
14	`amues`	edge viscosity, μ_e^*, dimensional
15	`it`	number of iterations
16	`anste`	Stanton number based on edge condition
17	`anstw`	Stanton number based on wall condition
18	`anue`	Nusselt number based on edge condition
19	`anuw`	Nusselt number based on wall condition
20	`eps`	$1/\sqrt{Re_{\text{ref}}}$
21	`p20`	total pressure at boundary-layer edge, nondimensional
22	`pes(i)`	boundary-layer edge pressure at location i (N/m^2 or lb/ft^2)
23	`qsd`	heat transfer at the wall (W/m^2 or $Btu/ft^2 \cdot sec$)
24	`roes`	edge density ($kg \cdot sec^2/m^4$ or $lb \cdot sec^2/ft^4$)
25	`redelt`	Reynolds number based on local displacement thickness
26	`res`	local Reynolds number

Number code	BL2D variable	Description of the output variable (output to file fort.7)
27	rethet	Reynolds number based on local momentum thickness
28	rftrue	recovery factor
29	rad(i)	body radius (m or ft)
30	smxp	maximum vorticity Reynolds number
31	rshk	local radius of shock wave (m or ft)
32	rvwal	suction or blowing mass flux normalized with edge value
33	rvwald	dimensional mass flux at the wall (Pa·s/m or lb·sec/ft^3)
34	x(i)	boundary-layer surface coordinate s^* (m or ft)
35	swang	local shock-wave angle in degrees
36	taud	wall shear stress (N/m^2 or lb/ft^2)
37	tes	dimensional edge temperature, T_e
38	theta	momentum thickness (m or ft)
39	trfct	intermittency distribution
40	twbtt1	T_w/T_0
41	ues	dimensional edge velocity, u_e^* (m/sec or ft/sec)
42	utau	friction velocity, $\sqrt{\tau/\rho}$ at wall (m/sec or ft/sec)
43	vw	transformed wall normal velocity at wall, w_w
44	alphah	$(\gamma-1)M_e^2$
45	xi(i)	ξ
46	ye	boundary-layer thickness (based on VELEDG), t^* (m or ft)
47	jpoint	normal grid index k, where turbulence model inner law = outer law
48	xa(i)	axial coordinate of body, x^* (m or ft)
49	zshk	axial coordinate of shock wave (m or ft)

APPENDIX E. DESCRIPTION OF MAIN COMPUTER VARIABLES IN BL2D

BL2D variable	Description
ad1,ad2,ad3	a_1, a_2, a_3; coefficients used in streamwise differencing $\partial/\partial\xi$
as1,as2,as3	coefficients used in streamwise differencing $\partial/\partial s^*$
ak	normal grid stretching parameter, k_s
al,alp	l, l'
al1,al1p	l_1, l_1'
al2,al2p	l_2, l_2'
amach,amache	M_∞, M_e
amu,amue	μ, μ_e
amues	edge viscosity, μ_e^*, dimensional
amufs	μ_∞^*
amurefs	μ^* at T_{ref}
amurs	Sutherland viscosity law constant
anste,anstw	Stanton number based on edge or wall condition
anue,anuw	Nusselt number based on edge or wall condition
bet,bet2	$\gamma/(\gamma-1)$, $(\gamma-1)/2$
betah	pressure gradient parameter, $2\xi\frac{\partial u_e^*}{\partial\xi}$
cfe,cfw	skin-friction coefficient based on edge or wall condition
conve	convergence criterion for variable entropy iteration
delfp,delhp	$\delta F', \delta H'$
dfptol,dhptol	convergence criteria on $\delta F', \delta H'$
disp	displacement thickness, δ^* (m or ft)
dpeds	pressure gradient, $\frac{\partial P_e}{\partial s^*}$
drdzs	slope of the shock curve
ds	step size in s^*
dsmxo	$\partial/\partial s^*$ of maximum vorticity Reynolds number
dxi,dxi1	step sizes in ξ; $\xi_i - \xi_{i-1}$, $\xi_{i-1} - \xi_{i-2}$

BL2D variable	Description
dsi, dsi1	step sizes in s^*
eps	$1/\sqrt{Re_{\text{ref}}}$
f, f1, f2	F at i, $i-1$, $i-2$
form	ratio of displacement thickness to momentum thickness
fp, fp1, fp2	F' at i, $i-1$, $i-2$
g, gam	γ
glar	array of z^*/δ^* values for which $N_{Pr,t}$ values are input
h, hh1, hh2	H at i, $i-1$, $i-2$
hd	heat transfer coefficient, h
hp, hp1, hp2	H' at i, $i-1$, $i-2$
i, i1	i, $i-1$
iacc	order of accuracy
iadd	flag for addition of normal grid points
ibody	flag for type of flow at $i = 1$
ientro	flag for variable entropy calculation
ift	flag for nonsimilar solution
ifs	flag for input of free-stream conditions
igas	flag for type of viscosity law
iord1, iord2	i indices to specify order of accuracy of the streamwise gradient
it, itmax	number of iterations and maximum number of iterations
ite, itemax	number of variable entropy iterations and its upper limit
itrans	flag to denote laminar, transitional, or turbulent regime (0, 1, or 2)
itro	number of variable entropy iterations
iunit	flag for choice of units, US or SI
iw	flag for transverse curvature term
iwall	flag for energy boundary condition at the wall
iyint	normal intermittency function
j	flag for two-dimensional or axisymmetric flow
k, k1	normal grid index $k, k-1$
nmax	greater value of (nzm, nxm)
ns, nsm	number of points defining the shock curve, upper limit for ns

BL2D variable	Description
num	number of input inviscid data points
numbl, numblm	number of input $N_{Pr,t}$ values, upper limit for numbl
nx, nxl	number of streamwise grid points, number of steps
nxlim	streamwise grid index at which to stop march, nxlim $\leq$ nx
nxm	maximum array dimension for streamwise grid
nz, nzm	number of normal grid points, upper limit for nz
nzi	number of normal grid points in the inner part of a two-part distribution
oz	$\sqrt{2\xi}$
p10	total pressure at boundary-layer edge for ientro = 1, non-dimensional
p20	total pressure at boundary-layer edge for ientro = 2, non-dimensional
pe	static pressure at boundary-layer edge at grid locations
pes	static pressure at boundary-layer edge, dimensional
pese	static pressure at boundary-layer edge at input data points, dimensional
pfs	free-stream static pressure, dimensional
phii	opening angle of body at $s^* = 0$, deg
prl, prt	Prandtl number, laminar or turbulent
prtar	input array of turbulent Prandtl number values
pts	free-stream total pressure, dimensional
qsd, qws	heat transfer at the wall (W/m^2 or $Btu/ft^2 \cdot sec$)
qwse	heat transfer at the wall at input data points (W/m^2 or $Btu/ft^2 \cdot sec$)
rad	body radius, dimensional
rade	body radius at input data points
redelt	Reynolds number based on local displacement thickness
refs	free-stream Reynolds number
reref	Re_{ref}
rethet	Reynolds number based on local momentum thickness
roe	edge density, nondimensional

BL2D variable	Description
rofs	free-stream density, dimensional
rrs	input shock curve radius, dimensional
rstar	gas constant, dimensional
ss	array of step sizes
sst	transition location
taud	wall shear stress (N/m^2 or lb/ft^2)
t10	boundary-layer edge total temperature, nondimensional
te	boundary-layer edge temperature, nondimensional
tf	free-stream temperature, nondimensional
tfs	free-stream temperature, dimensional
theta	momentum thickness, dimensional
tlngth	ratio of s^* at the end of transition zone to s^* at the beginning of transition zone
tts	total temperature, dimensional
tws	wall temperature, dimensional
twse	wall temperature at input data points, dimensional
ue	edge velocity, nondimensional
uee	edge velocity for ientro = 2, nondimensional
ufs	free-stream velocity, dimensional
veledg	value of F used to define edge of boundary layer
vis2c1,vis2c2	viscosity coefficients for igas = 2
w	transformed normal velocity
wave	shock wave angle at $s^* = 0$
wws	wall-normal velocity, dimensional
wwse	wall-normal velocity at input data points, dimensional
x(i)	body surface coordinate s^*, dimensional
xa(i)	axial length, dimensional
xae(i)	axial length at input data points, dimensional
xe(i)	body surface coordinate values at input data points, dimensional
xi	ξ
z	transformed normal grid array, ζ

BL2D variable	Description
zi	value of ζ that corresponds to the limit of the inner distribution
zmax	maximum value of ζ
zshk	axial coordinate of shock wave (m or ft)

C-2.

REPORT DOCUMENTATION PAGE

Form Approved
OMB No. 0704-0188

1. AGENCY USE ONLY *(Leave blank)*	2. REPORT DATE	3. REPORT TYPE AND DATES COVERED
	May 1995	Contractor Report

4. TITLE AND SUBTITLE

Computer Program BL2D for Solving Two-Dimensional and Axisymmetric Boundary layers

5. FUNDING NUMBERS

C NAS1-19672

WU 537-03-23-03

6. AUTHOR(S)

Venkit Iyer

7. PERFORMING ORGANIZATION NAME(S) AND ADDRESS(ES)

ViGYAN, Inc.
30 Research Drive
Hampton, VA 23666-1325

8. PERFORMING ORGANIZATION REPORT NUMBER

9. SPONSORING / MONITORING AGENCY NAME(S) AND ADDRESS(ES)

National Aeronautics and Space Administration
Langley Research Center
Hampton, VA 23681-0001

10. SPONSORING / MONITORING AGENCY REPORT NUMBER

NASA CR-4668

11. SUPPLEMENTARY NOTES

Langley Technical Monitor: Ajay Kumar

12a. DISTRIBUTION / AVAILABILITY STATEMENT

Unclassified/Unlimited

Subject Category 34

12b. DISTRIBUTION CODE

13. ABSTRACT *(Maximum 200 words)*

This report presents the formulation, validation, and user's manual for the computer program BL2D. The program is a fourth-order-accurate solution scheme for solving two-dimensional or axisymmetric boundary layers in speed regimes that range from low subsonic to hypersonic Mach numbers. A basic implementation of the transition zone and turbulence modeling is also included. The code is a result of many improvements made to the program VGBLP, which is described in NASA TM-83207 (February 1982), and can effectively supersede it. The code BL2D is designed to be modular, user-friendly, and portable to any machine with a standard `fortran77` compiler.

The report contains the new formulation adopted and the details of its implementation. Five validation cases are presented. A detailed user's manual with the input format description and instructions for running the code is included. Adequate information is presented in the report to enable the user to modify or customize the code for specific applications.

14. SUBJECT TERMS

boundary layer; computer program; two-dimensional; axisymmetric; compressible flow; laminar flow control; transition prediction; turbulence modeling

15. NUMBER OF PAGES

98

16. PRICE CODE

A05

17. SECURITY CLASSIFICATION OF REPORT	18. SECURITY CLASSIFICATION OF THIS PAGE	19. SECURITY CLASSIFICATION OF ABSTRACT	20. LIMITATION OF ABSTRACT
Unclassified	Unclassified	Unclassified	

National Aeronautics and
Space Administration
Langley Research Center
Mail Code 180
Hampton, VA 23681-0001